2011

The level and distribution of the GABA(B)R1 AND GABA(B)R2 receptor subunits in the rat's central auditory system

Lena Jamal
University of Windsor

THE LEVEL AND DISTRIBUTION OF THE $GABA_BR1$ AND $GABA_BR2$ RECEPTOR SUBUNITS IN THE RAT'S CENTRAL AUDITORY SYSTEM

By

Lena Jamal

A Thesis

Submitted to the Faculty of Graduate Studies through Biological Sciences in Partial Fulfillment of the Requirements for the Degree of Master of Science at the University of Windsor

Windsor, Ontario, Canada

2011

THE LEVEL AND DISTRIBUTION OF THE $GABA_BR1$ AND $GABA_BR2$ RECEPTOR SUBUNITS IN THE RAT'S CENTRAL AUDITORY SYSTEM

By Lena Jamal

APPROVED BY:

_____

Dr. Jerome Cohen
Department of Psychology

_____

Dr. Barbara Zielinski
Department of Biological Sciences

_____

Dr. Huiming Zhang, Advisor
Department of Biological Sciences

_____

Dr. Andrew Swan, Chair of Defense
Department of Biological Sciences

21 September 2011

DECLARATION OF CO-AUTHORSHIP / PREVIOUS PUBLICATION

I. Co-Authorship Declaration

I hereby declare that this thesis incorporates the outcome of joint research undertaken in collaboration with Hao Zhang, Dr. Paul G. Finlayson, Dr. Lisa A. Porter, and Dr. Huiming Zhang. This collaboration is covered in Section 3.2 of the thesis. The primary contributions including experimental protocol, procedures, and data analysis were performed by the author. The contribution of Hao Zhang was through the conduction of Western blotting procedures as described in Section 3.2. Dr. Paul G. Finlayson, Dr. Lisa A. Porter, and Dr. Huiming Zhang all played key roles in the contribution of major ideas, interpretation of data, and guidance throughout the project.

I am aware of the University of Windsor Senate Policy on Authorship and I certify that I have properly acknowledged the contribution of other researchers to my thesis, and have obtained written permission from each of the co-authors to include the above material in my thesis.

I certify that, with the above qualification, this thesis, and the research to which it refers, is the product of my own work.

II. Declaration of Previous Publication

This thesis includes 1 original paper that has been previously published in a peer reviewed journal, as follows:

Thesis Section	Publication title/full citation	Publication status
Section 3.2	*The level and distribution of the $GABA_BR2$ receptor subunit in the rat's central auditory system*	*Published 2011*

I certify that I have obtained written permission from the copyright owners to include the above published material in my thesis. I certify that the above material describes work completed during my registration as graduate student at the University of Windsor.

I declare that, to the best of my knowledge, my thesis does not infringe upon anyone's copyright nor violate any proprietary rights and that any ideas, techniques, quotations, or any other material from the work of other people included in my thesis, published or otherwise, are fully acknowledged in accordance with the standard referencing practices. Furthermore, to the extent that I have included copyrighted material that surpasses the bounds of fair dealing within the meaning of the Canada Copyright Act, I certify that I have obtained permission from the copyright owner(s) to include such material(s) in my thesis.

I declare that this is a true copy of my thesis, including any final revisions, as approved by my thesis committee and the Graduate Studies office, and that this thesis has not been submitted for a higher degree to any other University or Institution.

ABSTRACT

The $GABA_B$ receptor is important for the function of neurons in the central auditory system. A functional $GABA_B$ receptor is a heterodimer of the $GABA_BR1$ and $GABA_BR2$ subunits. In this thesis, I used immunohistochemical methods to examine the level and localisation of both subunits in the rat's central auditory system.

Results revealed that $GABA_BR1$ and $GABA_BR2$ subunits were expressed throughout the auditory system. High levels of immunoreactivity to both subunits were found in the superficial layers of the auditory cortex, medial geniculate nucleus, dorsal region of the inferior colliculus, and dorsal cochlear nucleus. While the expression of these subunits was generally parallel with each other, some differences were observed between the two subunits. Overall, distributions of the $GABA_BR1$ and $GABA_BR2$ subunits in auditory structures are consistent with inputs to these structures. The localisation of the subunits supports the contribution of functional $GABA_B$ receptors that are likely mediating auditory connections.

ACKNOWLEDGEMENTS

There are so many people I would like to thank for making my pursuit of a Master's degree an amazing experience. First and foremost, I would like to thank my advisor and mentor Dr. Huiming Zhang. With his guidance, advice, and patience, I was able to achieve so much more than I would have imagined possible in such a short time.

I would also like to thank my exceptional committee members, Dr. Barbara Zielinski and Dr. Jerome Cohen. I really appreciated their never ending support throughout my thesis and their flexibility in always making time for me. Their commitment to my success was clear and their insight was invaluable.

I would like to thank past and present members of the Zhang Lab for their support and friendship. Special thanks go to Chirag Patel, Carmela Redhead, Afifa Bokhari, Aruj Chawla, Ayesha Raza, Ariana Lumani, Sara Dawood, Grace Stephan, Stephanie Stephan, and Andrea Cervi.

I also need to express my immense gratitude to Dr. Barbara Zielinski and Dr. Lisa Porter for always being available for help and for being such great sources of information and advice. I would also like to thank all the wonderful members of the Zielinski and Porter Labs who always made me feel welcome. I am indebted to their assistance and friendship with special mention to Cory Ochs, Warren Green, and Ravneet Bhogal in the Zielinski Lab as well as Jiamila Maimaiti, Dorota Lubanska, Espanta Jalili, and Agnes Malysa in the Porter Lab. I also need to thank my previous colleague Hao Zhang as well as Dr. Paul Finlayson for being wonderful collaborators. Their input helped make it possible for me to have had published work during my Master's degree.

The technical staff at the University of Windsor is excellent and my research experience went a lot smoother thanks to Ingrid Churchill, Rodica Leu, Bob Hodge, Barbara Zimmerman, Nancy Barkley, Jacqueline Christie, and Elaine Rupke.

Finally, I am grateful for all of the wonderful people I have met these past two years. Everyone helped make this a wonderful and unforgettable experience. Most of all, I would like to thank my amazing family, who have always been there for me and encourage me to always do my best in everything I pursue. Without their immense and continued support I would not be where I am today.

Research was supported by NSERC and the University of Windsor

TABLE OF CONTENTS

LIST OF TABLES

LIST OF FIGURES

LIST OF ABBREVIATIONS

AC – auditory cortex

AMPA – α-amino-3-hydroxyl-5-methyl-4-isoxazole-propionate

AVCN – anteroventral cochlear nucleus

BSA – bovine serum albumin

CB – cerebellum

CN – cochlear nucleus

DAB – 3, 3’ diaminobenzidine tetrahydrochloride

DCN – dorsal cochlear nucleus

DNLL – dorsal nucleus of the lateral lemniscus

ECL – enhanced chemiluminescence

EPSP – excitatory post-synaptic potential

GABA – γ-aminobutyric acid

GCD – granule cell domain of the cochlear nucleus

G-protein – guanine nucleotide-binding protein

HRP – horseradish peroxidase

IC – inferior colliculus

ICc – central nucleus of the inferior colliculus

ICd – dorsal cortex of the inferior colliculus

ICx – external cortex of the inferior colliculus

HD – heptahelical domain

ILD – interaural level difference

IPSP – inhibitory post-synaptic potential

ITD – interaural time difference

LNTB – lateral nucleus of the trapezoidal body

LSO – lateral superior olivary nucleus

MG – medial geniculate nucleus

MGd – dorsal part of the medial geniculate nucleus

MGm – medial part of the medial geniculate nucleus

MGv – ventral part of the medial geniculate nucleus

MNTB – medial nucleus of the trapezoidal body

MSO – medial superior olivary nucleus

NDS – normal donkey serum

NLL – nucleus of the lateral lemniscus

NMDA – N-methyl-D-aspartic acid

PFA – paraformaldehyde

PB – phosphate buffer

PBS – phosphate buffer saline

PVCN – posteroventral cochlear nucleus

PVDF – polyvinylidene fluoride

SOC – superior olivary complex

SPN – superior paraolivary nucleus

TBST – tris-buffered saline tween

VCN – ventral cochlear nucleus

VFT – venus flytrap module

VNLL – ventral nucleus of the lateral lemniscus

VNTB – ventral nucleus of the trapezoidal body

1 INTRODUCTION

1.1 The auditory system

Hearing is essential to the biological fitness of mammals. It contributes to behaviours such as prey catching, predator avoidance, and species-specific communication. Acoustic signals are processed by the auditory system which consists of the peripheral and the central auditory systems. The auditory system has the ability not only to recognise and localise sounds, but also to differentiate behaviourally significant sounds from ambient noises.

The peripheral system consists of the outer, middle, and inner ear. The outer ear includes the external ear (pinna) and ear canal. The middle ear includes the oscicles and the inner ear includes the cochlea. The outer ear and middle ear are separated by the eardrum (tympanic membrane) and the middle and inner ear are separated by the oval window of the cochlea (Silverthorn, 2007). Sounds are directed by the pinna into the ear canal and the waves hit and vibrate the tympanic membrane. The vibrations are then transferred to the oval window through three connected oscicles, the malleus, incus, and stapes, which amplify the signal (Silverthorn, 2007). The vibrations from the oval window create waves within the fluid-filled cochlea causing hairs of hair cells to bend. Hair cells receiving mechanical stimulation (bending of hairs) release neurotransmitters which consequently excite spiral ganglion cells. Action potentials generated by ganglion cells travel by the cochlear nerve to the central auditory system (Silverthorn, 2007).

The central auditory system consists of six major structures: the cochlear nucleus (CN), the superior olivary nucleus (SOC), the nucleus of the lateral lemniscus (NLL), the inferior colliculus (IC), the medial geniculate nucleus (MG), and the auditory cortex (AC). These structures are organised in a hierarchical manner, with the CN being at the lowest level and the

AC at the highest. Each of these major central auditory structures can be divided into multiple subnuclei as seen in Figures 1A and 1B.

1.2 Central auditory structures

1.2.1 Cochlear Nucleus (CN)

The CN is located in the hindbrain and receives direct projections from the peripheral auditory system. The CN as a whole sends projections to the contralateral CN and IC, SOC, NLL and MG, and is the target of descending projections from the AC, IC, ventral NLL, and SOC (Schofield and Coomes, 2005). It is comprised of two main subdivisions: the ventral CN (VCN) and the dorsal CN (DCN). This can be seen in Figure 1A (upper panel).

Ventral Cochlear Nucleus (VCN)

The VCN can be further divided into two major subdivisions: the anterior VCN (AVCN) and the posterior VCN (PVCN). The VCN has five distinct cell types: spherical bushy, globular bushy, octopus, multipolar, and small cells. Characterisation of these cells can be seen in Figure 2. These cells receive inputs from the cochlear nerve (Osen et al., 1991). In addition to ascending inputs provided by auditory nerve fibres, all cells in the VCN (except for the octopus cells) receive descending input from the DCN and AC (Malmierca and Merchán, 2005).

Octopus cells in the PVCN send projections to the contralateral ventral NLL and bilaterally to the dorsal region of the SOC (Weiner and Schreiner, 2005). Globular bushy cells, which can be found in the rostral area of the PVCN and the caudal area of the AVCN, project to the contralateral ventral SOC (Warr, 1982). Spherical bushy cells in the AVCN project both ipsilaterally and contralaterally to the ventral SOC (Merchán et al., 1988). Multipolar and small

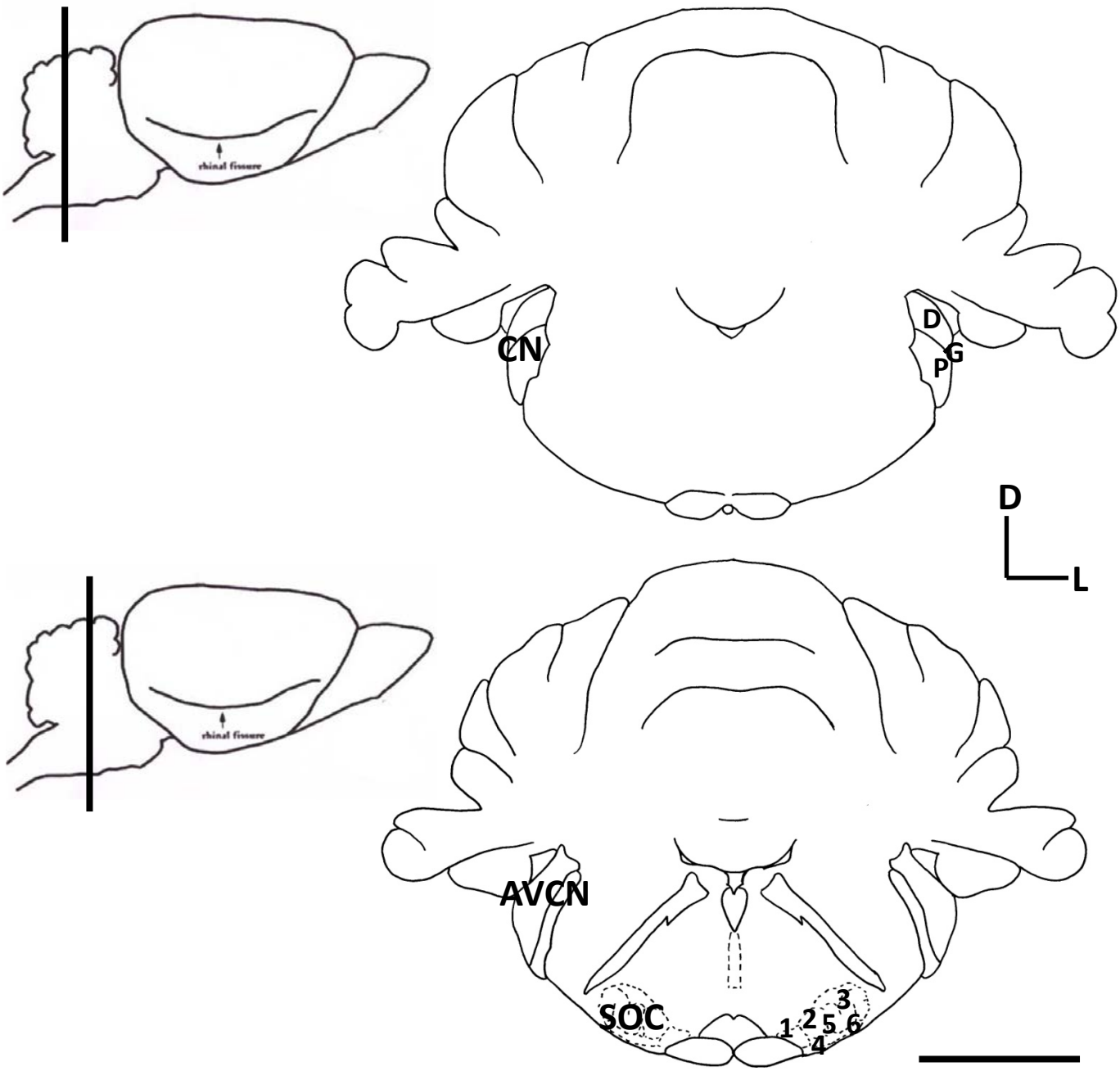

Figure 1A. Schematic representations of coronal sections of the rat brain containing the cochlear nucleus (CN, upper and lower panels) and the superior olivary complex (SOC, lower panel). The upper panel includes the posterior part of the CN which can be divided into the DCN (D), PVCN (P), and GCD (G). Lower panel contains the anterior part of the CN and the SOC. The anterior part of the CN is also called the anteroventral CN (AVCN). The SOC can be divided into the MNTB (1), SPN (2), LSO (3), VNTB (4), MSO (5), and LNTB (6). [*Redrawn and modified from Paxinos and Watson 2005*]

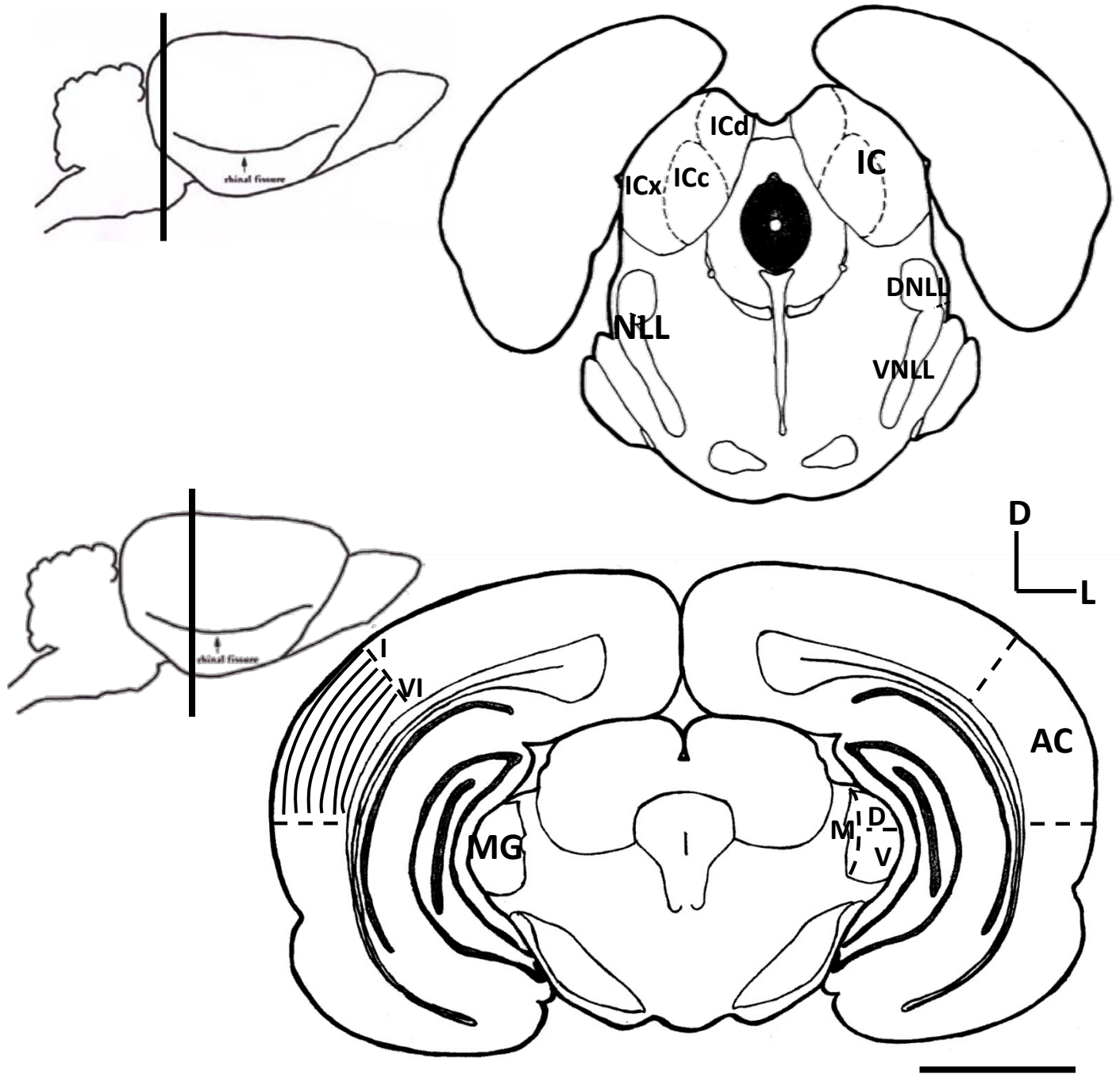

Figure 1B. Schematic representations of coronal sections of the rat brain containing the nucleus of the lateral lemniscus (NLL, upper panel), inferior colliculus (IC, upper panel), medial geniculate nucleus (MG, lower panel), and the auditory cortex (AC, lower panel). The NLL can be divided into the DNLL and VNLL. The IC can be divided into the ICd, ICx, and ICc. The MG can be divided into the MGD (D), MGV (V), and MGM (M). The AC can be divided into layers I, II, III, IV, V, and VI (represented as lines from the lateral to medial axis). [*Redrawn and modified from Paxinos and Watson 2005*]

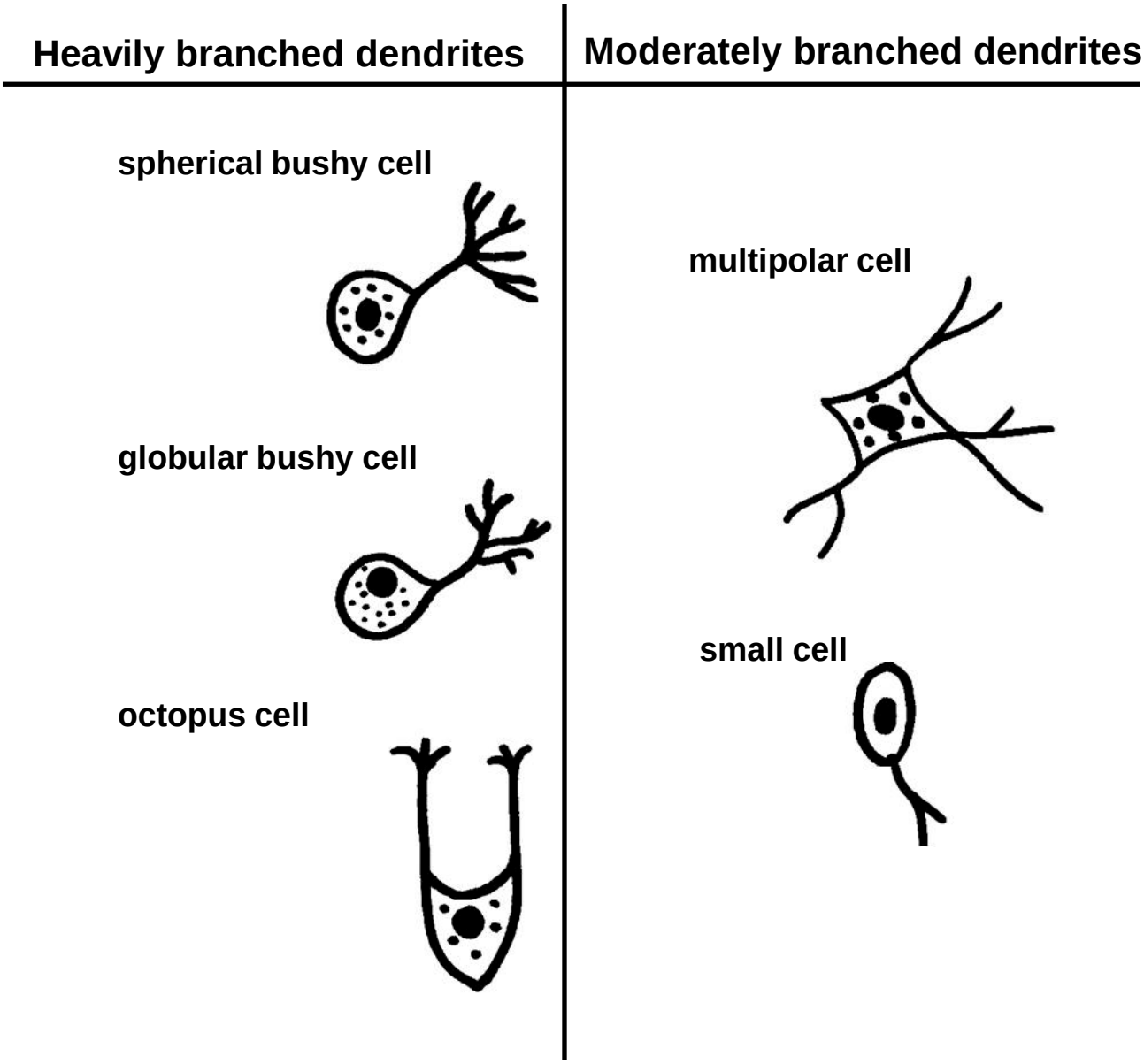

Figure 2. Schematic representations of cell types in the cochlear nucleus of the rat. Left panel contains schematic diagrams showing the morphologies of spherical bushy, globular bushy, and octopus cells respectively. These cells have dendrites that are heavily branched. Right panel contains schematic diagrams showing the morphologies of multipolar cells and small cells which have dendrites that are moderately branched. [*Redrawn from Malmierca and Merchan 2005*]

cells can be found throughout the VCN and have targets in the ipsilateral ventral IC, SOC, DCN, and contralateral CN.

Dorsal Cochlear Nucleus (DCN)

The DCN can be divided into 4 layers and a granule cell cap domain (GCD). Out of the four layers, the first three are superficial layers that are composed of pyramidal cells that receive projections from the VCN (Mugnaini et al., 1980, 1980b). These pyramidal cells send projections to the contralateral IC and the medial division of the MG (Schofield and Coomes, 2005). The fourth layer, referred to as the deep layer, is composed of giant or fusiform cells receiving local innervations from interneurons in neighbouring superficial layers and sending projections to the contralateral IC and MG (Malmierca et al., 2002).

The GCD is continuous with the first superficial layer, also known as the molecular layer, and can be found just above the DCN/PVCN border. It is made up of small cells that receive ascending projections from the cochlear nerve and VCN and the majority of corticocochlear projections from the AC (Mugnaini et al., 1980, 1980b). The GCD projects to the pyramidal cells in the superficial layers of the DCN, IC, medial MG, and bilaterally to the SOC (Schofield and Coomes, 2005).

1.2.2 Superior Olivary Complex (SOC)

The SOC is located in the hindbrain and is made up of a group of nuclei that are closely associated with one another. This structure consists of the lateral nucleus of the trapezoidal body (LNTB), the ventral nucleus of the trapezoidal body (VNTB), the medial nucleus of the trapezoidal body (MNTB), the lateral superior olivary nucleus (LSO), the medial superior olivary

nucleus (MSO), and the superior paraolivary nucleus (SPN). This can be seen in Figure 1A (lower panel).

Lateral Nucleus of the Trapezoidal Body (LNTB)

The LNTB can be found subjacent to the LSO. The main source of input to this structure includes all cell types within the CN except for octopus cells (Warr, 1982). The LNTB returns descending projections to the CN, providing a feedback mechanism in the auditory brainstem. Other outputs include those to ipsilateral IC as well as the neighbouring MSO (Spangler et al., 1987).

Ventral Nucleus of the Trapezoidal Body (VNTB)

The VNTB can be found in the most ventral region of the SOC. Inputs to this structure include ascending projections from globular bushy and octopus cells within the contralateral VCN. The ipsilateral IC and multipolar cells within the ipsilateral and contralateral PVCN provide additional inputs to the VNTB (Huffman and Henson, 1990; Warr and Beck, 1996). The VNTB has a broad range of outputs including the cochlea and molecular and deep layer of the DCN on both sides of the brain, as well as the ipsilateral LSO, IC, and VCN (Warr and Beck, 1996).

Medial Nucleus of the Trapezoidal Body (MNTB)

The MNTB, lies on the medial edge of the SOC near the vertical midline of the brain. This structure almost exclusively contains cells that are elongated in shape. The main source of input includes globular bushy cells within the contralateral AVCN. The axons of these bushy cells form Calyces of Held terminals that contact neurons in the MNTB (Morest, 1973). The MNTB projects to all neighbouring subdivisions of the SOC as well as the VNLL (Grothe and Koch, 2011).

Lateral Superior Olivary Nucleus (LSO)

The LSO is an S-shaped structure that includes a medial and a lateral limb. Within this subdivision there are two main types of cells: bipolar and multipolar cells. Inputs include direct projections from spherical bushy cells in the ipsilateral AVCN as well as indirect projections from globular bushy cells in the contralateral VCN through the MNTB (Grothe and Koch, 2011). This convergence of input is important for the localisation of high frequency sounds in the horizontal plane using interaural level differences (ILD). An additional input to the LSO includes that from the local MSO. Outputs of this structure include ascending projections to the NLL and IC on both sides of the brain (Schneiderman and Henkel, 1987).

Medial Superior Olivary Nucleus (MSO)

The MSO can be described as a small oval-shaped structure. It contains multipolar cells with dendrites that extend along the medial and lateral axis on either side of the cells (Hassfurth et al., 2010). Inputs to this structure include direct as well as indirect projections from spherical bushy cells in the ipsilateral and contralateral AVCN. Indirect inputs to the MSO are those through neighbouring LNTB and MNTB subdivisions respectively (Grothe and Koch, 2011). Outputs of the MSO include those to the ipsilateral dorsal NLL and the ventral IC. Because of the binaural sources of input, the MSO contributes to the localisation of low frequency sounds in the horizontal plane using interaural time differences (ITD).

Superior Paraolivary Nucleus (SPN)

The SPN is a circular structure. The SPN contains multipolar cells that are among the largest in the SOC. Sources of input to this structure includes octopus cells in the ipsilateral VCN and multipolar cells within the ipsilateral and contralateral PVCN, as well as the ipsilateral

MNTB (Friauf and Ostwald, 1988; Schofield, 1995). Targets of the SPN include the ipsilateral IC (Faye-Lund, 1986; Saldaña and Berrebi, 2000).

1.2.3 Nucleus of the Lateral Lemniscus (NLL)

The NLL is a fibrous structure that lies on the lateral edge of the brain and beneath the IC. It consists of two main divisions: the ventral division of the NLL (VNLL) and the dorsal division of the NLL (DNLL). This can be seen in Figure 1B (upper panel).

Ventral Nucleus of the Lateral Lemniscus (VNLL)

The VNLL contains mainly two cell types: bushy cells and multipolar cells (Merchán et al., 1988). These cells receive contralateral inputs primarily from octopus and multipolar cells within the VCN (Warr, 1982). Similar to the MNTB, there are Calyx of Held terminals within the ventral portion of the VNLL that are believed to originate from octopus cells in the CN (Malmierca et al., 1999a, 1999b). Other projections to the VNLL arise from the ipsilateral MNTB and SPN that target the dorsal portion of the VNLL (Grothe and Koch, 2011).

Interestingly, almost every single neuron in this subdivision projects to the ipsilateral ventral IC (Zhao and Wu, 2001). Because of this, it seems more than likely that the primary role of this subdivision is to act as a relay point for the ventral IC subdivision. However, this does not exclude the possibility of some level of processing occurring within the VNLL.

Dorsal Nucleus of the Lateral Lemniscus (DNLL)

In contrast to the VNLL, the DNLL receives bilateral inputs driven by both ears. This suggests a difference in function between the two subdivisions. While the VNLL may serve to relay information from the contralateral ear to the IC, the DNLL processes binaural cues for sound localisation (Grothe et al., 20011). There are two main cell types in this subdivision:

multipolar and small cells (Merchán et al., 1988). This structure is the target of projections from the contralateral VCN, LSO, and DNLL as well as the ipsilateral LSO, MSO, SPN and VNLL subdivisions (Kelly et al., 2009). The DNLL projects to both sides of the IC as well as the contralateral DNLL through the Commissure of Probst (Winer and Schreiner, 2005).

1.2.4 Inferior Colliculus (IC)

The IC, located in the midbrain, is a major auditory processing center. The IC receives diverse inputs from multiple brainstem sources and high structures. It is the primary source of input to the MG, which projects to the AC. The IC can be divided into three regions, including the central nucleus of the inferior colliculus (ICc), the external cortex of the inferior colliculus (ICx), and the dorsal cortex of the inferior colliculus (ICd). This can be seen in Figure 1B (upper panel).

Central Nucleus of the Inferior Colliculus (ICc)

The ICc receives input primarily from lower structures including the ipsilateral VNLL and MSO, the contralateral CN, and the DNLL and LSO on both sides of the brain (Beyerl, 1978). Differences exist in the location of these subcollicular terminals within the ICc. For example, afferents from the SOC end in the ventral portion of the ICc while afferents from the CN and DNLL end in the dorsal region of the ICc (Malmierca et al., 1999a, 1999b). The ICc also receives local inputs from the ICx and the ICd on both sides of the brain (Winer, 2005). Some direct inputs to the ICc from higher structures do exist, including a weak projection from the AC (Schofield, 2009). Targets of projections of the ICc include the ventral region of the MG on both sides of the brain. The ICc also provides weaker projections to the medial and dorsal regions of the MG as well as the contralateral IC (Malmierca and Merchán, 2005). As the ICc receives

inputs from almost all the important auditory areas, it plays a very important role in central auditory processing. It's noted that while the primary role of the ICc is auditory processing, the ICd and ICx contribute to other sensory systems as well (Winer and Schreiner, 2005).

External Cortex of the Inferior Colliculus (ICx)

The ICx is a superficial structure that is located in the lateral region of the IC and can be divided into 3 layers. The main sources of input to this structure include the ipsilateral MG, neighbouring ICc and ICd, and the AC on both sides of the brain (Malmierca et al., 1999a, 1999b). The ICx also receives weak projections from the NLL and cerebral cortex (Faye-Lund, 1985 Huffman and Henson, 1990; Herbert et al., 1991). The ICx projects to the medial and dorsal regions of the MG.

Dorsal Cortex of the Inferior Colliculus (ICd)

The ICd is divided into 4 layers (Faye-Lund and Osen, 1985). The function of the ICd is not yet been established. The main sources of input to this subdivision arise from the ipsilateral and contralateral AC (Bajo et al., 2007). Other sources of input include the ipsilateral ICx and ICc, contralateral IC, DNLL, SPN, and CN. The ICd projects to the dorsal region of the MG and ICc (Malmierca and Merchán, 2005).

1.2.5 Medial Geniculate Nucleus (MG)

The MG is a thalamic structure and is the last major structure before the AC in the ascending auditory pathway. This structure sends ipsilateral projections almost exclusively to the AC (Winer and Schreiner, 2005). The MG has three subdivisions i.e., the ventral division (MGv), the dorsal division (MGd), and the medial division (MGm). This can be seen in Figure 1B (lower panel).

Ventral Division of the Medial Geniculate Nucleus (MGv)

The MGv is the major source of input to the AC in the ascending pathway. The MGv receives inputs primarily from the ipsilateral ICc and a weak input from the contralateral ICc (González-Hernádez et al., 1991). The major output of this subdivision is to the ipsilateral AC (Winer and Schreiner, 2005). Much like the ICc, the MGv is mainly involved in auditory processing while the other auditory geniculate subdivisions are involved in the integration between inputs from auditory as well as other sensory systems (Bordi and LeDoux, 1994).

Medial Division of the Medial Geniculate Nucleus (MGm)

The MGm is the smallest of the three divisions of the MG and consists of a thin layer in the medial portion of the MG. The MGm has a wide range of ascending inputs including those from ICx, CN, SOC, and VNLL (LeDoux et al., 1987). This subdivision also receives descending input from the AC and reticular thalamic nucleus (Winer, 2005). The major source of output is the ICd, ICx, and AC (LeDoux et al., 1987; Winer, 1992).

Dorsal Division of the Medial Geniculate Nucleus (MGd)

The MGd is the major target of descending projections from the AC as well as ascending projections primarily from the ICd and to a lesser extent from the ICx (Winer, 2005). A feedback loop may exist between the MGd and the ICx, as the MGd does send projections to the ICx (Winer, 1992).

1.2.6 AC

The AC is part of the neocortex and is a thin structure that can be found on the dorso-lateral surface of the brain. The AC is believed to be involved in processing complex auditory stimuli that are novel in comparison to ambient noises (Gaese and Ostwald, 1995). It can be

divided into six layers, layers I through VI, of which each is anatomically and physiologically distinct from another. This can be seen in Figure 1B (lower panel).

Layers I-IV

Layer I is the most superficial layer and contains a very small number of neurons. The primary sources of input are those from the MGm and nearby cortical cells within the same layer (Winer, 1992; Winer and Schreiner, 2005). Layer II contains many small neurons that are pyramidal and non-pyramidal and project to neighbouring layers III and IV (Winer, 1992). Layer III also has pyramidal and non-pyramidal neurons. These neurons receive intrinsic connections from layer II in the ipsilateral AC. Other inputs to this layer include those from the contralateral AC as well as subcortical projections from the MGv. Among all the cortical layers, layer IV is the thinnest layer and contains densely packed non-pyramidal small neurons (Games and Winer, 1988). Layer IV is the target of projections from subcortical structures including the MGv as well as direct projections from layer II (Winer and Schreiner, 2005).

Layer V

Layer V is the thickest layer in the AC and can be characterised by the numerous pyramidal neurons with long apical dendrites perpendicular to the surface of the brain. Inputs to this layer are primarily local as dendrites from this layer can be found in layers III and IV. Due to the placement of these dendrites, layer V receives indirect projections from the MG as well (Huang and Winer, 2000).

There is some segregation in output among neurons within this layer. Large neurons with long apical dendrites that reach towards layer I project to the ICd and ICx on both sides of the brain. These neurons are present mostly in the deep region of the layer (Games and Winer, 1988). Small neurons located in the superficial region of this layer were found to project to the

contralateral AC, while medium-sized cells were found to project to both the AC and IC. Only pyramidal neurons have been found to project to the IC (Games and Winer 1988). Neurons in the most superficial and deepest regions of layer V project to the ipsilateral MGd and MGv (Winer and Prieto, 2001).

Layer VI

Neurons in layer VI can be either pyramidal or non-pyramidal in shape and are relatively small and densely packed (Schofield, 2009). Sources of input to the layer VI include the MGm (Winer and Schreiner, 2005). Neurons in this layer project almost exclusively to ipsilateral structures including the MGd and MGv as well as the ICd and ICx and possibly weakly to the ICc (Schofield, 2009). There are also targets in layer IV of the AC, the SOC and CN.

1.3 Ascending vs. descending auditory systems

The major central auditory structures form a complex network that is heavily interconnected. Within this network there are numerous projections that originate from a lower structure and target a higher structure. These projections are referred to as ascending projections. There are also projections originating from higher structures and targeting lower structures. These projections are referred to as descending projections. These pathways can become quite complex and intricate due to the high level of connectivity. Major ascending and descending projections can be seen in Figures 3A and 3B.

Ascending auditory pathways have been extensively studied compared to descending pathways. Major projections in the ascending pathway include those from the CN bilaterally to the SOC, NLL, and IC; the SOC to the ipsilateral IC; bilateral projections from the NLL to the IC; the IC bilaterally to the MG and; the MG ipsilaterally to the AC (Hutson and Morest 1996;

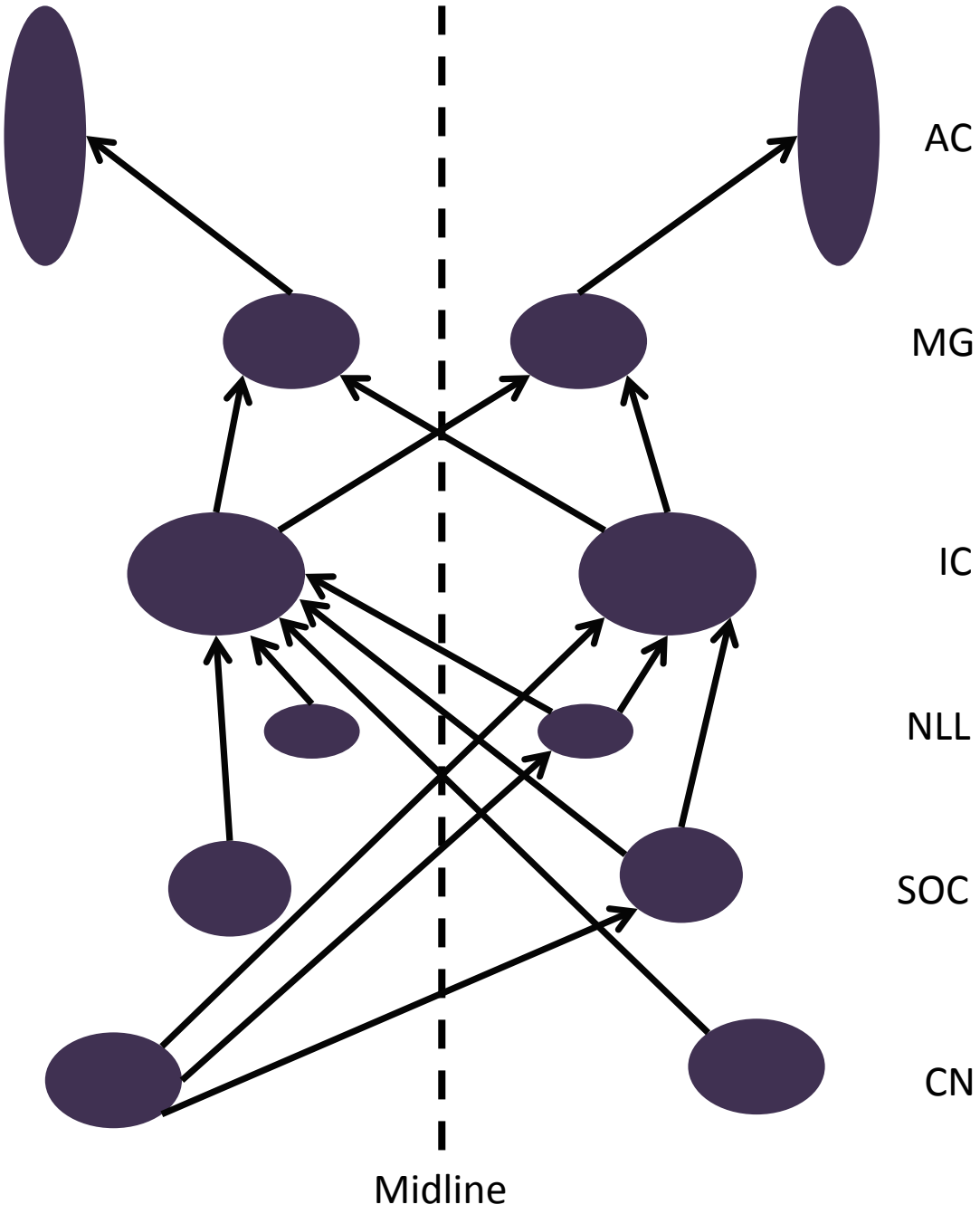

Figure 3A. Schematic representation of the major ascending projections in the central auditory system. Local and commissural connections have been omitted for clarity. [*Redrawn and modified from Winer and Schreiner 2005*]

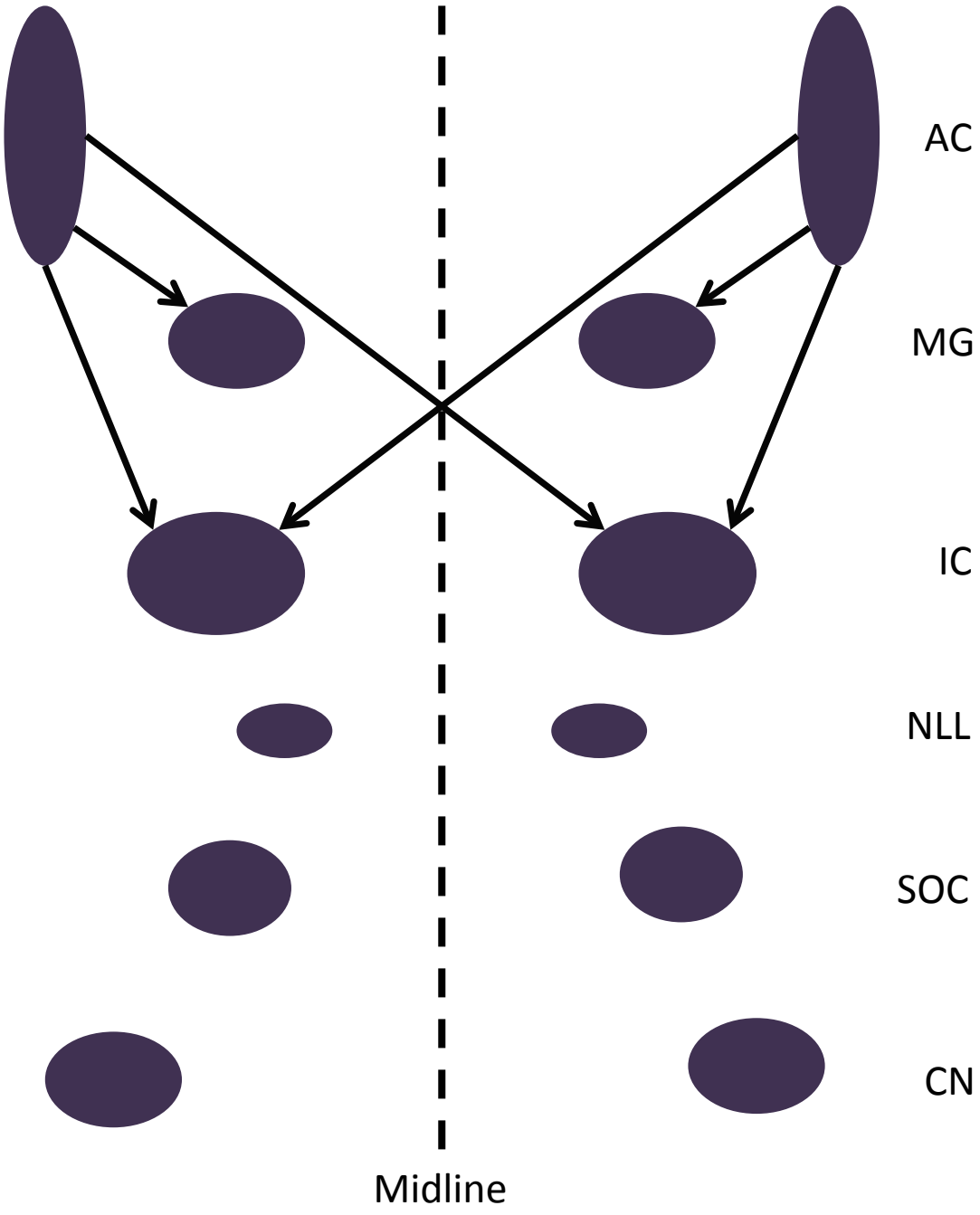

Figure 3B. Schematic representation of the major descending projections in the central auditory system. Local and commissural connections have been omitted for clarity. [*Redrawn and modified from Winer and Schreiner 2005*]

Friauf and Ostwald 1988; Gulick et al., 1989; Winer and Schreiner, 2005; Malmierca and Merchán, 2005).

The descending pathway consists primarily of corticofugal, or projections from the AC. The possible roles of these projections are include coordination and modulation of subcortical activity. Main descending projections include corticofugal projections that target the MG ipsilaterally and the IC on both sides of the brain (Schreiner and Winer, 2005; Schofield, 2009).

Other pathways in the auditory system include local intrinsic connections within the same subdivision and structure as well as commissural connections that cross the midline and connect the structure counterpart on the other side of the brain.

1.4 Major types of neurotransmission in the auditory system

The processing of acoustic information in the central auditory system is dependent on both excitatory and inhibitory neurotransmission. Major excitatory neurotransmitters in the central auditory system include glutamic acid (glutamate) and major inhibitory neurotransmitters include γ-aminobutyric acid (GABA) and glycine.

1.4.1 Glutamatergic neurotransmission

Glutamate is the most abundant excitatory neurotransmitter in the central nervous system (Silverthorn, 2007). Glutamate neurotransmitters are stored in the synaptic vesicles of pre-synaptic cells. Action potentials trigger glutamate release into the synaptic cleft. Receptors for glutamate are located post-synaptically and are activated through glutamate binding. These receptors can be either ionotropic or metabotropic. There are three major types of ionotropic glutamate receptors: α-amino-3-hydroxy-5-methyl-4-isoxazolepropionic acid (AMPA), N-Methyl-D-aspartic acid (NMDA), and kainate receptors (Silverthorn, 2007).

1.4.2 Glutamate receptors

AMPA- gated channels are permeable to sodium and potassium ions. When activated by glutamate, the channel opens to allow sodium ions to flow through the channel into the cell and potassium ions to flow out. The net effect of these ion influxes is cell membrane depolarization that results in an excitatory post-synaptic potential or EPSP. This EPSP has a fast time course.

NMDA- gated channels are permeable to calcium in addition to sodium and potassium ions. Activation by glutamate results in a net effect of excitation. The ion channel associated with an NMDA receptor is normally blocked by magnesium ions. This blockage can be removed by a depolarisation event caused by nearby AMPA receptors (Silverthorn, 2007). Increased calcium in a neuron upon NMDA receptor activation, can serve as a second messenger that triggers an intracellular cascade leading to an elevated excitability of the neuron. This neurophysiological change is known as long term potentiation. It has the ability to perpetuate its excitatory effect upon the post-synaptic cell for an extended period of time. Longterm potentiation is believed to play a major role in learning and memory (Silverthorn, 2007).

1.4.3 GABAergic neurotransmission

GABA is one of the main inhibitory neurotransmitters found in the central nervous system. In the central auditory system, it has been found that GABAergic neurotransmission contributes mostly to ascending pathways; as descending pathways are likely excitatory (Feliciano and Potashner, 1995). GABA is a product resulting from the removal of carbon dioxide from glutamate by the glutamate decarboxylase catalyst (Caspary et al., 1990).

GABA is stored in vesicles within pre-synaptic cells, which are usually interneurons (Silverthorn, 2007). Upon release, GABA can activate three main classes of receptors including

$GABA_A$, $GABA_B$, and $GABA_C$ receptors (Enna, 2001). Previous autoradiographical studies have found $GABA_A$ and $GABA_B$ receptors regionally in auditory structures in the rat including the brainstem, thalamus, and IC (Bowery et al., 1987; Charles et al., 2001; Milbrandt et al., 1994) as well as in other animals (big brown bat: Fubara et al., 1996; guinea pig: Juiz et al., 1994). While $GABA_A$ and $GABA_B$ receptors have been found in the auditory system, $GABA_C$ receptors are found primarily in the retina of vertebrae (Bormann and Feigenspan, 1995) and seem to play an important role in visual processing.

1.4.4 $GABA_A$ receptors

The $GABA_A$ receptor is an ionotropic receptor. The activation of a $GABA_A$ receptor opens an ion channel to allow chloride ions to flow inside the cell. Binding of the $GABA_A$ receptor by GABA produces a fast inhibitory response with a short time course preventing an action potential from occurring (Huang et al., 2006).

1.4.5 $GABA_B$ receptors

The $GABA_B$ receptor is a metabotropic receptor. It is indirectly connected to an ion channel by a guanine nucleotide-binding protein or G-protein (Chalifoux and Carter, 2011). The binding of a $GABA_B$ receptor by GABA activates the G-protein, leading to the opening of an ion channel (Silverthorn, 2007). Because its activation requires more steps, the activation of $GABA_B$ receptors has a relatively slower onset compared to that of $GABA_A$ receptors. This process can be seen in Figure 4, which illustrates the mechanism of activation of the $GABA_B$ receptor upon ligand binding.

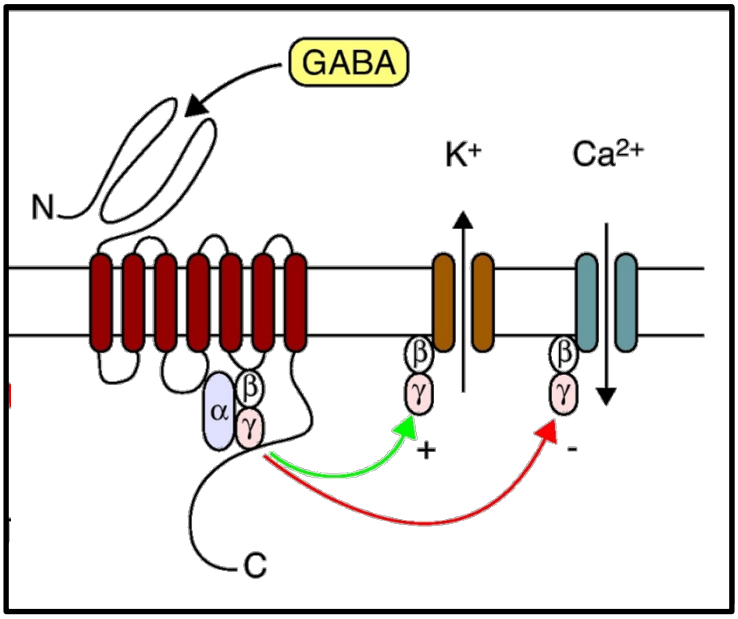

Figure 4. Mechanism of $GABA_B$ receptor activation. Binding of GABA to the $GABA_B$ receptor causes dissociation of G-proteins. The βγ subunits of the G-protein diffuse locally to open potassium channels and close calcium channels. [*Chalifoux and Carter 2011*]

$GABA_B$ receptors can be found both pre- and post-synaptically. Pre-synaptically, the activation of $GABA_B$ receptors can inhibit the release of GABA or glutamate neurotransmitters from nerve terminals (Kornau, 2006). Thus, activation of the $GABA_B$ receptor can result in a net excitatory or inhibitory effect on a post-synaptic cell depending on the neurotransmitter regulated by the pre-synaptic $GABA_B$ receptor. Post-synaptically, it produces a prolonged inhibition by activating K^+ channels to induce hyperpolarisation (Ulrich et al., 2007). Because of the ability to modulate the release of both excitatory and inhibitory neurotransmitters, the $GABA_B$ receptor has often been linked to function as a regulator, as seen previously in nociceptive as well as other nervous systems (Malcangio and Bowery, 1996). This inhibition is done by preventing calcium release through voltage-activated Ca^{2+} channels (López-Bendito et al., 2002). Additionally, it has a longer duration in effects and can contribute to long-term potentiation. Because of these characteristics, the $GABA_B$ receptor makes a unique contribution to neural processing.

$GABA_B$ receptor subunits

A functional $GABA_B$ receptor is a heterodimer consisting of one $GABA_BR1$ and one $GABA_BR2$ subunit. Both subunits share similar conformations and are about 30% identical in sequence (Pin et al., 2004). Each subunit protein contains a venus flytrap (VFT) module and a heptahelical domain (HD). The characterisation as well as proposed binding mechanism of the two receptor subunits can be seen in Figure 5.

The $GABA_BR1$ subunit has two well-documented splice variants, $GABA_BR1\alpha$ and $GABA_BR1\beta$, which are identical in structure except for the repeating sushi sequence on the N-terminal of the $GABA_BR1\alpha$ isoform (Huang et al., 2006). This difference has been attributed to a division of roles between the two subunits. It has been found that because of this extra sushi

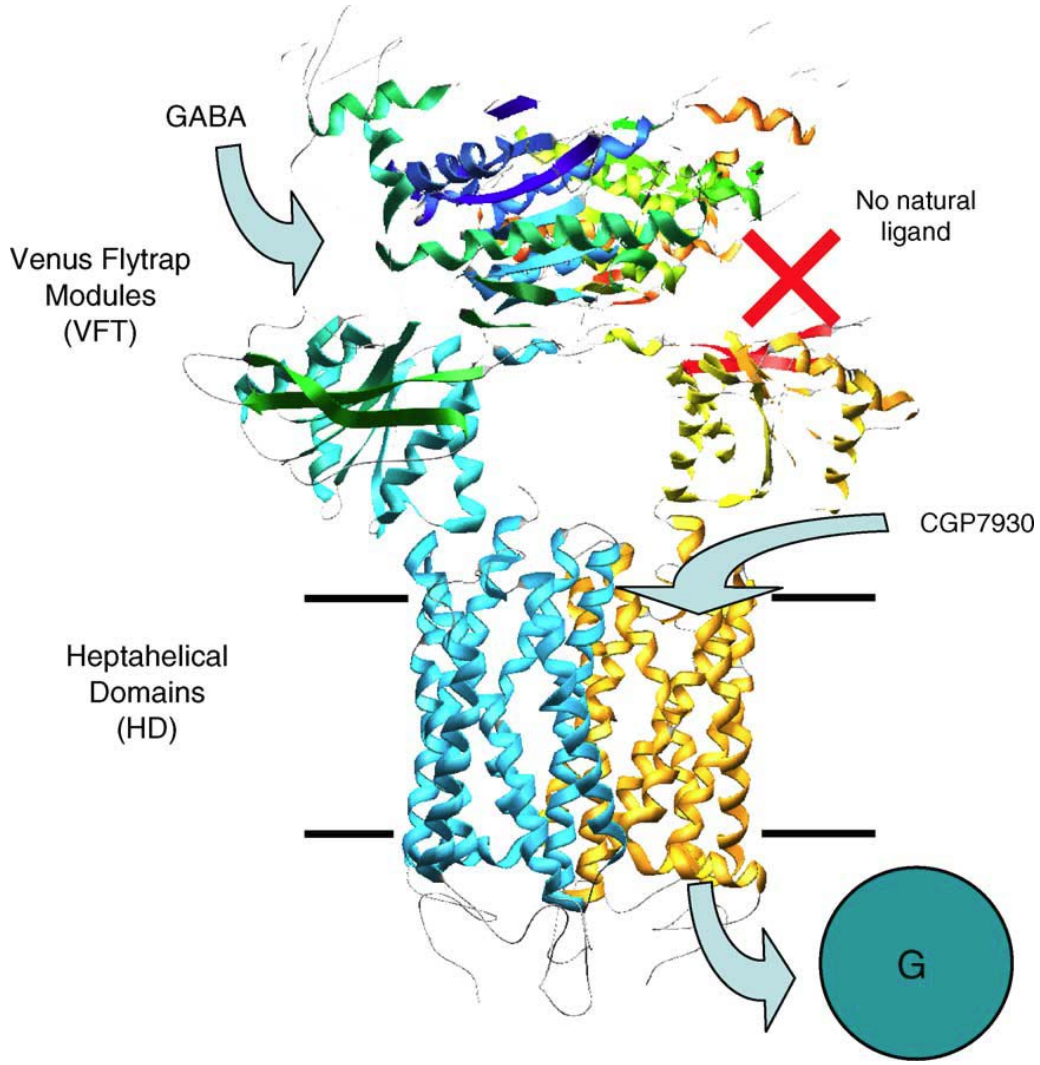

Figure 5. Binding structure of the $GABA_B$ receptor. Proposed binding structure between the $GABA_BR1$ and $GABA_BR2$ subunits in the formation of a functional $GABA_B$ receptor. The $GABA_BR1$ subunit is depicted on the left in blue. The $GABA_BR2$ subunit is depicted on the right in yellow. Each subunit is composed of a venus flytrap (VFT) module and a heptahelical domain (HD). The cleft of the VFT in the $GABA_BR1$ subunit binds GABA. The HD in the $GABA_BR2$ is involved in G-protein activation. These subunits have been found to interact directly at the level of the VFT in addition to the level of the HD. [*Pin et al. 2004*]

domain, the $GABA_BR1\alpha$ isoform is targeted towards pre-synaptic terminals to play a major role in the release of glutamate (Chalifoux and Carter, 2011). While both isoforms are present at the post-synaptic cell membrane, the $GABA_BR1\beta$ isoform in particular is necessary for a post-synaptic $GABA_B$ receptor as this splicing variant binds to potassium channels to allow the K^+ current to flow (Chalifoux and Carter, 2011).

Previous studies have suggested additional isoforms for $GABA_BR1$ and $GABA_BR2$ subunits, but little is known about their characteristics or functions. The $GABA_BR1$ subunit could have as many as 6 isoforms, $GABA_BR1(\alpha–f)$, while the $GABA_BR2$ is thought to have at least 3 isoforms, which have not been properly characterised (Enna, 2001). It is important to note that not all potential isoforms necessarily lead to functional receptors. For example, the $GABA_BR1e$ isoform is believed to bind to the $GABA_BR2$ subunit as a form of regulation. This is because binding between the $GABA_BR1e$ isoform and $GABA_BR2$ subunit does not lead to a functional receptor. This binding may limit the availability of the $GABA_BR2$ subunit to bind to other $GABA_BR1$ isoforms that may form a functional $GABA_B$ receptor (Enna, 2001).

Functionality of each $GABA_B$ receptor subunit

Variants of the $GABA_BR1$ and the $GABA_BR2$ subunits are formed in the endoplasmic reticulum (ER) (Ige et al., 2000). As part of a stringent trafficking sequence, the $GABA_BR1$ subunits remain within this structure due to a retention signal located on the protein (Restituito et al., 2005). The $GABA_BR2$ subunit is necessary for the release of the $GABA_BR1$ subunit from the ER as the $GABA_BR1$ and $GABA_BR2$ subunits assemble at the C terminal tail (Pin et al., 2004). This binding masks the retention signal, allowing the assembled heterodimer to migrate towards the plasma membrane (Restituito et al., 2005).

In order to study the function of both subunits in forming a functional receptor, previous studies have introduced mutations in order to modify specific shapes and/or sequences of each subunit. Altering or removing the retention signal in the $GABA_BR1$ subunit allows it to migrate to the cell surface however its presence alone will not be functional (Pin et al., 2004). This demonstrated the necessity of the $GABA_BR2$ subunit for proper assembly. The G-protein is believed to be associated with the HD of the $GABA_BR2$ subunit, which is necessary for receptor activation (Enna, 2001). Additionally, upon binding of the two receptor subunits, the $GABA_BR2$ subunit increases the affinity of the $GABA_BR1$ subunit for binding GABA (Pin et al., 2004). The $GABA_BR1$ subunit is also essential for a functional $GABA_B$ receptor as the GABA binding domain is located on the VFT module of the $GABA_BR1$ subunit (Enna, 2001).

1.4.6 Glutamatergic and GABAergic neurotransmission in the auditory system

All aforementioned neurotransmitters and receptors play different roles in neural processing in the central auditory system. Glutamate is the main excitatory neurotransmitter while GABA and glycine are inhibitory neurotransmitters. Previous researchers have tried to isolate the types of neurotransmission that mediate connections among neurons in auditory structures. Some key pathways are mentioned below.

Local GABAergic connections have been found in the DCN that project to neighbouring layers (Moore, 1996). Projections from the AVCN to the ipsilateral LSO have been found to be glutamatergic. The MSO receives excitatory input from the ipsilateral MNTB and LNTB and sends excitatory projections to the NLL (Grothe and Koch, 2011). The SPN sends projections to the IC that may be either GABAergic or glutamatergic in nature (Kulesza, 2000). The majority

of NLL neurons are GABA-positive. In addition, most neurons in the DNLL send GABAergic projections to the ipsilateral and contralateral IC (Wu and Kelly, 1985).

The MG is the target of GABAergic input from extrinsic sources such as the ICc and reticular thalamic nucleus. The MG also receives glutamatergic inputs from the ICc. A large portion of glutamatergic projections from the IC to the MG are from GABA-positive neurons (Malmierca and Merchán, 2005). While pyramidal neurons in the AC are likely the source of excitatory projections to subcortical structures, they are the target of GABAergic innervations by local neurons (Winer and Larue, 1989).

1.4.7 The $GABA_B$ receptor in the central nervous system

Previous studies have been conducted on the localisation and distribution of the $GABA_B$ receptor in the brain. Autoradiographical studies have found the $GABA_B$ receptor throughout the central nervous system (Bowery et al., 1987; Chu et al., 1990; Gehlert et al., 1985). One autoradiography study looked specifically at the auditory structures in the big brown bat (Fubara et al., 1996). Relatively high levels of $GABA_B$ receptor expression were found in the AC, MG, and the dorsal region of the IC while low levels of expression were found in the ventral region of the IC, NLL, SOC, and CN. Several other studies have used autoradiography to quantify the level of the $GABA_B$ receptor in specific auditory structures in the auditory system of the rat, as well as in other animals, and found similar distribution levels among these species (the guinea pig's CN: Juiz et al., 1994; the rat's IC: Mibrandt et al., 1994).

A previous immunohistochemical study examined the distribution of the $GABA_B$ receptor subunits throughout the rat's central nervous system (Charles et al., 2001). This study provided some insight into the distribution of the $GABA_B$ receptor subunits in the central

auditory system. Results from this study were consistent with those from autoradiography studies as high levels of expression were found in the MG and AC and intermediate levels were found in the IC. Other immunohistochemistry studies have found the $GABA_B$ receptor in the DCN and the MSO (Luján et al., 2004; Hassfurth et al., 2010).

Previous physiological studies have also supported the existence of the $GABA_B$ receptor in different structures of the central auditory system. These structures include the CN (Lim et al., 2000), the SOC (Isaacson, 1998; Sakaba and Neher, 2003; Yamauchi et al., 200), the IC (Faingold et al., 1989; Ma et al., 2002; Sun et al., 2006; Sun and Wu, 2009; Vaughn et al., 1996; Zhang and Wu, 2000), the MG (Peruzzi et al., 1997; Bartlett and Smith, 1999), and the AC (Buonomano and Merzenich, 1998; Metherate and Ashe, 1994; Bandrowski et al., 2001).

1.5 Objectives of my thesis research

$GABA_B$ receptors likely make important contributions to central auditory processing by regulating excitatory and inhibitory neurotransmitters from pre-synaptic terminals and by mediating inhibitory post-synaptic potentials. While previous studies have used immunohistochemical techniques to localise the $GABA_B$ receptor cellularly and sub-cellularly in certain structures of the rat's central nervous system (Panzanelli et al., 2004; Kulik et al., 2003; López-Bendito et al., 2002, Ige et al., 2000), knowledge about the level and distribution of the $GABA_B$ receptor in the central auditory system is yet to be advanced. This knowledge will allow for insight into the role of the receptor in auditory processing. Therefore, the major focus of my thesis research was to determine the levels and distributions of both the $GABA_BR1$ and $GABA_BR2$ subunits in major auditory structures and their subdivisions. I also wanted to find whether the two receptor subunits are co-localised in auditory neurons.

2 MATERIALS AND METHODS

2.1 Tissue preparation

Experiments were performed on adult male Wistar rats obtained from Charles River Laboratories Inc. (St. Constant, QC). All rats used were between 250 to 350 grams in weight and were housed in the Animal Quarters at the University of Windsor for at least 1 week prior to experimentation. The noise level in the Animal Quarters was about 55-60 decibels (dB) sound pressure level (SPL). Four rats were used for Western blotting procedures and thirteen rats were used for immunohistochemistry trials. All experimental procedures were approved by the University of Windsor Animal Care Committee and were in accordance with the guidelines of the Canadian Council on Animal Care.

2.2 Western blotting procedures

Western blotting procedures were used to ensure the specificity of primary antibodies for probing the $GABA_BR1$ and $GABA_BR2$ receptor subunits in rat neural tissue.

2.2.1 Tissue collection

A rat was euthanized with an overdose of pentobarbital (120 mg/kg) and the brain was extracted immediately. Tissue from the cerebellum and liver was collected into a single Eppendorf tube containing homogenization buffer and protease inhibitors (see appendices).

2.2.2 Sample preparation

The collected tissue was kept on ice and homogenised manually using a plastic pestle. The tissue homogenate was centrifuged at 3400 rpm for 20 minutes at 4°C to remove cell debris and nuclei. The supernatants were transferred into fresh Eppendorf tubes on ice and centrifuged at the same speed for an additional 10 minutes at 4°C. The protein content of the final

supernatant was determined using a Bradford assay (Sigma-Aldrich, Oakville, ON, Canada) and quantified using a Biomate5 spectrophotometer (Thermo Scientific, Surrey, UK).

2.2.3 Immunoblotting

Values obtained via the Bradford assay were used to prepare 100 μL samples containing 30 μg of protein in 4X sample buffer in excess homogenization buffer. The samples were loaded and separated using 10% sodium dodecyl sulphate-polyacrylamide gel electrophoresis (SDS-PAGE). The gel was transferred to a polyvinylidene fluoride PVDF membrane (PVDF)-Plus 0.45μm membrane (Osmonics Inc., Minnetonka, MN, USA) for 2 hours at 30V. The membrane was blocked with 3% bovine serum albumin (BSA) in Tris-buffered saline tween (TBST) (see appendices) and then incubated in primary antibody overnight. Following 3 washes in TBST, the membrane was incubated in secondary antibody for 2 hours and washed 3 additional times before detection using an enhanced chemiluminescence (ECL) kit (Pierce, Rockford, IL, USA). Images were acquired using an HD2 gel imaging system and AlphaEase digital analysis software (Alpha Innotech, CA, USA).

2.3 Immunohistochemistry

Immunohistochemistry was used to examine the cellular localisation and regional distribution of the $GABA_BR1$ and $GABA_BR2$ subunits in the auditory system. Two procedures were employed respectively for examinations of immunolabelling using light and fluorescence microscopy.

2.3.1 Tissue sample collection

The rat was euthanized with an overdose of pentobarbital (120 mg/kg) and transcardially perfused with 200 ml of 0.9% physiological saline followed by 400 ml of 4% paraformaldehyde (PFA) in 0.1M phosphate buffer (PB). After the brain was extracted, it was placed in a sucrose gradient (10%, 20%, and 30%) until it sank for cryoprotection. It was sectioned using a CM1050 S cryostat (Leica Microsystems, Heidelberg, Germany) in either the coronal or sagittal plane at a thickness of 30 μm. The sections were collected on SuperFrost Plus glass slides (Fisher Scientific, Pittsburg, PA, USA) for use in subsequent immunoreactions.

2.3.2 Immunohistochemical procedures for light microscopy

Slides were incubated in the primary antibody against either the $GABA_BR1$ or $GABA_BR2$ subunit in 0.1M phosphate buffer saline (PBS) containing 0.05% Triton and 5% normal donkey serum (NDS) overnight. After washes in 0.1M PBS, sections were placed in keepers with secondary antibody in 0.1M PBS containing 2% NDS at room temperature for 2 hours. After 3 additional washes in 0.1M PBS, slides were placed in ExtrAvidin®-peroxidase (E2886, 1:400, Sigma-Aldrich, Oakville, ON, Canada) in 0.1M PBS for 1.5 hours at room temperature. After further washes in 0.1M PBS, the probed subunit was visualised using 0.05% 3,3'-diaminobenzidine tetrahydrochloride (DAB, G3660, Sigma-Aldrich) in 0.1M PB with 0.12% H_20_2 as the substrate. The DAB reaction was terminated by immersing the slides in 0.1M PBS. The sections were dehydrated through an ethanol gradient (60%, 70%, 95%, 100%, and 100%) and cleared with xylene twice. The slides were mounted with Permount (SP-500, Fisher Scientific) and coverslipped. Sections were examined using a Leica CTR 6500 microscope and images were photographed using a DFC 425 digital camera (Leica Microsystems). For

presentation, images were adjusted for contrast and brightness with Photoshop CS4 Extended (Adobe Systems, San Jose, CA, USA).

2.3.3 Immunohistochemical procedures for fluorescence microscopy

Fluorescence microscopy was used to study the co-localisation of the $GABA_BR1$ and $GABA_BR2$ subunits in auditory neurons. Sections were incubated overnight in solution containing both primary antibodies against $GABA_BR1$ and $GABA_BR2$ subunits in 0.1M PBS with 0.05% Triton and 5% NDS. After 3 washes in 0.1 M PBS, slides were placed in secondary antibodies against the primary antibody of the $GABA_BR1$ subunit in 0.1M PBS with 2% NDS for 1 hour at room temperature. After another set of 3 washes, slides were placed in a keeper containing Alexa Fluor® 647 streptavidin conjugate (S21374, 1:500, Invitrogen, Burlington, ON, Canada) in 0.1M PBS for 45 minutes at room temperature. After 3 further washes in 0.1M PBS, slides were placed in the secondary antibody against the primary antibody of the $GABA_BR2$ subunit in 0.1M PBS with 2% NDS for 1 hour at room temperature. After another set of washes in 0.1M PBS, slides were exposed to Alexa Fluor® 568 streptavidin conjugate (S11226, 1:500, Invitrogen) in 0.1M PBS for 45 minutes at room temperature. The slides were mounted with Fluoromount (F4680, Sigma-Aldrich) and coverslipped. Sections were examined using a Leica CTR 6500 microscope and images were photographed using a DFC 380 FX digital camera (Leica Microsystems). Subunits tagged with the Alexa Fluor® 568 fluorophore were viewed using the Texas Red (TXR) filter cube and were pseudo-coloured red using Leica advanced fluorescence (AF) software (Leica Microsystems). Subunits tagged with the Alexa Fluor® 647 fluorophore were viewed using the far red Y5 filter cube and pseudo-coloured green. Co-localisation was indicated by yellow, a mixture of red and green when both channels were

superimposed on one another or merged. For presentation, images were adjusted for contrast and brightness with Photoshop CS4 Extended (Adobe Systems, San Jose, CA, USA).

2.4 Antibodies and control experiments

2.4.1 Antibodies

One primary antibody was used to target the $GABA_BR1$ subunit and one other primary antibody was used to target the $GABA_BR2$ subunit in the current study. The antibody used against the $GABA_BR1$ subunit was rabbit polyclonal $GABA_BR1$ antiserum (R-300, 1:1000, Santa Cruz Biotechnology Inc., Santa Cruz, CA). The antibody used against the $GABA_BR2$ subunit was affinity purified guinea-pig polyclonal $GABA_BR2$ antiserum (AB5394, 1:1000, Chemicon, Temecula, CA). Complete information regarding these primary antibodies can be found in Table 1. Two additional mouse monoclonal primary antibodies were used in Western blotting procedures for detecting Actin (MAB1501, 1:1000, Chemicon) and α-Tubulin (05-829, 1:1000, Chemicon) respectively.

Secondary antibodies used in Western blotting experiments were all conjugated to horse-radish peroxidase (HRP). Goat anti-rabbit IgG-HRP (sc-2004, 1:6000, Santa Cruz Biotechnology Inc.) and goat anti-guinea pig IgG-HRP secondary antibodies (AQ108, 1:6000, Chemicon) were used for probing $GABA_BR1$ and $GABA_BR2$ subunits respectively. Anti-mouse IgG (12-349, 1:5000, Santa Cruz Biotechnology Inc.) was used as a secondary antibody for probing α-Tubulin and Actin. For immunohistochemistry procedures, secondary antibodies for the $GABA_BR1$ and $GABA_BR2$ subunits included the biotinylated donkey anti-rabbit IgG (711-005-152, 1:400, Jackson ImmunoResearch Laboratories, Burlington, ON, Canada) and biotinylated donkey anti-guinea pig IgG (706-065-148, 1:400, Jackson ImmunoResearch Laboratories) respectively.

Table 1. Datasheet of primary antibodies used to detect $GABA_BR1$ and $GABA_BR2$ subunits.

Antibody	Anti-$GABA_BR1$	Anti-$GABA_BR2$
Format	Purified	Purified
Antibody Type	Polyclonal	Polyclonal
Host Species	Rabbit	Guinea Pig
Vendor	Santa Cruz Biotechnology	Chemicon (Millipore)
Target	amino acids 929-958 at the C-terminus	amino acids 42- 54 at the N-terminus
Molecular Size of the Subunit	100 and 130 kDa	120 kDa
Sequence of the Subunit	960 amino acids	941 amino acids

2.4.2 Control experiments

Experiments were done to ensure the specificity of the antibodies used against the $GABA_BR1$ and $GABA_BR2$ subunits. In order to make sure that the primary antibodies were specific to neural tissue, Western blots were run on tissues collected from the cerebellum and liver. Bands corresponding to the molecular weights of each subunit ($GABA_BR1$: 130kDa and 100kDa; $GABA_BR2$: 120kDa) should be seen in the lanes containing cerebellar tissue but absent in the lanes containing liver tissue as $GABA_B$ receptors have been found in the cerebellum and not in the liver (Charles et al., 2001). Actin bands were probed on the blot as an even loading control between the cerebellum and liver samples, as both structures contain Actin. α-Tubulin is found in brain tissue and not in liver tissue and serves as a positive control.

For immunohistochemistry procedures, the cerebellum was used as a positive control. Previous studies have revealed the existence and distribution of the $GABA_BR1$ and $GABA_BR2$ receptor subunits in the cerebellum (Charles et al., 2001; Ige et al., 2000). These distributions were compared with distribution levels of the receptor subunits obtained in this study. As a negative control, the primary antibody was replaced by 0.1M phosphate buffer saline (PBS). This ensured that the secondary antibody was unable to bind to tissue in the absence of primary antibody. No selective labelling was observed. For cases where immunofluorescence was used for detection of both antibodies within a single section, the order of the subunit exposed to the sequence of signal detection was alternated in order to remove any potential biases resulting from possible cross-reactivity.

2.5 Data analysis

2.5.1 Densitometry for immunohistochemistry procedures

Densitometry was used to assess the level of expression of the $GABA_BR1$ and $GABA_BR2$ receptor subunits in all the major auditory structures. For sections from different auditory structures, images were taken using the microscope (Leica Microsystems) under identical settings and were exported as tagged image file format (TIFF) files to evaluate densitometry values. Pixel intensities were obtained from the subdivisions of the AC, MG, IC, NLL, SOC, and CN using ImageJ software (National Institute of Health). Boundaries of the auditory structures and their subdivisions were made in reference to the Rat Brain Atlas in Stereotaxic Coordinates (Paxinos and Watson, 2007).

In the cerebellum, labelling is high in the molecular layer and absent in the white matter for both $GABA_B$ receptor subunits (Ige et al., 2000). Therefore, densitometry values from the molecular and white layers of the cerebellum obtained in this study were used as standards to calculate the relative level of $GABA_B$ receptor subunits in each auditory area within the same case. Furthermore, using the cerebellum as a standard allowed for comparisons across different cases as well. Relative expression levels within the same case were calculated using the following formula:

$$L = (Aud-Cw)/(Cm-Cw)$$

where L is the relative level of labelling in an auditory region,

Aud is the densitometry value of an auditory area,

Cw is the densitometry value of the white matter of the cerebellum, and

Cm is the densitometry value of the molecular layer of the cerebellum.

Values of L obtained by this equation were assigned scores of '+', '++', '+++', and '++++' when values were between 0-0.2, 0.2-0.4, 0.4-0.6, and 0.8-1.0, respectively (Jamal et al., 2011).

RESULTS

3.1 Specificity and effectiveness of the antibodies for the $GABA_BR1$ and $GABA_BR2$ receptor subunits

3.1.1 Specificity and effectiveness of the antibody for the $GABA_BR2$ receptor subunit

Collaborating Western blotting experiments from a previous colleague confirmed the specificity of the primary antibody used to probe the $GABA_BR2$ subunit (Jamal et al., 2011). A single band at 110 kDa can be seen in the lane containing cerebellar tissue but not in the lane containing liver tissue (Figure 6A, upper panel) confirming previous findings (Charles et al., 2001). In addition, the signal of Actin in each lane was equal, confirming even sample loading (Figure 6A, middle panel). Our results also indicated that α-Tubulin can serve as a selective control for brain tissue as a band was present in the lane containing brain tissue (cerebellum) but absent in the lane containing liver tissue (Figure 6A, lower panel).

Immunohistochemistry trials conducted in seven independent cases (i.e. seven animals) further corroborated the specificity of the primary antibody against the $GABA_BR2$ subunit. $GABA_BR2$ subunit immunoreactivity in the cerebellum was high in the molecular layer, moderate in the granule cell layer, and absent in the white matter (Figure 6B). Distinctly labelled Purkinje cells were seen in between the molecular and granule cell layers. These results were in

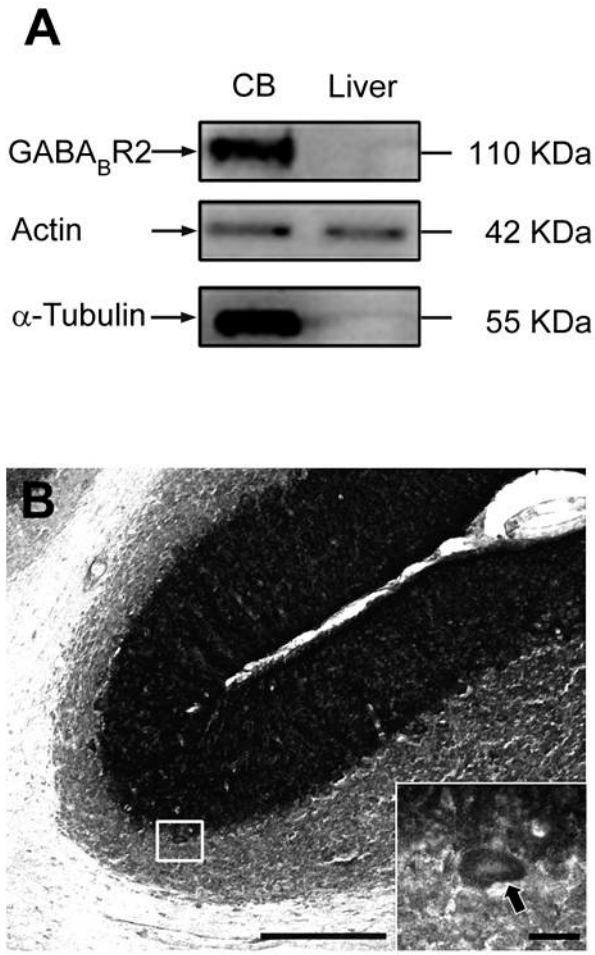

Figure 6. Immunoreactivity to the $GABA_BR2$ subunit antibody in the cerebellum**.** (A) Western blots revealing $GABA_BR2$ subunit antibody immunoreactivity in the cerebellum and the liver (top panel). Actin is used as a general loading control (middle panel) and α-Tubulin is used as a brain tissue-specific loading control (lower panel). (B) Immunoreactivity to the $GABA_BR2$ subunit in a coronal section of the cerebellum showing molecular, Purkinje cell, and granule cell layers and white matter. Inset in (B) shows a labelled soma of a Purkinje cell as well as adjacent areas in the molecular and granule layers. Arrow with white outline points toward a labelled Purkinje cell. Scale bars: 200 μm in the low magnification image; 20 μm in the inset. [*Jamal et al. 2011*]

agreement with previous findings (Ige et al., 2000). No labelling was seen in sections when the primary antibody was replaced by 0.1M PBS.

Therefore, Western blotting and immunohistochemical results confirmed that the primary antibody used in this study was effective and specific for detecting the $GABA_BR2$ subunit in the rat's neural auditory structures.

3.1.2 Specificity and effectiveness of the antibody for the $GABA_BR1$ receptor subunit

Western blotting experiments confirmed the specificity of the primary antibody used for detecting the $GABA_BR1$ subunit. Two bands at 130 kDa and 100 kDa can be seen in the lane containing cerebellar tissue but not in the lane containing liver tissue (Figure 7A, upper panel). This result is consistent with those reported in previous literature regarding molecular weights of the $GABA_BR1\alpha$ and $GABA_BR1\beta$ isoforms (Panzanelli et al., 2004). In addition, the level of Actin in each lane was equal, confirming even sample loading (Figure 7A, middle panel). α-Tubulin can serve as selective control for neural tissue as a band was present in the lane containing cerebellum and absent in the lane containing liver (Figure 7A, lower panel).

Immunohistochemistry in four individual cases (i.e. four animals) further confirmed the specificity of the antibody. $GABA_BR1$ subunit immunoreactivity in the cerebellum was high in the molecular and granule cell layers, and was almost absent in the white matter (Figure 7B). Numerous densely labelled Purkinje cells were labelled between the molecular and granule cell layers and were even stronger in immunoreactivity to the $GABA_BR1$ subunit. This result was in agreement with previous findings (Ige et al., 2000). Furthermore, no labelling was seen in sections run with 0.1M PBS in place of the primary antibody against the $GABA_BR1$ subunit. Thus, Western blotting and immunohistochemical results demonstrated that the antibodies used

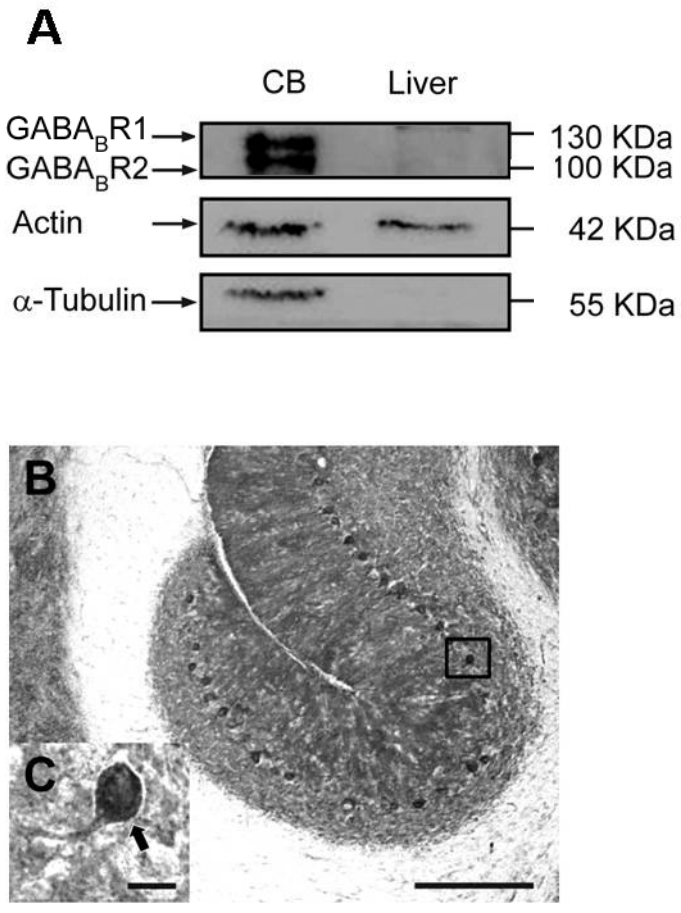

Figure 7. Immunoreactivity to the $GABA_BR1$ subunit antibody in the cerebellum. (A) Western blots revealing $GABA_BR1$ subunit antibody immunoreactivity in the cerebellum and the liver (top panel). Actin is used as a general loading control (middle panel) and α-Tubulin is used as a brain tissue-specific loading control (lower panel). (B) Immunoreactivity to the $GABA_BR1$ subunit in a coronal section of the cerebellum showing molecular, Purkinje cell, and granule cell layers and white matter. Inset in (B) shows a labelled soma of a Purkinje cell as well as adjacent areas in the molecular and granule layers. Arrow with white outline points toward a labelled Purkinje cell. Scale bars: 200 μm in the low magnification image; 20 μm in the inset.

in this study were effective and specific for detecting the $GABA_BR1$ subunit in the rat's neural auditory structures.

3.2 The level and distribution of the $GABA_BR2$ receptor subunit in the rat's central auditory system

3.2.1 The level of the $GABA_BR2$ receptor subunit in major central auditory structures

Overall levels of the $GABA_BR2$ receptor subunit were compared among auditory structures using coronal and sagittal sections. For five of the seven animals, the brain was sectioned in the coronal plane. For the other two of the animals, the brain was sectioned in the sagittal plane.

Figure 8 shows low magnification images of four sections obtained from one single animal. These sections were corresponding to plates 83, 105, 118, and 123 in The Rat Brain Atlas in Stereotaxic Coordinates (Paxinos and Watson, 2007). The first section contains the AC and MG (Figure 8, upper left panel), the second section contains the IC and NLL (Figure 8, upper right panel), the third section contains the SOC and AVCN (Figure 8, lower left panel), and the fourth section contains the DCN and PVCN (Figure 8, lower right panel). These sections indicate that the immunoreactivity to the antibody against the $GABA_BR2$ receptor subunit was high in the AC and MG, moderate in the IC and low in the NLL and SOC and CN.
Sections from the same animal but at rostrocaudal locations other than plates 83, 105, 118, and 123 in The Rat Brain Atlas in Stereotaxic Coordinates (Paxinos and Watson, 2007) were also used to conduct immunohistochemical experiments. Immunolabelling by the antibody against the $GABA_BR2$ subunit was analysed in these additional sections. Results from these additional

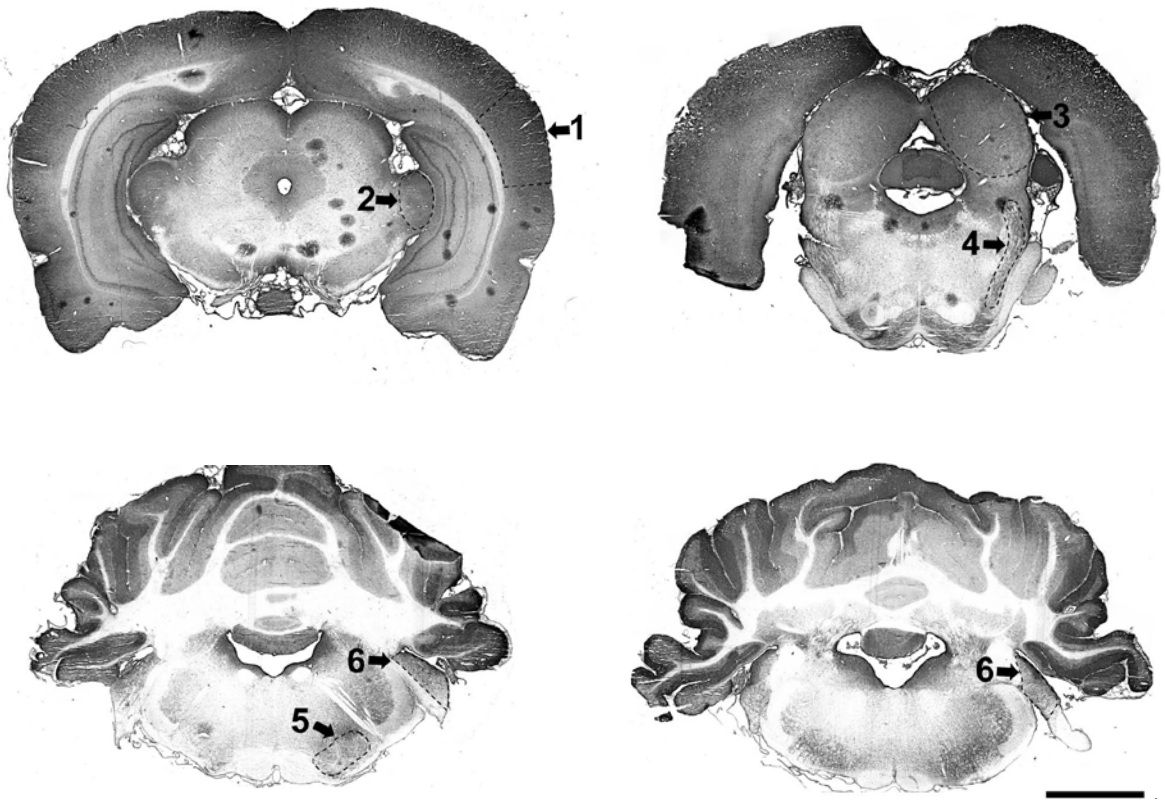

Figure 8. Low magnification images showing immunoreactivity to the $GABA_BR2$ subunit in auditory structures in coronal sections. Upper left panel contains the auditory cortex (AC, 1) and the medial geniculate nucleus (MG, 2). Upper right panel contains the inferior colliculus (IC, 3) and the nucleus of the lateral lemniscus (NLL, 4). Lower left panel contains the superior olivary complex (SOC, 5) and anterior cochlear nucleus (CN, 6). Lower right panel contains the posterior CN (6). Scale bar: 2500 μm

sections (not shown) confirmed those from plates 83, 105, 118, and 123. Scores obtained were used to corroborate the scores obtained from the set of sections presented in Figure 8.

Densitometry scores were obtained from individual auditory areas in the 5 coronal cases. A score of labelling is given by using the densitometry value (see section 2.5.1 for method). Scores from all the auditory areas are presented in Table 2. Based on the scores obtained, the level of labelling was the highest in the DCN, dorsal IC, MG, and the superficial layers of the AC, and the lowest in the SOC, and NLL. Moderate scores were found in the ventral IC and VCN.

Two cases were sectioned in the sagittal plane. Results revealed that the $GABA_BR2$ subunit was labelled in all the major auditory structures. Figure 9 shows low magnification images of two sections from a single case, with the IC presented in Figure 9A and the MG and CN presented in Figure 9B. Results from these sagittal sections regarding the immunoreactivity to the $GABA_BR2$ subunit are consistent in findings from coronal sections. Labelling was dense in the entire MG. In the CN, labelling was high in the DCN and moderate in the anterior and posterior regions of the VCN. In the IC, labelling was moderate in the ventral region where the ICc is located. High levels of labelling were observed in the rostral and caudal edges as well as the dorsal region. These regions are where the ICx and ICd are located respectively.

In the following subsections, I will present immunohistochemical results from a single case regarding the regional distribution and cellular localisation of the $GABA_BR2$ receptor subunit in major central auditory structures (Figures 10 through 15). Results from this case were confirmed by results obtained by the four other cases.

Table 2. Densitometry scores of the $GABA_BR2$ subunit in the auditory structures. Densitometry values of immunoreactivity in auditory structures to the $GABA_BR2$ subunit as revealed by immunohistochemical labelling and densitometry analysis (n=5). [*Jamal et al. 2011*]

Auditory structure	Subdivision	Densitometry value
AC	Layer I	+++
	Layers II/III	++++
	Layer IV	+++
	Layer V	+++
	Layer IV	++
MG	MGd	+++
	MGv	+++
	MGm	+++
IC	ICc	++
	ICd	++++
	ICx	+++
NLL	DNLL	+
	Dorsal VNLL	++
	Ventral VNLL	+
SOC	LSO	++
	MSO	++
	SPN	+
	LNTB	++
	VNTB	++
	MNTB	+
CN	DCN molecular/fusiform cell layers	++++

	DCN Deep layers	++
	GCD	++++
	AVCN	++
	PVCN	++
CB	Molecular/Purkinje cell layers	++++
	Granule cell layer	++
	White matter	-

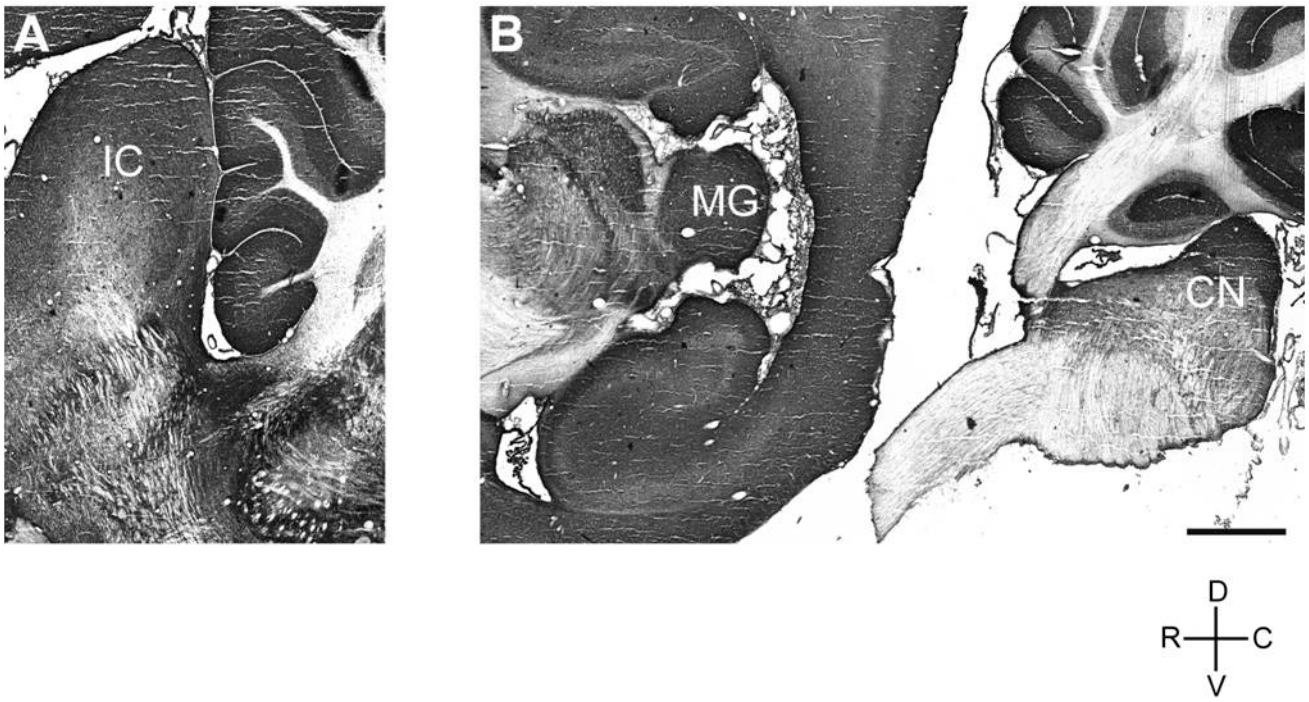

Figure 9. Immunoreactivity to the $GABA_BR2$ subunit in a parasagittal section with the inferior colliculus (IC, A) and a parasagittal section with the medial geniculate nucleus (MG, B) and the cochlear nucleus (CN, B). Scale bar: 1000 μm. The cross symbol below (B) indicates the orientation of sections. R: rostral; C: caudal; D: dorsal; V: ventral. [*Jamal et al. 2011*]

3.2.2 Regional and cellular distribution of the $GABA_BR2$ subunit

Cochlear Nucleus (CN)

Overall, the CN was moderately labelled by the antibody against the $GABA_BR2$ subunit (Figure 10A and 10B). The lateral edge of the DCN was heavily labelled. In particular, the neuropil (i.e., dendrites and axons around cell bodies) and cell bodies of the molecular layer and GCD were highly immunoreactive to the antibody for the $GABA_BR2$ subunit (Figures 10A, 10C, and 10D). In contrast, in the deeper layers, labelling of the neuropil was much lighter. Labelling was localised primarily to possible pyramidal and fusiform cells. In the PVCN (Figure 10A) and AVCN (Figure 10B), overall labelling was moderate with punctate labelling both on somata and in neuropil. Cell bodies resembling globular bushy, octopus, and multipolar cells were labelled in the PVCN (Figure 10E). Presumable spherical and globular bushy cells in the AVCN were also labelled (Figure 10F). In the AVCN, some large immunoreactive neurons had a fainter labelled outline surrounding the cell (Figure 10F). These outlines could suggest the possible existence of Calyx of Held synapses. This will be further discussed in section 4.1.4.

Superior Olivary Complex (SOC)

Each subnucleus of the SOC was immunoreactive to the $GABA_BR2$ subunit to a certain extent (Figure 11A). The MNTB had an overall low level of labelling due to light neuropil immunoreactivity as well as an abundance of fibres that reside on the medial side. Cells within this region were distinctly labelled (Figure 11B). Like in the AVCN, some neurons with a faint outline indicative of a possible Calyx of Held were observed in the MNTB. The SPN also had a low overall $GABA_BR2$ subunit density due to light punctate neuropil labelling (Figure 11C). Unlike neurons in the other subnuclei of the SOC, the SPN has relatively large neurons with thick dendrites clearly labelled. The LSO demonstrated a moderate level of labelling (Figure

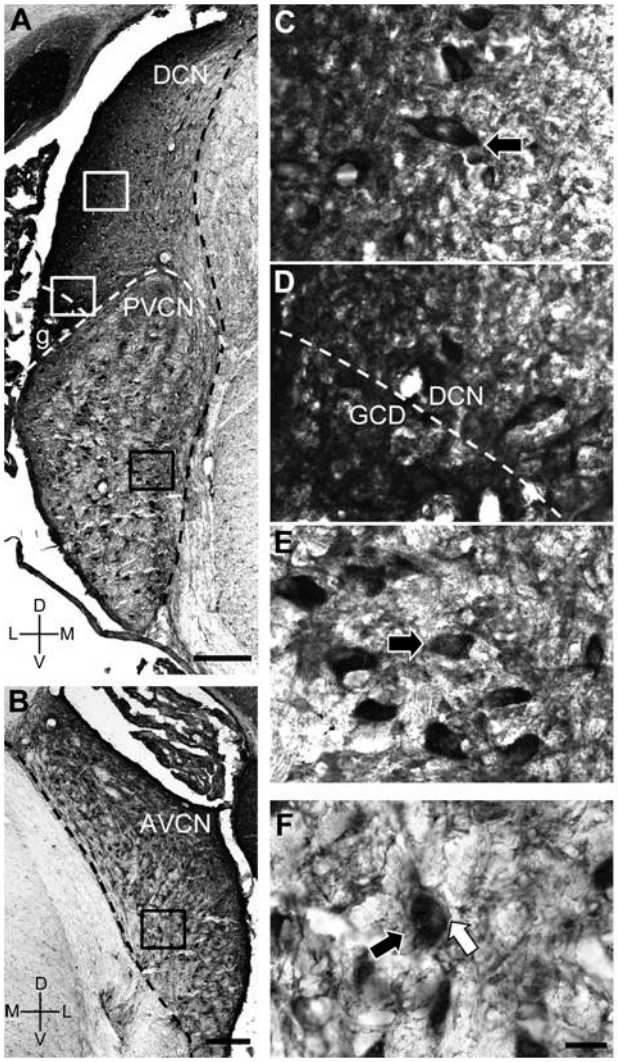

Figure 10. Immunoreactivity to the $GABA_BR2$ subunit in the cochlear nucleus (CN). Low magnification images show labelling in the caudal CN (A, with DCN, GCD, and PVCN) and the rostral CN (B, with AVCN). "g" indicates the GCD. High magnification images show labelling in areas in the DCN (C), GCD along with ventral DCN (D), PVCN (E), and AVCN (F). Dashed curves in (A), (B), and (D) indicate boundaries of subdivisions in the CN. Black arrows with white outlines point toward labelled cell bodies. The white arrow with a black outline in (F) points toward a weakly labelled area surrounding a cell body. Scale bars: 200 μm in (A, B); 20 μm in (C-F). The cross symbols in (A, B) indicate the orientation of sections. L: lateral; M: medial; D: dorsal; V: ventral. [*Jamal et al. 2011*]

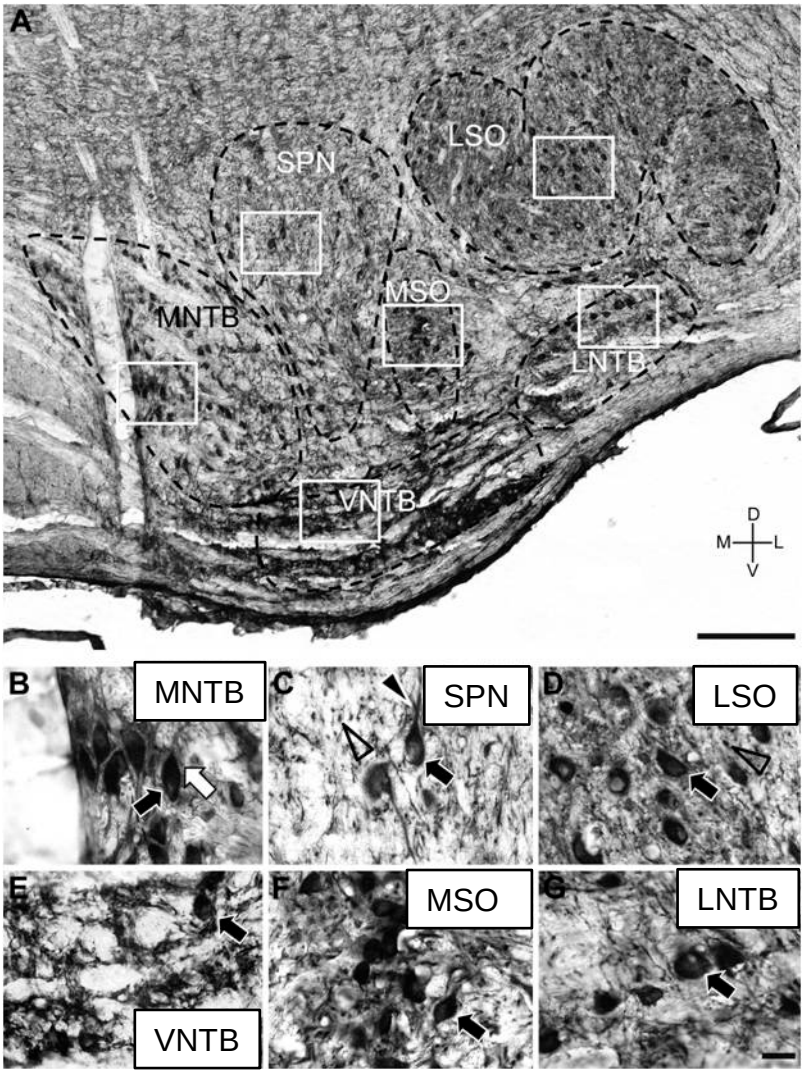

Figure 11. Immunoreactivity to the $GABA_BR2$ subunit in the superior olivary nucleus (SOC). Low magnification image shows labelling in the entire SOC (A). High magnification images show labelling in areas in the MNTB (B), SPN (C), LSO (D), VNTB (E), MSO (F), and LNTB (G). Enclosed dashed curves indicate subdivisions of the SOC. Black arrows with white outlines point toward labelled cell bodies. A black arrowhead with a white outline in (C) points toward a labelled dendrite. Black open arrowheads in (C, D) point towards labelled puncta. A white arrow with a black outline in (B) points towards a weakly labelled area surrounding a labelled MNTB cell. Scale bars: 200 μm in (A); 20 μm in (B–G). The cross symbol in (A) indicates the orientation of the section. L: lateral; M: medial; D: dorsal; V: ventral. [*Jamal et al. 2011*]

11D). Cells and neuropil in the lateral and medial limbs of the LSO were clearly labelled. The labelled neuropil revealed its structural boundaries. Labelling in the VNTB consisted of relatively strong neuropil labelling with possible immunoreactive cells (Figure 11E). The MSO demonstrated a moderately light immunoreactivity to the $GABA_BR2$ subunit (Figure 11F). Distinctively labelled multipolar cells were lined along the middle of this structure including associated axons. Both somata and neuropil were labelled in a punctate distribution. The LNTB had moderately labelled cells and surrounding neuropil (Figure 11G).

Nucleus of the Lateral Lemniscus (NLL)

The NLL appeared to have an overall low level of immunoreactivity to the $GABA_BR2$ subunit (Figure 12A). This appeared to be partly due to the abundance of fibres in this region. The presence of fibres affected the labelling in the DNLL the most among all the subareas of the NLL (Figure 12B). In between fibres, the DNLL had somewhat relatively dense labelling in the somata and neuropil. The dorsal region of the VNLL had a relatively high level of immunoreactivity and cell packing density (Figure 12C). The somata and neuropil of the DNLL and dorsal VNLL were labelled relatively more densely compared to the ventral region of the VNLL. The ventral region of the VNLL contained labelled cells however the neuropil was the lightest in all the three regions (Figure 12D).

Inferior Colliculus (IC)

There were differences in the distribution of $GABA_BR2$ subunit immunoreactivity within the three subdivisions of the IC (Figure 13A). The ICd and ICx were densely labelled in contrast to the moderately labelled ICc. In the ICd, both neuropil and cell body were heavily labelled (Figure 13B). Within the ICx, differences existed in the level of labelling, revealing three layers of the structure (Figure 13D). The second layer displayed moderate labelling in the neuropil and

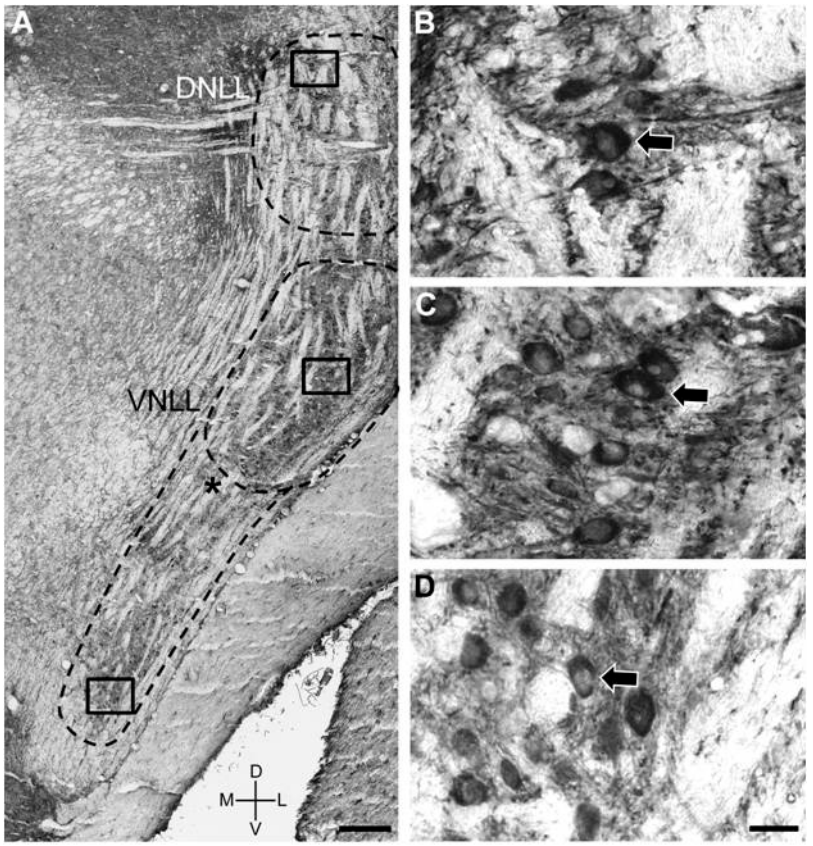

Figure 12. Immunoreactivity to the $GABA_BR2$ subunit in the nucleus of the lateral lemniscus (NLL). Low magnification image shows labelling in the entire NLL (A). High magnification images show labelling in areas in the DNLL (B), dorsal part of the VNLL (C), and ventral part of the VNLL (D). Dashed curves indicate subdivisions of the NLL. Within the VNLL, the dashed curve with an asterisk indicates the boundary between the dorsal and the ventral regions of the VNLL. Black arrows with white outlines point towards labelled cell bodies. Scale bars: 200 μm in (A); 20 μm in (B–D). The cross symbol in (A) indicates the orientation of the section. L: lateral; M: medial; D: dorsal; V: ventral. [*Jamal et al. 2011*]

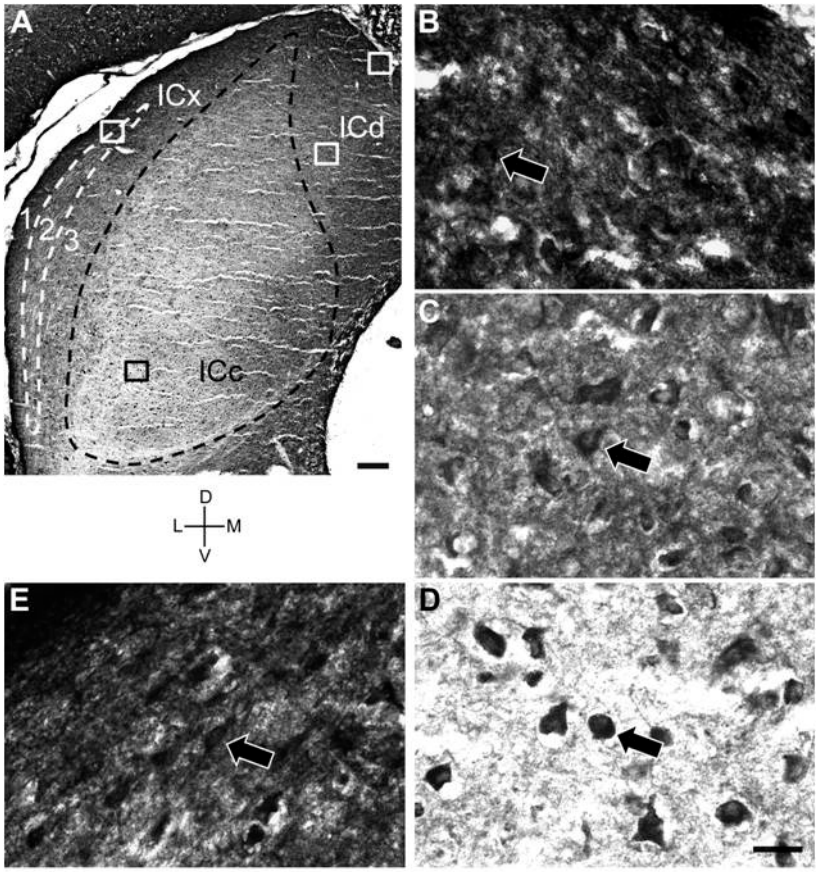

Figure 13. Immunoreactivity to the $GABA_BR2$ subunit in the inferior colliculus (IC). Low magnification image shows labelling in the entire IC (A). High magnification images show labelling in areas in the dorsal part of the ICd (B), the border region between the ICd and the ICc (C), the ventral part of the ICc (D), and layers I and II of the ICx (E). Dashed curves indicate subdivisions of the IC as well as layers in the ICx. Numbers in the ICx indicate layers. Black arrows with white outlines point toward labelled cell bodies. Scale bars: 200 μm in (A); 20 μm in (B–E). The cross symbol below (A) indicates the orientation of the section. L: lateral; M: medial; D: dorsal; V: ventral. [*Jamal et al. 2011*]

somata in contrast to the high levels of expression in the first and third layers. Labelling in the ICc was the lowest in the three subdivisions, with relatively weaker neuropil labelling but strong cell body labelling (Figure 13E).

A gradient existed in the level of labelling between the ICd and ICc. In between these two structures, there was a gradual decrease of neuropil labelling along the dorsomedial to ventrolateral axis (Figure 13C). While the ICd was heavily labelled, and the ICc was moderately labelled, the dorsal region of the ICc bordering the ICd was of intermediate immunoreactivity. Between the ICc and ICx, there seemed to be a more defined boundary separating the two subdivisions.

Medial Geniculate Nucleus (MG)

Distribution of the $GABA_BR2$ subunit appeared to be homogenous across all subdivisions of the MG (Figure 14A). In the MGd, somata and neuropil were densely labelled with a cluster of cells clearly seen in the dorsal cap region (Figure 14B). In the rest of the MGd, as well as the MGv, strong labelling was seen in cell bodies and neuropil (Figure 14B and 14C). The MGm contained large highly immunoreactive cell bodies (Figure 14D).

Auditory Cortex (AC)

The AC displayed a laminar distribution in the immunoreactivity to the $GABA_BR2$ subunit (Figure 15A). Layer I appeared moderately labelled with small neurons labelled along with numerous fibres (Figure 15B). Layers II and III shared similar distributions and displayed the highest neuropil immunoreactivity in all the six layers of the AC. Clusters of pyramidal neurons and their apical dendrites as well as non-pyramidal neurons within this layer were labelled (Figure 15C and 15D). The neuropil in layer IV was labelled at a similar level to neuropil in layer I (Figure 15E). Labelled fibres perpendicular to the lateral surface of the AC

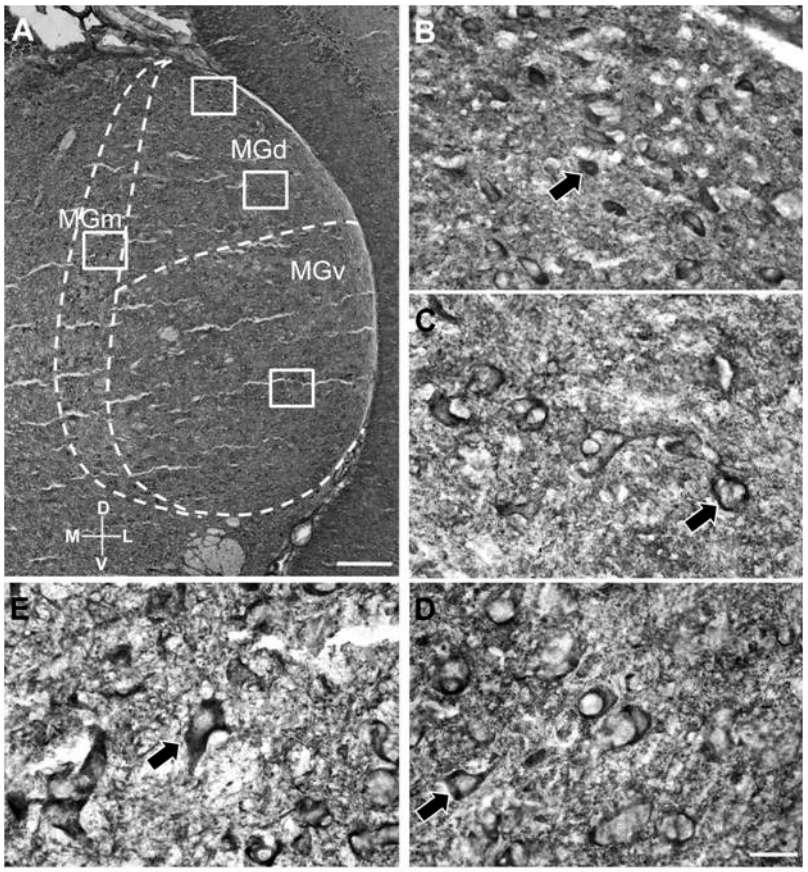

Figure 14. Immunoreactivity to the $GABA_BR2$ subunit in the medial geniculate nucleus (MG). Low magnification image shows labelling in the entire MG (A). High magnification images show labelling in the dorsal part of the MGd (B), ventral part of the MGd (C), MGv (D), and MGm (E). Dashed curves indicate subdivisions of the MG. Black arrows with white outlines point toward labelled neurons. Scale bars: 200 μm in (A); 20 μm in (B–E). The cross symbol in (A) indicates the orientation of the section. L: lateral; M: medial; D: dorsal; V: ventral. [*Jamal et al. 2011*]

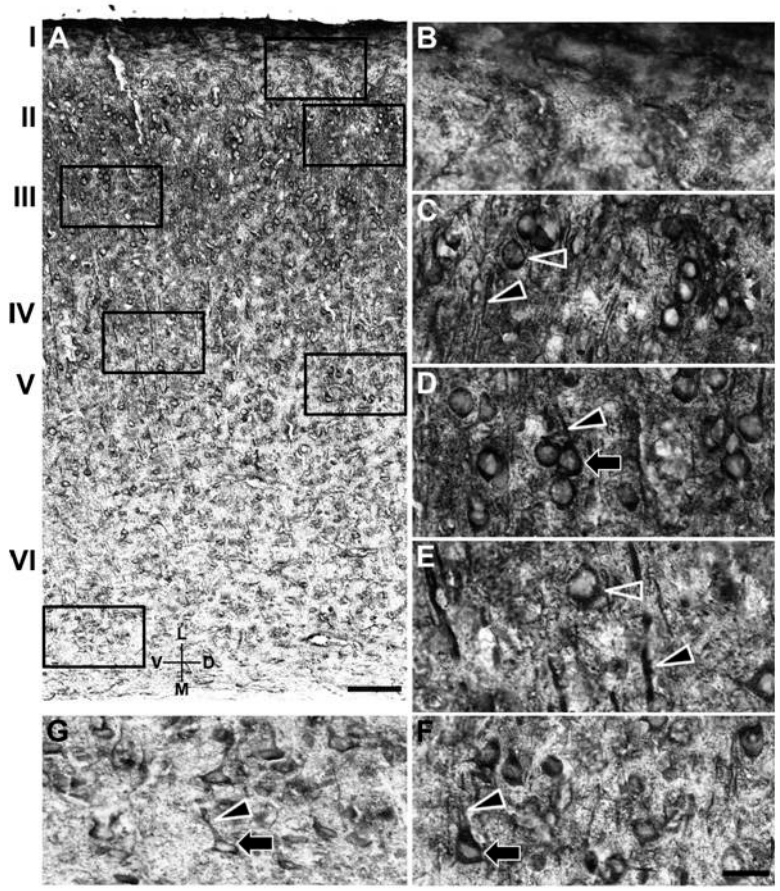

Figure 15. Immunoreactivity to the $GABA_BR2$ subunit in the auditory cortex (AC). Low magnification image shows labelling across six cortical layers (A). High magnification images show labelling in layers I through VI (B–G), respectively. Black arrows with white outlines point toward labelled pyramidal neurons. White open arrowheads point toward labelled non-pyramidal neurons. Black arrowheads with white outlines point toward labelled dendrites. Layers of the AC are indicated on the left side of (A). Scale bars: 100 μm in (A); 50 μm in (B–G). The cross symbol at the bottom of (A) indicates the orientation of the section. L: lateral; M: medial; D: dorsal; V: ventral. [*Jamal et al., 2011*]

and not associated with any particular neuron within this layer were also seen. These fibres are likely from pyramidal neurons in the layers V and VI of the auditory cortex. The neuropil in layer V was not as strongly labelled as the superficial layers (Figure 15F). Neuropil within layer VI had the lowest immunoreactivity of the six layers, although labelled pyramidal and non-pyramidal neurons could be seen (Figure 15G). Pyramidal neurons in layers V and VI had labelled dendrites perpendicular to the lateral surface of the AC that extended towards superficial layers.

3.3 The level and distribution of the $GABA_BR1$ receptor subunit and the co-localisation of this subunit with the $GABA_BR2$ subunit

3.3.1 The level of the $GABA_BR1$ receptor subunit in major central auditory structures

Overall levels of the $GABA_BR1$ receptor subunit was studied in major auditory structures using coronal sections collected from four separate animals. The four sections presented in Figure 16 were obtained from one single case. These sections were corresponding to plates 83, 105, 118, 123 in The Rat Brain Atlas in Stereotaxic Coordinates (Paxinos and Watson, 2007). The first section contains the AC and MG (Figure 16, upper left panel), the second section contains the IC and NLL (Figure 16, upper right panel), the third section contains the SOC and AVCN (Figure 16, lower left panel), and the fourth section contains the DCN and PVCN (Figure 16, lower right panel). Results from this case indicate that the labelling was high in the AC and MG, moderate in the IC and low in the NLL and SOC and CN. This distribution of the $GABA_BR1$ subunit was parallel to that seen for the $GABA_BR2$ subunit.

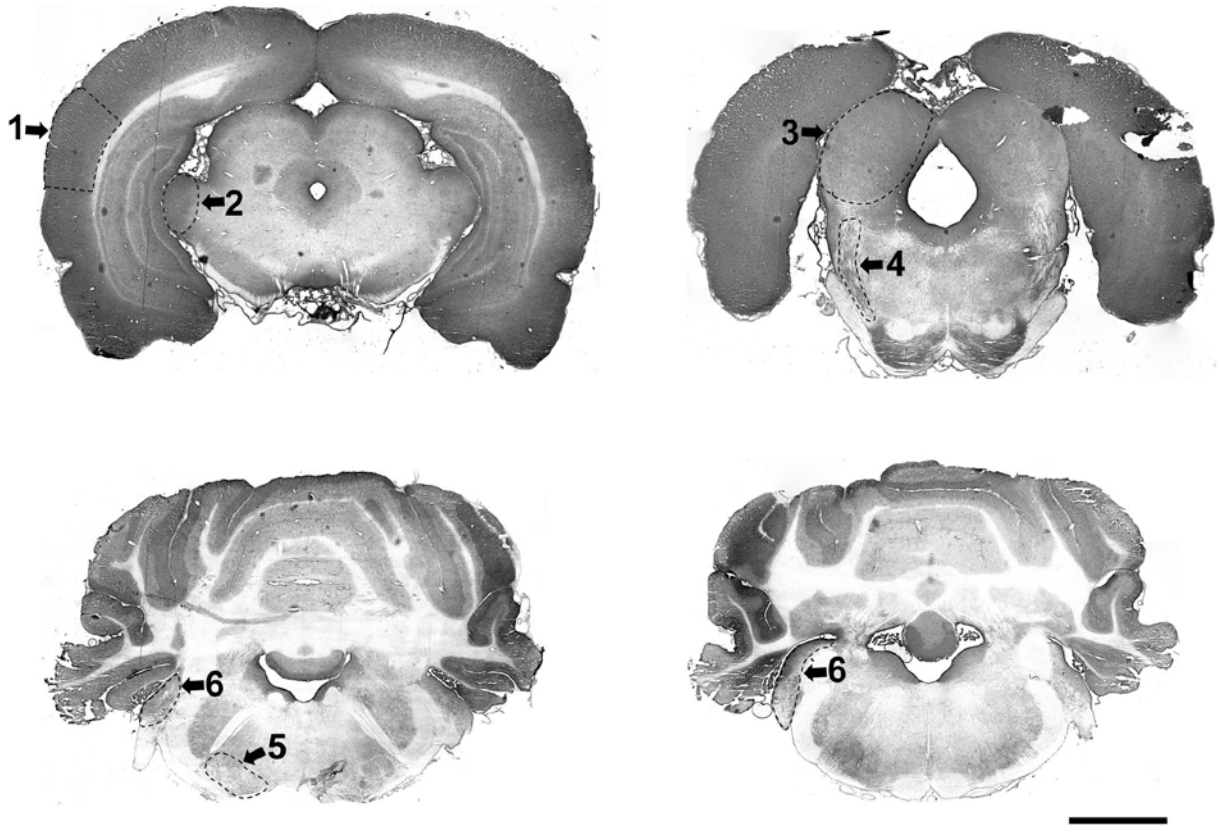

Figure 16. Low magnification images showing immunoreactivity to the $GABA_BR1$ subunit in auditory structures in coronal sections. Upper left panel contains the auditory cortex (AC, 1) and the medial geniculate nucleus (MG, 2). Upper right panel contains the inferior colliculus (IC, 3) and the nucleus of the lateral lemniscus (NLL, 4). Lower left panel contains the superior olivary complex (SOC, 5) and the anterior cochlear nucleus (6). Lower right panel contains the posterior cochlear nucleus (6). Scale bar: 2500 μm

Sections from the same animal but at rostrocaudal locations other than plates 83, 105, 118, and 123 in The Rat Brain Atlas in Stereotaxic Coordinates (Paxinos and Watson, 2007) were also used to conduct immunohistochemical experiments. Immunolabelling by the antibody against the $GABA_BR1$ subunit was analysed in these additional sections. Results from these additional sections (not shown) confirmed those from plates 83, 105, 118, and 123. Scores obtained were used to corroborate the scores obtained from the set of sections presented in Figure 16.

Densitometry scores were obtained from individual auditory areas in four individual cases (i.e. four separate animals). A score of labelling is given by using the densitometry value (see section 2.5.1 for method). Scores from all the auditory areas are presented in Table 3. Based on the scores obtained, the level of labelling was the highest in the DCN, dorsal IC, MG, and the first four layers of the AC, and the lowest in the ventral IC, NLL, and SOC. Moderate scores were found in the AVCN and PVCN. The level of expression of the $GABA_BR1$ subunit in auditory subdivisions was generally in parallel with that of the $GABA_BR2$ subunit.

In the following subsections, I will present results from a single case regarding the regional distribution and cellular localisation of the $GABA_BR1$ receptor subunit in major central auditory structures (Figures 17 through 22, left panels). These results will be presented alongside and compared with those from the same case regarding the regional distributions and cellular localisations of the $GABA_BR2$ receptor subunit (Figures 17 through 22, right panels). Immunohistochemical reactions for the $GABA_BR1$ and $GABA_BR2$ subunits were conducted by using alternating sections from this case. Results from this case were confirmed by results obtained by the other three cases.

Table 3. Densitometry scores of the $GABA_BR1$ subunit in the auditory structures. Densitometry values of immunoreactivity in auditory structures to the $GABA_BR1$ subunit as revealed by immunohistochemical labelling and densitometry analysis (n=4).

Auditory structure	Subdivision	Densitometry value
AC	Layer I	++++
	Layers II/III	++++
	Layer IV	+++
	Layer V	++
	Layer IV	+
MG	MGd	+++
	MGv	+++
	MGm	+++
IC	ICc	+
	ICd	+++
	ICx	++
NLL	DNLL	+
	Dorsal VNLL	+
	Ventral VNLL	+
SOC	LSO	++
	MSO	++
	SPN	+
	LNTB	++
	VNTB	++
	MNTB	+
CN	DCN molecular/fusiform cell layers	+++
	DCN Deep layers	++

	GCD	+++
	AVCN	++
	PVCN	++
CB	Molecular/Purkinje cell layers	++++
	Granule cell layer	+++
	White matter	-

3.3.2 Regional and cellular distribution of the $GABA_BR1$ subunit

Cochlear Nucleus (CN)

In the CN, the DCN (Figure 17A, left panel), PVCN (17A, left panel), and AVCN (Figure 17B, left panel) were all immunoreactive to the $GABA_BR1$ subunit. The highest level of labelling was in the DCN, due to the molecular layer and GCD (Figure 17C, left panel). Both cell body and neuropil were heavily labelled. Abundant labelled puncta were observed. In deeper layers, neuropil labelling was significantly weaker. Labelled puncta were also observed (Figure 17D, left panel). Cells resembling fusiform and pyramidal neurons were clearly labelled. In the PVCN (Figure 17E, left panel) and AVCN (Figure 17F, left panel), multiple types of neurons were immunoreactive for the $GABA_BR1$ subunit and these neurons likely consisted of bushy, octopus, and multipolar cells. Both labelled puncta and fibres could be seen in the neuropil surrounding the cells in the PVCN and AVCN. In the AVCN, a few neurons demonstrated a surrounding faint outline of labelling. This outline might be associated with a possible Calyx of Held terminal (Figure 17F, left panel). In general, both regional and cellular distributions of labelling within the CN were parallel between the $GABA_BR1$ and $GABA_BR2$ subunits.

Superior Olivary Complex (SOC)

Most subnuclei in the SOC had relatively low immunoreactivities for the $GABA_BR1$ subunit (Figure 18A, left panel). The cells within the MNTB were not as distinctly labelled by the antibody against the $GABA_BR1$ subunit as by the antibody against the $GABA_BR2$ subunit (Figure 18B, right panel). It was difficult to tell whether any labelling was associated with Calyx of Held terminals were in the MNTB. The SPN had clearly labelled cells that were surrounded by weak punctate neuropil labelling (Figure 18C, left panel). The boundaries of the LSO could be seen due to relatively densely labelled neuropil and cell bodies (Figure 18D, left panel). Cell

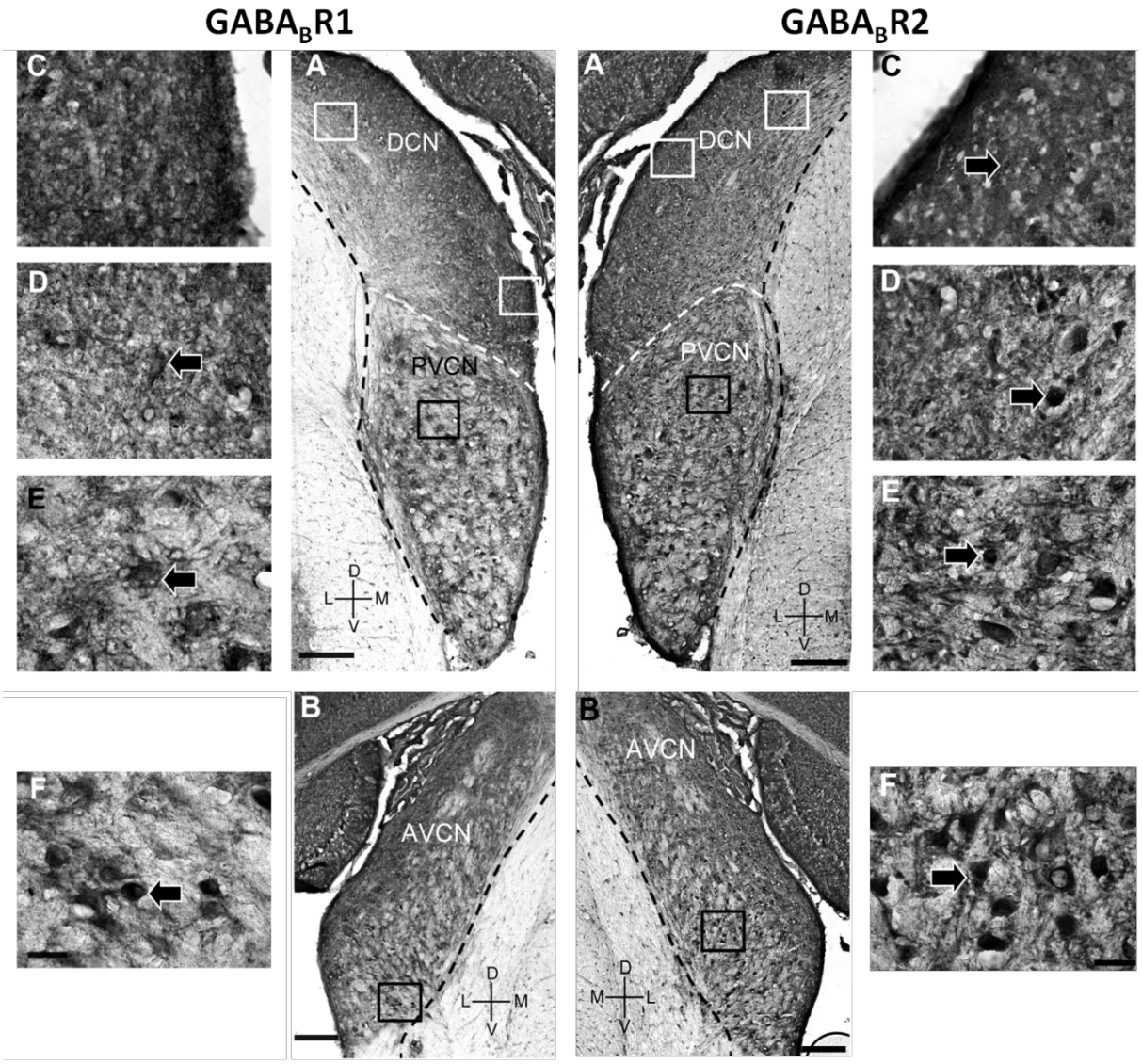

Figure 17. Immunoreactivity to the $GABA_BR1$ and $GABA_BR2$ subunits in the cochlear nucleus (CN). Low magnification images show labelling in the caudal part of the CN including the DCN and PVCN (A) and in the AVCN (B). High magnification images showing labelling in areas in the DCN (C, D), PVCN (E), and AVCN (F). Black arrows with white outlines point toward labelled neurons.
Scale bars: 200 μm in A and B; 20 μm in C-F.

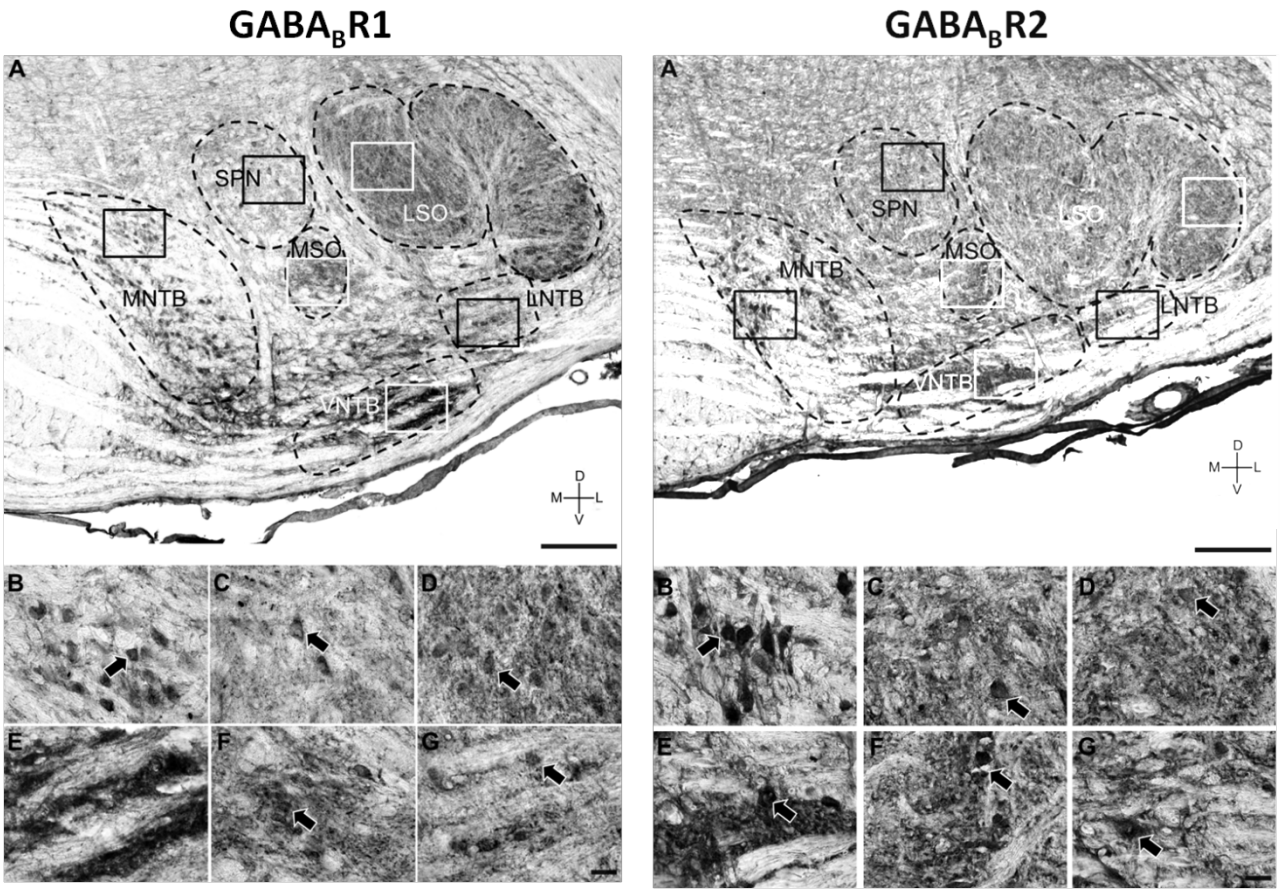

Figure 18. Immunoreactivity to the $GABA_BR1$ and $GABA_BR2$ subunits in the superior olivary complex (SOC). Low magnification image shows labelling in the entire SOC (A). High magnification images show labelling in areas in the MNTB (B), SPN (C), LSO (D), VNTB (E), MSO (F), and LNTB (G). Black arrows with white outlines point toward labelled neurons.
Scale bars: 200 μm in A; 20 μm in B-G.

packing density within the LSO was high, especially in the lateroventral area of the lateral limb. The level of $GABA_BR1$ immunoreactivity in the VNTB was relatively high as well (Figure 18E, left panel). Fibres and cells within this subdivision were densely labelled. The MSO had distinctly labelled multipolar cells as well as surrounding neuropil that were punctate in distribution (Figure 18F, left panel). Cells in the LNTB were found to contain $GABA_BR1$ subunits (Figure 18G, left panel). However, surrounding neuropil was only weakly labelled. Except for the MNTB and LSO, expression of the $GABA_BR1$ subunit in the SOC was similar to that of the $GABA_BR2$ subunit.

Nucleus of the Lateral Lemniscus (NLL)

In the NLL, overall labelling of the $GABA_BR1$ subunit was quite low, likely due to the abundance of fibres in this region (Figure 19A, left panel). The labelling in all subdivisions of the NLL shared similar distributions with somata and neuropil labelling in between fibres (Figures 19B, 19C, and 19D, left panel). The somata and neuropil of the dorsal region of the VNLL were labelled somewhat more densely compared to the ventral region of the VNLL and DNLL. Cell packing density of immunoreactive neurons was also higher in the dorsal region of the VNLL compared to the DNLL. Similar to that of the $GABA_BR2$ receptor, the level of expression was quite low in all NLL subdivisions despite cell body and neuropil labelling in these subdivisions.

Inferior Colliculus (IC)

The overall immunoreactivity level to the $GABA_BR1$ subunit in the IC was moderately high (Figure 20A, left panel). Similar to the distribution of the $GABA_BR2$ subunit within this structure, there was a contrast in labelling among different subdivisions. The ICd and ICx were densely labelled in contrast to the lightly labelled ICc. In the ICd, both neuropil and cell body

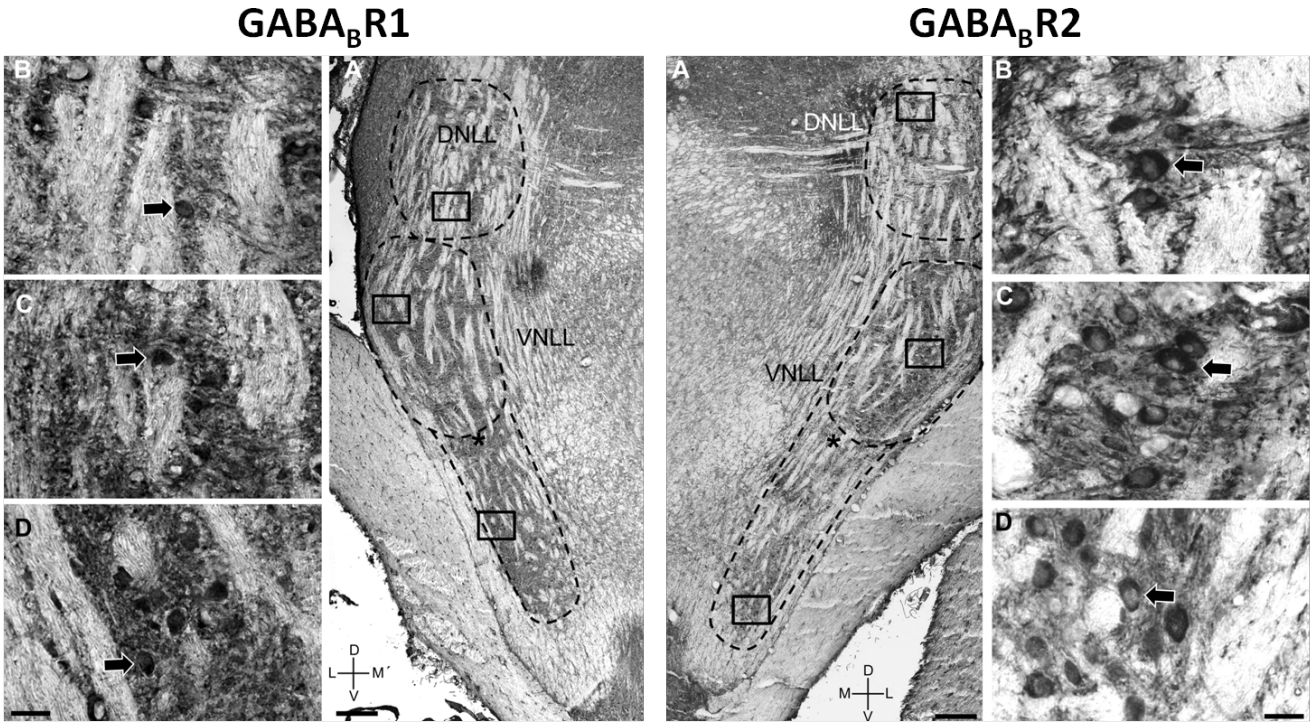

Figure 19. Immunoreactivity to the $GABA_BR1$ and $GABA_BR2$ subunits in the nucleus of the lateral lemniscus (NLL). Low magnification image shows labelling in the entire NLL (A). High magnification images shows labelling in areas of the DNLL (B), dorsal part of the VNLL (C), and ventral part of the VNLL (D). Black arrows with white outlines point toward labelled neurons.
Scale bars: 200 μm in A; 20 μm in B-D.

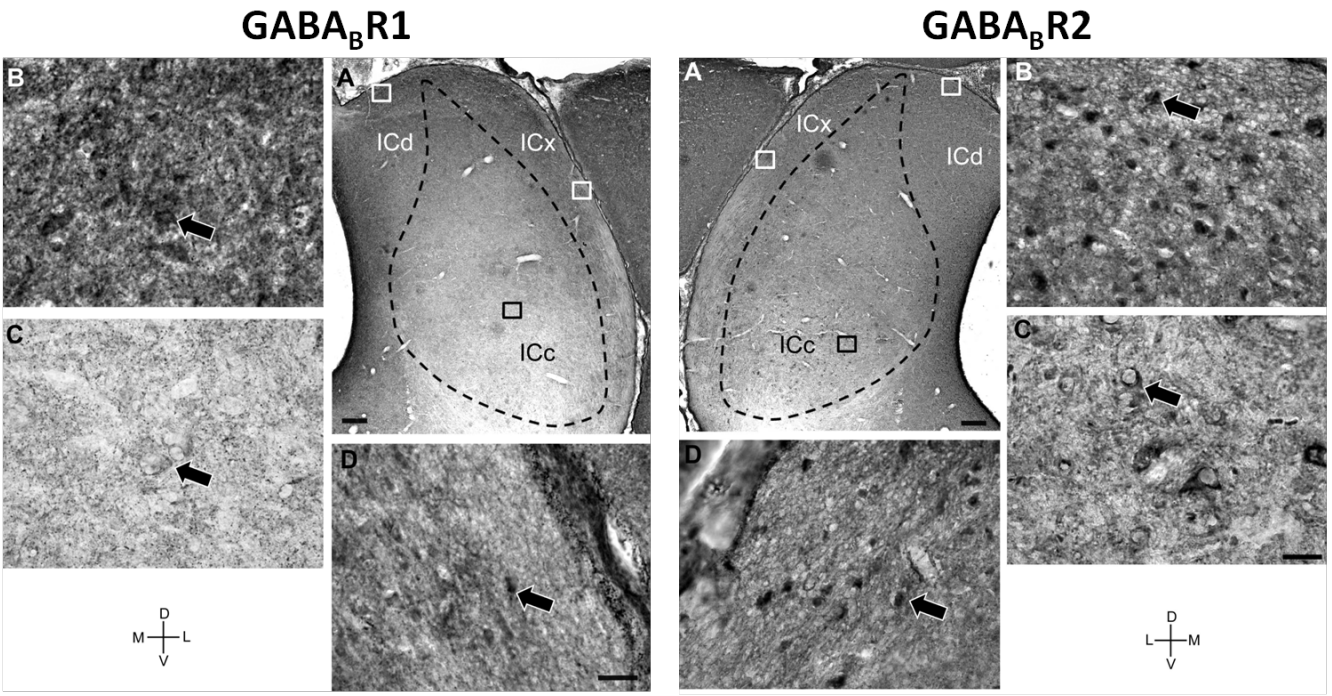

Figure 20. Immunoreactivity to the GABA$_B$R1 and GABA$_B$R2 subunits in the inferior colliculus (IC). Low magnification image shows labelling in the entire IC (A). High magnification images show labelling in areas in the ICd (B), ICc (C), and ICx (D). Black arrows with white outlines point toward labelled neurons.
Scale bars: 200 μm in A; 20 μm in B-D.

were heavily labelled. Abundant labelled puncta were observed (Figure 20B, left panel). Not unlike the distribution seen with the $GABA_BR2$ subunit, three possible layers could be seen in the ICx with fainter labelling in the second superficial layer (Figure 20D, left panel). No such layers could be seen in the ICd. In the ICc, cell bodies and neuropil were labelled in a punctate pattern that was quite light, with cell bodies somewhat distinguishable from surrounding labelled neuropil (Figure 20C, left panel). This differed from labelling by the $GABA_BR2$ subunit which was found to label cell bodies quite strongly and distinctly from the moderately labelled neuropil.

A gradient existed between the ICd and ICc in the level of immunoreactivity to the antibody against the GABABR1 subunit, very similar to that of the antibody against the $GABA_BR2$ subunit. In between these two structures, there was a gradual decrease of immunoreactivity in neuropil along the dorsomedial to ventralateral axis (Figure 20C, left panel). While the dorsal ICd was heavily labelled, and the ventral ICc was weakly labelled, the dorsal region of the ICc bordering the ICd was of intermediate immunoreactivity. Between the ICc and ICx, there seemed to be a more defined boundary separating the two subdivisions.

Medial Geniculate Nucleus (MG)

The overall immunoreactivity to the $GABA_BR1$ antibody in the MG was relatively high (Figure 21A, left panel). Like the distribution seen with the $GABA_BR2$ subunit, labelling across all subdivisions was quite homogenous. In the MGd, somata and neuropil were densely labelled with a cluster of cells clearly seen in the dorsal cap region (Figure 21B, left panel). The rest of the MGd also contained numerous labelled cells and abundant labelled neuropil. The labelling was punctate (Figure 21C, left panel). In the MGv, strong labelling of a level similar to that in the MGd was seen in cell bodies and neuropil (Figure 21D, left panel). The MGm contained

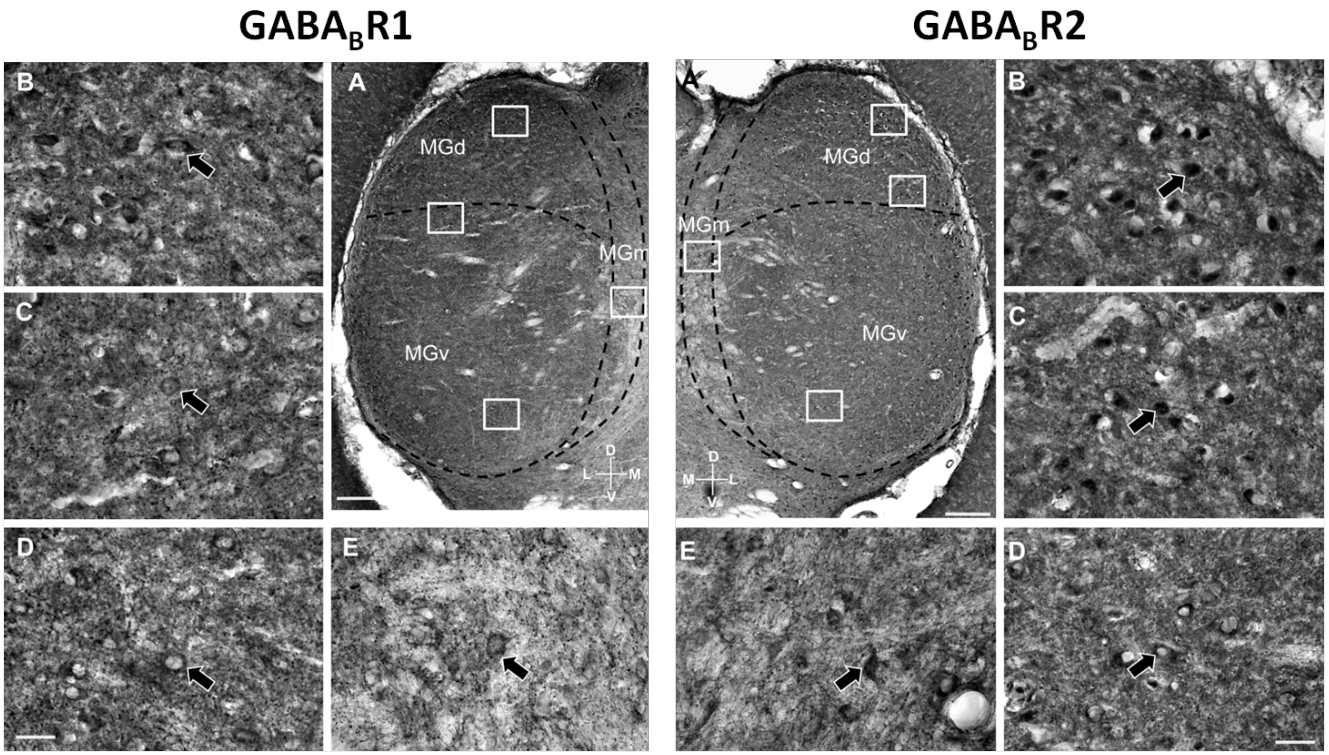

Figure 21. Immunoreactivity to the $GABA_BR1$ and $GABA_BR2$ subunits in the medial geniculate nucleus (MG). Low magnification image showing labelling in the entire MGN (A). High magnification images show labelling in MGd (B), at the border between the MGd and the MGv (C), in the MGv (D), and in the MGm (E). Black arrows with white outlines point toward labelled neurons.
Scale bars: 200 μm in A; 20 μm in B-E.

relatively irregularly shaped cell bodies that were labelled in a punctate pattern (Figure 21E, left panel). Generally, the distribution of the $GABA_BR1$ subunit in the MG was very similar to that of the $GABA_BR2$ subunit.

Auditory Cortex (AC)

Overall immunoreactivity to the $GABA_BR1$ subunit was high in the AC (Figure 22A, left panel). Similar to that to the $GABA_BR2$ antibody, distribution of immunoreactivity to the $GABA_BR1$ antibody was laminar and varied across different layers. The first three superficial layers demonstrated the highest levels of neuropil labelling. In layer I, a few immunoreactive cells surrounded by numerous fibres can be seen (Figure 22B, left panel). Layers II and III shared similar distributions of cell body and neuropil immunoreactivities to the $GABA_BR1$ subunit (Figures 22C and 22D respectively, left panel). Both contained densely packed pyramidal and non-pyramidal cell bodies that were labelled in addition to heavily labelled surrounding neuropil. Compared to layers II and II, cell packing density as well as neuropil labelling in layer IV were not as strong (Figure 22E, left panel). Labelled cell bodies were round in shape and most likely non-pyramidal. Some fibres were seen in this layer perpendicular to the surface of the AC and may have arisen from apical dendrites belonging to pyramidal neurons in deeper layers (not shown). In layer V, the level of neuropil labelling was somewhat lighter than that in layer IV. In this layer, pyramidal and non-pyramidal cells were immunoreactive to the $GABA_BR1$ subunit (Figure 22F, left panel). Labelled pyramidal cells were large with long apical dendrites that extended toward the more superficial layers. Overall neuropil labelling in layer VI was lighter than that of layer V, and become progressively lighter towards the white matter (Figure 22G, left panel). Similar to layer V, layer VI contained both pyramidal and non-pyramidal cells that were labelled. In addition, there were numerous cell bodies with elongated

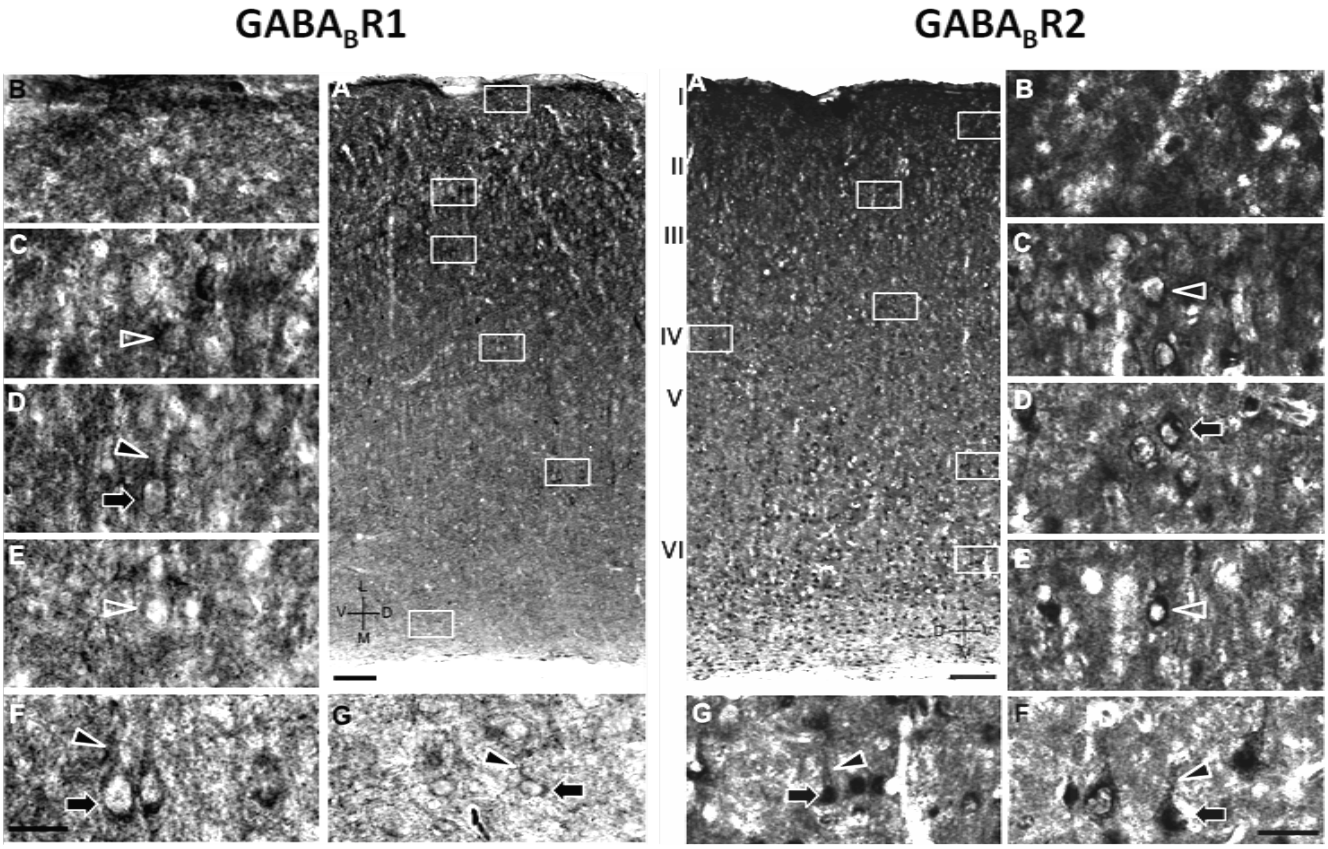

Figure 22. Immunoreactivity to the $GABA_BR1$ and $GABA_BR2$ subunits in the auditory cortex (AC). Low magnification image shows labelling across six cortical layers (A). High magnification images show labelling in layers I though VI (B-G), respectively. Layers of the AC are indicated between the two low magnification images. Black arrows with white outlines point toward labelled pyramidal neurons. White open arrowheads point toward labelled non-pyramidal neurons. Black arrowheads with white outlines point toward labelled dendrites.
Scale bars: 100 μm in A; 25 μm in B-G.

forms that were distinctly labelled. These cells were exclusively found in the deepest region of this layer, bordering cortical white matter.

Overall laminar distribution appeared to be parallel between the $GABA_BR1$ subunit and the $GABA_BR2$ subunit. A difference appears to exist in immunoreactivity between the two subunits in layer VI. Neuropil labelled by the $GABA_BR1$ subunit appears to be relatively lighter compared to that labelled by the $GABA_BR2$ subunit, similar to what was seen in the ICc.

3.3.3 Co-localisation of the $GABA_BR1$ and $GABA_BR2$ subunits

Immunofluorescence experiments were conducted to localise both subunits in auditory neurons. Cell bodies and neuropil labelled by the antibody against the $GABA_BR1$ subunit were pseudo-coloured in green while those labelled by $GABA_BR2$ subunit were pseudo-coloured in red. Cell bodies and neuropil labelled by both antibodies appeared yellow (a mixture of green and red). Double immunofluorescence experiments were conducted by using sections containing auditory structures from two independent cases (i.e. two animals). Preliminary results were obtained from these cases about the co-localisation of $GABA_BR1$ and $GABA_BR2$ subunits in neurons in brainstem auditory structures.

As a positive control, the distributions of the $GABA_BR1$ and $GABA_BR2$ subunits were compared in the cerebellum. In agreement with results from immunohistochemical experiments using light microscopy, both subunits had high expression levels in the molecular and granule cell layers and little to no expression in the white matter (Figure 23). Although Purkinje cells were highly immunoreactive to both subunits, the labelling by the antibody against the $GABA_BR1$ subunit was clearly stronger in these cells in merged images. The expression levels of both subunits in the cerebellum were in agreement with previous findings (Ige et al., 2000).

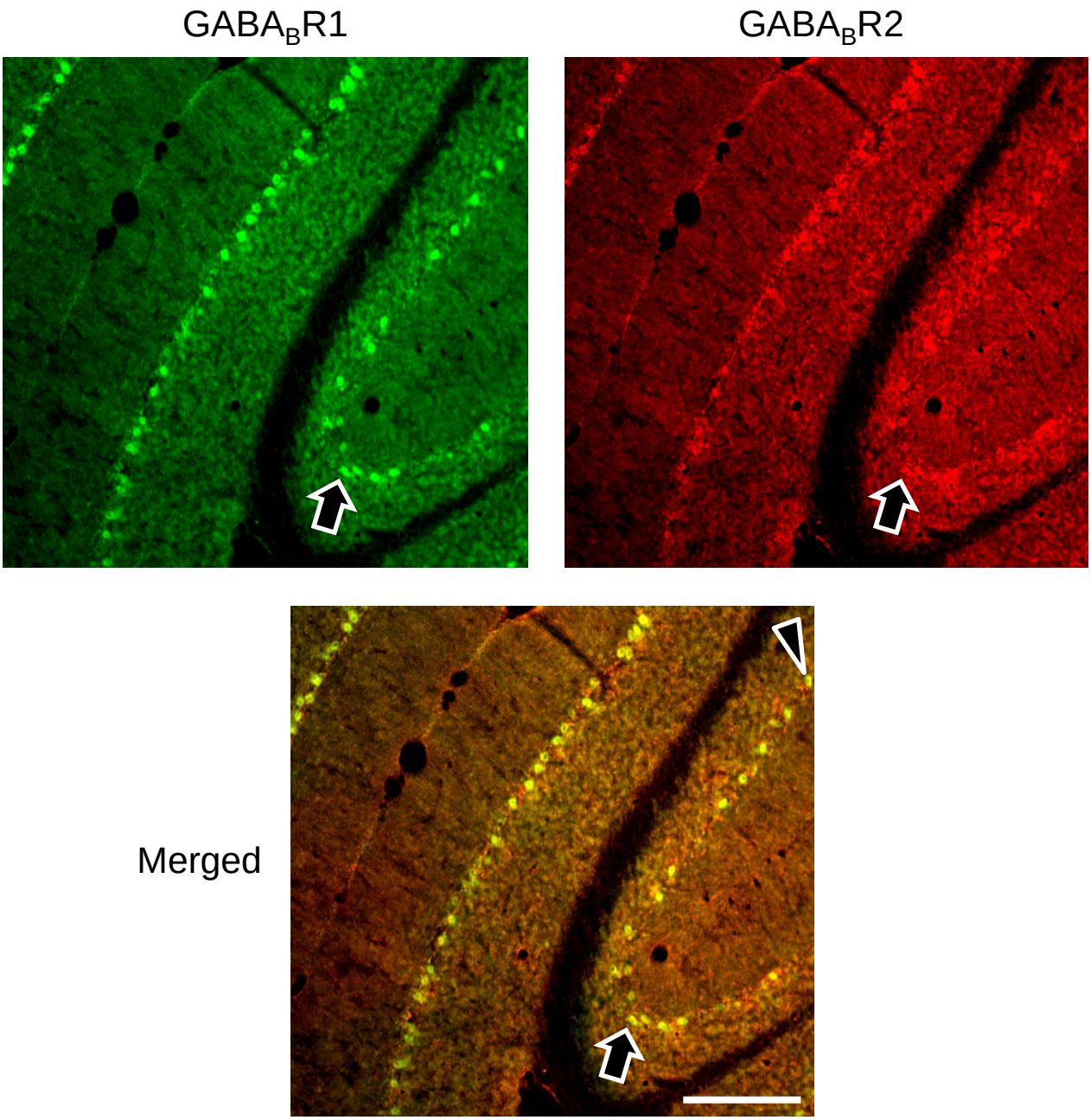

Figure 23. Co-localisation of the GABA$_B$R1 and GABA$_B$R2 subunits in the cerebellum. Coronal section of cerebellum showing molecular, Purkinje cell, and granule cell layers and white matter. Black arrow with white outline points towards a cell showing co-localisation of immunoreactivities to the GABA$_B$R1 and GABA$_B$R2 antibodies. Black arrowhead with white outline points towards a cell that is more highly immunolabelled by the GABA$_B$R1 subunit than the GABA$_B$R2 subunit.
Scale bar: 200 μm

Cochlear Nucleus (CN)

In the CN, the majority of neurons and neuropil were double labelled in all subdivisions (Figures 24A and 24B). Pyramidal cells in the DCN were immunoreactive to both subunits (Figure 24A). The GCD displayed stronger immunoreactivity to the antibody for the $GABA_BR2$ subunit than that to the antibody for the GABABR1 subunit. Small cells were stained by both fluorophores but the staining of the neuropil was more intense for the $GABA_BR2$ subunit. In the PVCN and AVCN, both subunits were highly co-localised (Figure 24B).

Superior Olivary Complex (SOC)

The $GABA_BR1$ and $GABA_BR2$ subunits were not always co-localised in the SOC. In the MNTB, the majority of cells were co-localised (Figure 25A). There were also some cells that were solely labelled for the $GABA_BR1$ subunit. Very few neurons were labelled only for the $GABA_BR2$ subunit. In the LNTB (Figure 25A) and SPN (Figure 25B), cell bodies and neuropil labelling demonstrated co-localisation of both subunits. In the MSO, multipolar cells that line the dorsal-ventral axis were stained for the $GABA_BR2$ subunit more intensely than the $GABA_BR1$ subunit (Figure 25B). In the neuropil surrounding these neurons, the two receptor subunits displayed a high level of co-localisation. In the LSO, the majority of cell bodies were immunoreactive to both subunits (Figure 25C). In some cells, intensity of labelling by the antibody for the $GABA_BR2$ subunit appeared to be stronger. The neuropil of the LSO was also labelled by both subunits and appeared to have a higher immunoreactivity for the $GABA_BR1$ subunit. Clearly labelled cells could be seen throughout the VNTB (Figure 25C), with a large number distributed in the medial region with a high cell packing density. Most cells were double-labelled with some neurons that were solely labelled by the $GABA_BR2$ subunit. Additionally,

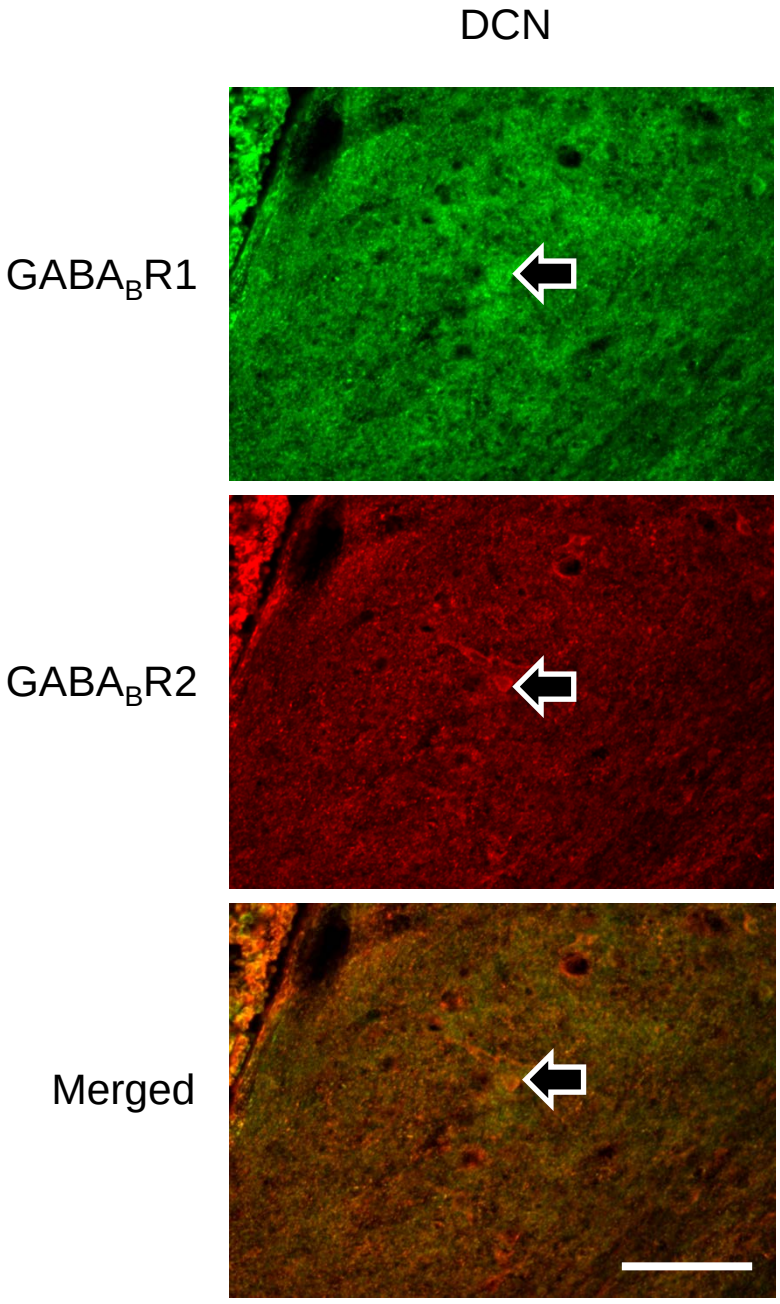

Figure 24A. Co-localisation of the GABA$_B$R1 and GABA$_B$R2 subunits in the dorsal cochlear nucleus (DCN). Black arrow with white outline points towards a cell showing co-localisation of the GABA$_B$R1 and GABA$_B$R2 subunits.
Scale bar: 100 μm

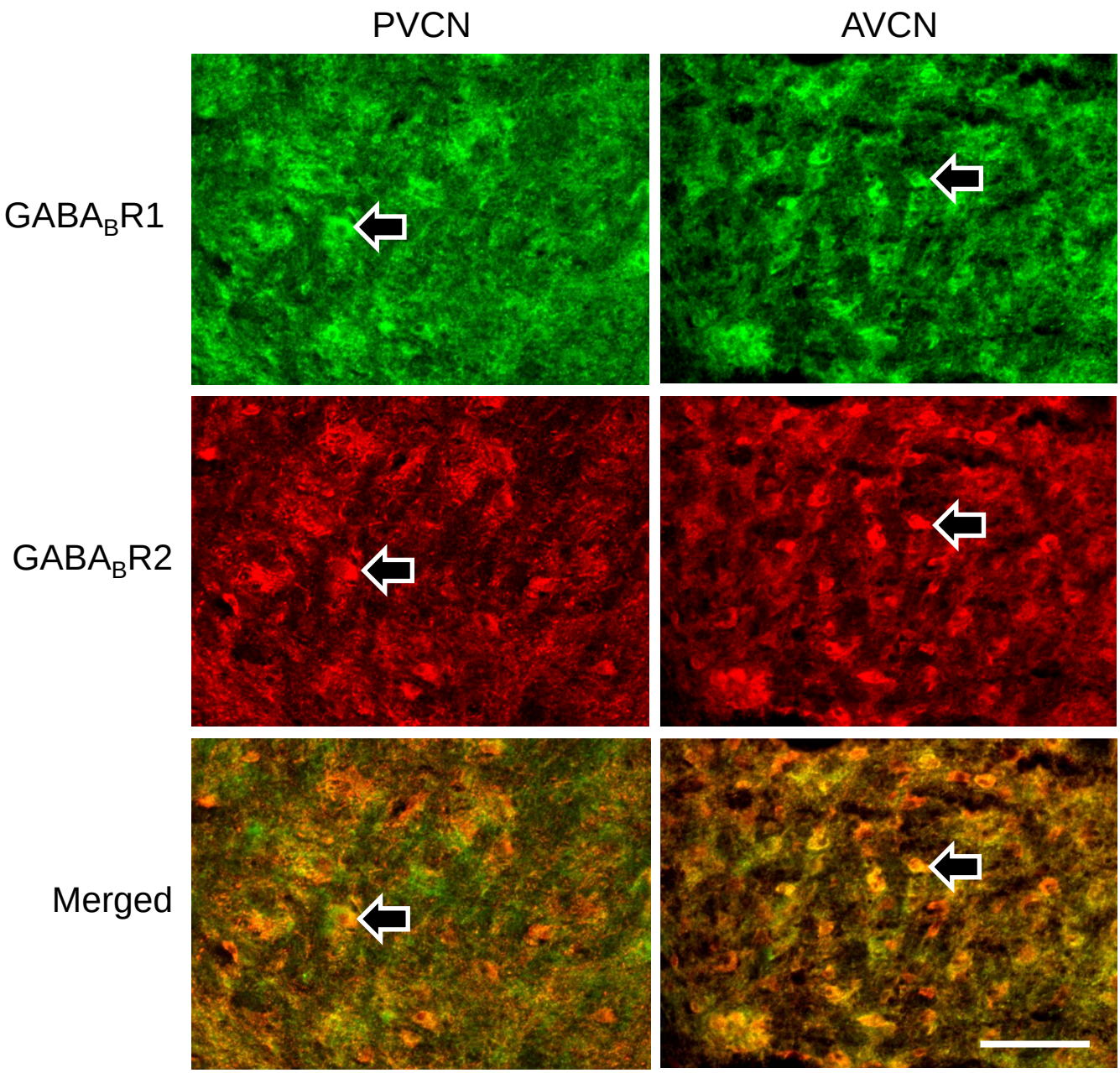

Figure 24B. Co-localisation of the GABA$_B$R1 and GABA$_B$R2 subunits in the posterior ventral cochlear nucleus (PVCN, left panel) and anterior ventral cochlear nucleus (AVCN, right panel). Black arrow with white outline points towards a cell showing co-localisation of the GABA$_B$R1 and GABA$_B$R2 subunits.
Scale bar: 100 μm

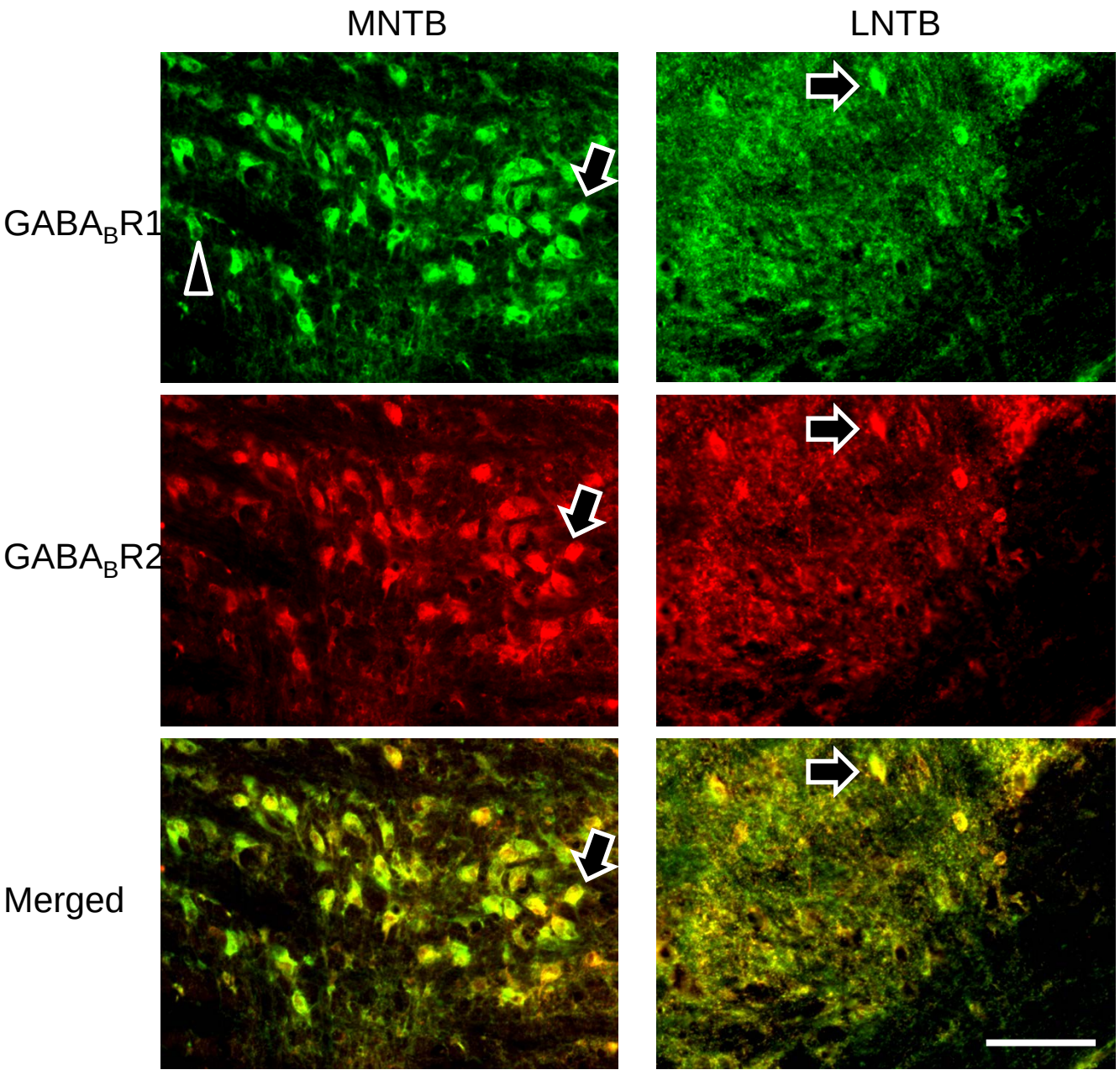

Figure 25A. Co-localisation of the GABA$_B$R1 and GABA$_B$R2 subunits in the medial nucleus of the trapezoidal body (MNTB, left panel) and the lateral nucleus of the trapezoidal body (LNTB, right panel). Black arrow with white outline points towards a cell showing co-localisation of the GABA$_B$R1 and GABA$_B$R2 subunits. Black arrowhead with white outline points toward a cell that is more highly immunoreactive to the GABA$_B$R1 subunit than the GABA$_B$R2 subunit.
Scale bar: 100 μm

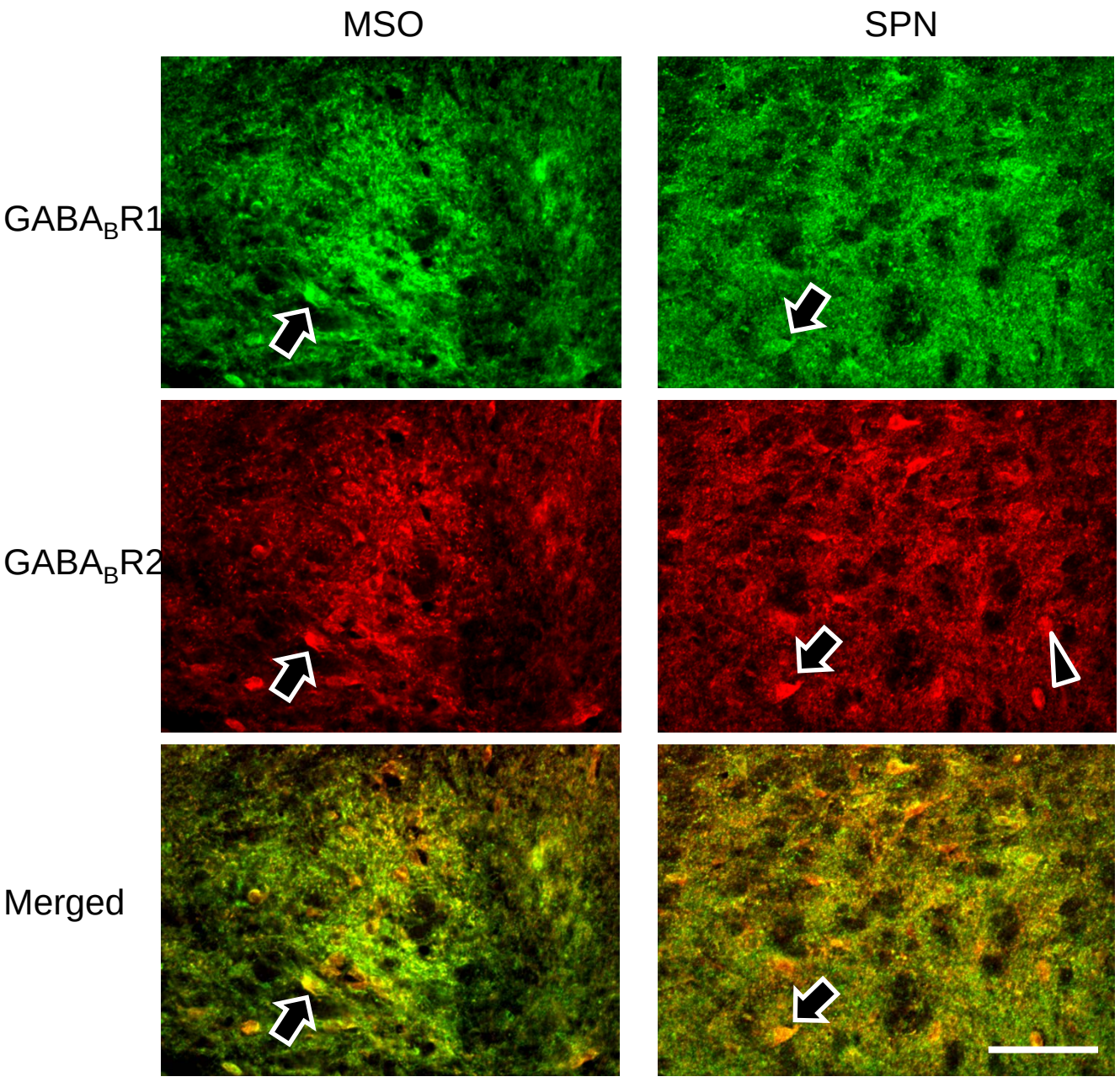

Figure 25B. Co-localisation of the GABA$_B$R1 and GABA$_B$R2 subunits in the medial superior olivary nucleus (MSO, left panel) and the superior paraolivary nucleus (SPN, right panel). Black arrow with white outline points towards a cell showing co-localisation of the GABA$_B$R1 and GABA$_B$R2 subunits. Black arrowhead with white outline points towards a cell that is possibly immunoreactive to the GABA$_B$R2 subunit and not the GABA$_B$R1 subunit.
Scale bar: 100 μm

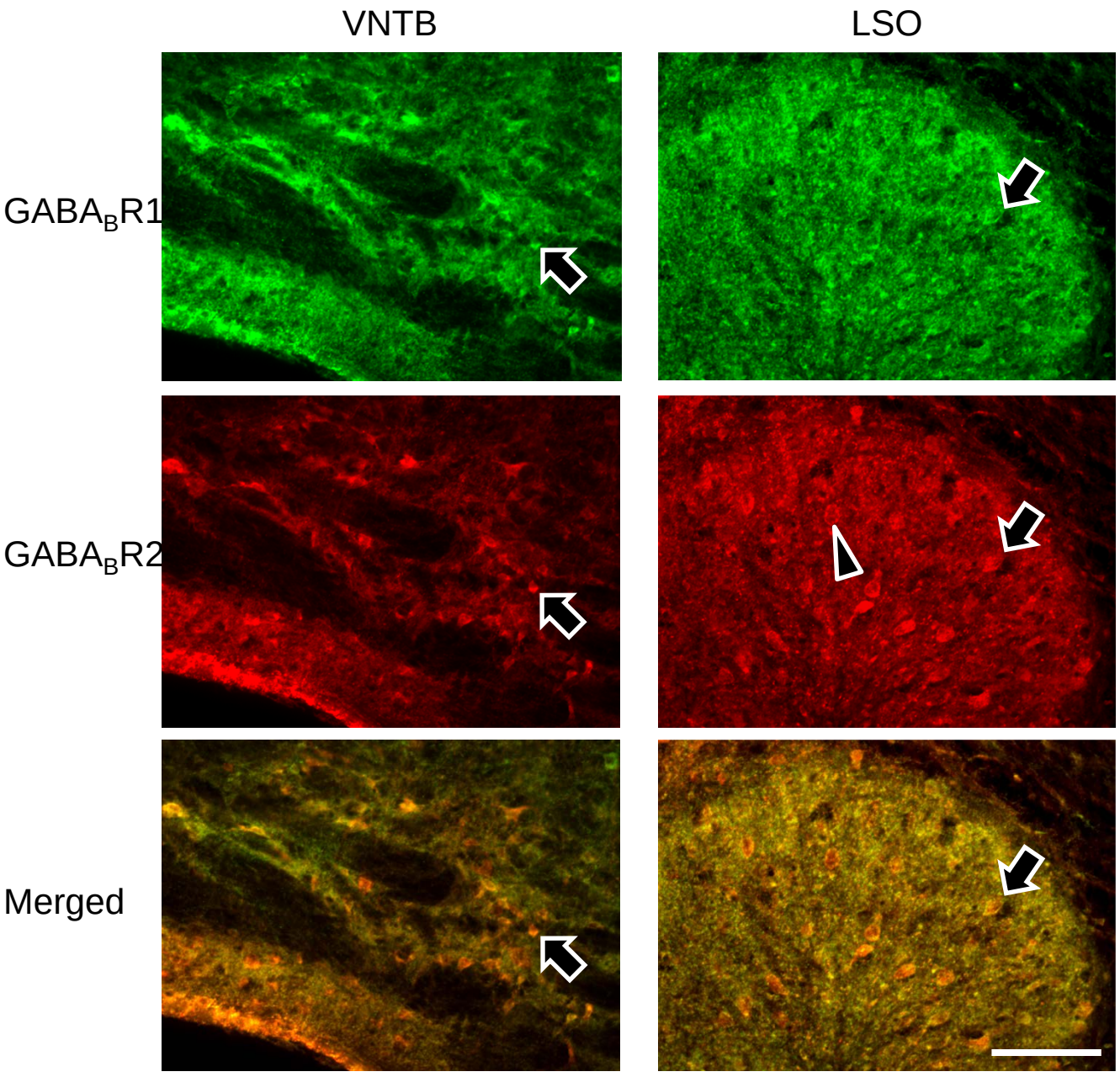

Figure 25C. Co-localisation of the GABA$_B$R1 and GABA$_B$R2 subunits in the ventral nucleus of the trapezoidal body (VNTB, left panel) and the lateral superior olivary nucleus (LSO, right panel). Black arrow with white outline points toward a cell showing co-localisation to the GABA$_B$R1 and GABA$_B$R2 subunits. Black arrowhead with white outline points towards a cell that is immunoreactive to the GABA$_B$R2 subunit and not the GABA$_B$R1 subunit.
Scale bar: 100 μm

fibres in this region were double-labelled with a somewhat stronger intensity of $GABA_BR1$ subunit immunoreactivity.

4 DISCUSSION

4.1 The level and distribution of the $GABA_BR1$ and $GABA_BR2$ receptor subunits and their co-localisation in the central auditory system

Immunohistochemistry and double immunofluorescence techniques were used to study the localisation and distribution of the $GABA_BR1$ and $GABA_BR2$ receptor subunits in the central auditory system. The receptor subunits were found in all auditory structures and their subdivisions. Overall, the distributions of these subunits were parallel. High levels of labelling were found in structures including layers I-V of the AC, MG, ICd, ICx, and DCN while low levels of labelling was found in the NLL and SOC. Moderate levels of labelling were found in the VCN and low to moderate levels were found in the IC. There were differences in distribution between the two subunits in specific subdivisions. $GABA_BR1$ subunit immunoreactivity in cell bodies and neuropil was relatively lower than that of the $GABA_BR2$ subunit in layer VI of the AC as well as the ICc.

Preliminary results from immunofluorescence experiments indicated that the majority of auditory neurons in the CN and SOC contained co-localised receptor subunits. However, there were instances where cellular distributions differed between the two subunits. Neurons solely labelled by the $GABA_BR1$ subunit were found in the MNTB. Neurons that were solely labelled by the $GABA_BR2$ subunit were found in the MSO and LSO. Intensity of neuropil labelling in the LSO, MSO, and SPN was higher for the $GABA_BR1$ subunit than that for the $GABA_BR2$ subunit.

4.1.1 Levels of the $GABA_BR1$ and $GABA_BR2$ receptor subunits across different auditory structures

The overall levels of distribution of both the $GABA_BR1$ and $GABA_BR2$ subunits are in agreement with those of the $GABA_B$ receptor previously reported for the big brown bat (Fubara et al., 1996). Functional $GABA_B$ receptors within the bat's auditory system were found to be expressed at higher levels in the forebrain (AC and MG) versus midbrain (IC) and brainstem structures (NLL, SOC, CN).Therefore for both species, the level of the $GABA_B$ receptor was higher in higher auditory structures and lower in lower structures. This structural dependence of $GABA_B$ receptor distribution may be a common feature across mammalian species (Jamal et al., 2011).

The distribution found in the current study also confirms previous audioradiographical findings regarding the level of $GABA_B$ receptors in the rat's central nervous system. Bowery and colleagues found the highest concentration of $GABA_B$ receptors to be in the molecular layer of the cerebellum (Bowery et al., 1987). According to the regional density scores obtained in this present study, this layer did receive one of the highest score ratings for both $GABA_BR1$ and $GABA_BR2$ subunits. Additionally, a previous quantitative analysis found the MG to contain high levels of $GABA_B$ receptor binding sites while lower levels of binding sites were found in the ICc and VCN (Chu et al., 1990).

A previous study using immunohistochemical methods to locate the $GABA_BR1$ and $GABA_BR2$ subunits in the rat's central nervous system demonstrates trends similar to those found by autoradiography studies. High expression levels of both subunits were found in the AC and thalamus while moderate levels of expression were found in the IC (Charles et al., 2001).

4.1.2 The relation between the expression of the $GABA_B$ receptor in auditory structures and synaptic inputs

The regional distribution was parallel between the $GABA_BR1$ and $GABA_BR2$ receptor subunits. Both subunits demonstrated similar variations in expression levels across auditory structures and within subdivisions of these structures. This variation corresponds to the differences in the inputs and functions of each area within the auditory system.

Cochlear Nucleus (CN)

All the subdivisions of the CN are immunoreactive to both $GABA_BR1$ and $GABA_BR2$ receptor subunits. This is in agreement with previous autoradiography studies that found $GABA_B$ receptors in the entire CN (Bowery et al., 1987; Fubara et al., 1996; Chu et al., 1990). High levels of immunoreactivity to both subunits are seen in the DCN, particularly in the molecular layer and GCD, while moderate levels of immunoreactivity are seen in the AVCN and PVCN. This contrast was also seen in previous studies (Bowery et al., 1987; Chu et al., 1990). Neurons within these subdivisions are major targets of GABAergic inputs from both local and extrinsic sources.

Local GABAergic connections to the molecular layer of the DCN likely include those from local interneurons that may be GABA-positive (Moore, 1996; Ottersen et al., 1995) as well as from pyramidal cells in deeper layers (Adams and Mugnaini, 1987). Pyramidal cells are most likely contacted by GABAergic inputs originating from GABA-positive stellate and Golgi cells (Mugnaini, 1985). Golgi cells have been found to also contact fusiform (giant) cells in the deepest layer of the DCN as well as cells within the GCD (Kolston et al., 1992).

Extrinsic sources of GABAergic input to neurons within the CN include those from the SOC and VNLL (Schofield and Cant, 1999; Thompson and Schofield, 2000). Large neurons in

the SPN have been found to project to the ipsilateral GCD as well as to other areas in the CN (Schofield, 1991; Shore and Moore, 1998). There are also GABAergic bilateral projections from the VNTB, LNTB, LSO, and VNLL that innervate the CN (Shore and Moore, 1998; Winter et al., 1989; Schofield, 1991).

The diverse sources of input may explain the variation in the levels of expression between the subdivisions of the CN.

Superior Olivary Complex (SOC)

The immunoreactivity of the VNTB, LNTB, LSO, and MSO to the $GABA_BR1$ and $GABA_BR2$ subunits was relatively strong compared to that of the MNTB and SPN in the SOC. This is in agreement with previous reports of $GABA_B$ receptor distribution in other species. In the cat and gerbil, $GABA_B$ receptor staining was found in all subnuclei of the SOC, with prominent labelling in the LSO and MSO (Grothe et al., 2011). The difference in staining levels in these subdivisions is most likely due to the variation in sources of GABAergic input as well as different roles in the modulation of neurotransmission.

The LSO has been found to contain many neurons that release GABA (Roberts et al., 1987). The main target of these neurons has been found to be the LSO itself and that this connection may act as a feedback circuit (Magnusson et al.., 2008).

The MSO most likely does not have this feedback loop as the multipolar cells in the MSO have been found not to be GABAergic. It does receive GABAergic projections from other subnuclei including glycine- and GABA-positive neurons in the LNTB and VNTB (Cant and Hyson, 1992; Adams and Mugnaini, 1990; Adams and Wenthold, 1987; Helfert et al., 1989; Thompson et al., 1985). Other sources of GABAergic input to the MSO could include the SPN

as well as descending fibres from the IC, although these inputs have not yet been confirmed (Schwartz et al., 1976; Kiss et al., 1983).

The LNTB and MNTB receive inputs from GABAergic neurons in the VNTB (Thompson and Schofield, 2000; Roberts et al., 1987). Interestingly, the main inhibitory projections from the MNTB are glycinergic and have targets in the MSO and LSO and can be modulated by $GABA_B$ receptors (Kotak et al., 1998; Smith et al., 2000; Nabekura et al., 2004; Magnusson et al., 2005).

While it is clear that the $GABA_B$ receptor are distributed across the different subnuclei and most likely play major roles in auditory transmission, its specific role in neurotransmission among each subdivision is still under investigation.

Nucleus of the Lateral Lemniscus (NLL)

In the NLL, the immunoreactivity to both subunits was found to be the highest in the dorsal region of the VNLL. The difference in labelling between the dorsal and ventral regions of the VNLL and likely reflected a difference in the sources of input to these regions. The main sources of input to the dorsal region of the VNLL include projections from the contralateral VCN as well as the ipsilateral LSO, MSO, SPN, MNTB, and the neighbouring ventral region of the VNLL (Kelly et al., 2009; Sommer et al., 1993; Warr and Beck, 1996). Major projections to the ventral region of the VNLL include the contralateral VCN and ipsilateral MNTB which is glycinergic (Magnusson et al., 2008). Inputs to the dorsal region of the VNLL include those from the LSO and SPN, known to have GABA-positive neurons (Helfert et al., 1989; Kulesza and Berrebi, 2000; Kumoi et al., 1993). These GABAergic projections, as well as the multiple sources of input, may explain why immunoreactivity is somewhat higher in the dorsal area of the VNLL versus the ventral region and the DNLL (Jamal et al., 2011).

Inferior Colliculus (IC)

Overall expression of both $GABA_BR1$ and $GABA_BR2$ receptor subunits in the IC is the highest in the ICd and ICx and the lowest in the ICc. This is in agreement with the distribution of $GABA_B$ receptors seen in rats and bats (Milbrandt et al., 1994; Fubara et al., 1996). These studies found the dorsomedial region of the IC to have a higher concentration of $GABA_B$ receptor binding sites compared to the ventral region of the IC.

Furthermore, Charles and colleagues found that both $GABA_BR1\alpha$ and $GABA_BR1\beta$ isoforms and the $GABA_BR2$ subunits were expressed at a moderate level in the IC as a whole (Charles et al., 2001). Our study supports these previous findings. The levels of both receptor subunits were moderate in the entire IC as a whole. Parallel distributions of the two subunits in the IC were found in the current study and support that functional receptors require both subunits.

The sources of GABAergic input to the ICd and ICx are unlikely to be from higher structures as corticofugal projections are likely glutamatergic (Feliciano and Potashner, 1995) and less than 1% of neurons in the MG are GABAergic (Winer and Larue, 1996). Thus the high level of expression of both subdivisions is likely from intrinsic sources including the ICc as well as possible commissural inputs from the contralateral IC (Moore et al., 1988; Saldaña and Merchán, 1992; Yang et al., 2000).

The difference in the immunoreactivity in the ICd and the ICc formed a gradient that decreased in the level of expression of both subunits along the mediodorsal and lateroventral axis. This gradient corresponds to the gradient of inputs to this structure (Jamal et al., 2011). The highly immunoreactive ICd and ICx subdivisions likely receive GABAergic projections from the midbrain itself, while the ICc is the target of afferents from lower brainstem structures including

the CN, SOC, and DNLL. The region of the IC that is moderately stained includes the border area between the ICd and ICc. This area has been found to receive an overlap of innervations from the midbrain and brainstem structures (Saldaña et al., 1996).

Within the ICc, the gradient continues to a certain extent where labelling in the dorsal region has a relatively higher expression than that of the most ventral area. This could reflect the segregation of inputs within this subdivision. The moderately labelled dorsal area receives projections from the CN and DNLL while the weakly labelled neuropil ventral area could be associated with afferents from the SOC. This difference in labelling could be indicative of segregation in the types of neurotransmission, although no conclusions can be made without further investigation.

Medial Geniculate Nucleus (MG)

High expression levels of both $GABA_BR1$ and $GABA_BR2$ subunits were found in this structure. This is in agreement with previous studies that have found relatively high concentrations of $GABA_B$ receptor binding sites in the thalamus (Bowery et al., 1987; Chu et al., 1990). Additionally, similar to the current study, the immunohistochemical study by Charles and colleagues found equally high levels of expression by both subunits among the three subdivisions of the MG (Charles et al., 2001). In addition to providing evidence of functional $GABA_B$ receptors in the MG, this also suggests that the subdivisions of this structure may share similar sources of inputs (Jamal et al., 2011).

The source of GABAergic input to these subdivisions is unlikely to be intrinsic. As discussed in the previous section, only 1% of neurons within the MG send GABAergic projections. Thus, labelling seen within the MG most likely arises from extrinsic sources (Jamal et al., 2011). Possible sources of GABAergic input to the MG include the ICc (Bartlett and

Smith, 1999; Bartlett et al., 2000; Peruzzi et al., 1997) as well as the auditory sector of the reticular thalamic nucleus (Bartlett and Smith, 1999; Bartlett et al., 2000; Montero, 1983).

Because all the subdivisions of the MG receive inputs from the IC and reticular thalamic nucleus, this could explain the homogenous immunoreactivity that was found to both receptor subunits in this structure (Jamal et al., 2011).

Auditory Cortex (AC)

In general, the AC has one of the highest expression levels of both receptor subunits of all the auditory structures. The distribution of both receptor subunits differed between individual layers. Layers II and III were found to have the highest level of immunoreactivity while layer VI had the lowest level. This laminar distribution was also found in a previous study of the neocortex that looked at the co-localisation of the $GABA_BR1$ and $GABA_BR2$ subunits in different layers (López-Bendito et al., 2002). Moderate to high levels of neuropil labelling was found across all layers. Additionally, the same authors had found tangentially migratory cells in the deep region of layer VI of the AC. These cells strongly resemble the cells that were found in this study that were heavily labelled for the $GABA_BR1$ subunit.

Similar to the previous study by Charles and colleagues (Charles et al., 2001), the layers of the AC were found to have high and parallel immunoreactivities to both subunits. However, there were differences between their findings and the findings of this study in the distributions of both subunits in different layers. They found the immunoreactivities of the $GABA_BR1$ and $GABA_BR2$ receptor subunits to be relatively the same across all layers while scores obtained in this study demonstrate a gradient in expression levels. The overall co-localisation of both subunits as well as their parallel distribution to the expression levels of functional $GABA_B$

receptors, lends further support to the need of both receptor subunits to heterodimerize in order to form functional $GABA_B$ receptors.

The majority of GABAergic inputs to the AC most likely do not arise from other auditory structures. This is because the MG is the main source of input to the AC but contains few GABA-positive neurons. Thus, GABAergic projections likely arise from within the AC including interneurons in local layers (Peterson, Prieto and Winer, 1990; Collía et al., 1990; Romanski and LeDoux, 1993) as well as inputs from the contralateral AC (Winer and Larue, 1989).

4.1.3 Co-localisation of the $GABA_BR1$ and $GABA_BR2$ subunits

The high level of co-localisation of both subunits supports previous findings that the $GABA_BR1$ and $GABA_BR2$ subunits heterodimerize in order to form functional $GABA_B$ receptors. This co-localisation has also been found in other brain regions in previous studies (e.g., cerebellum: Ige et al., 2000; neocortex: López-Bendito et al., 2002; hippocampus: López-Bendito et al., 2004; olfactory bulb: Panzanelli et al., 2004).

In the SOC, there were variations in the levels of co-localisation among subnuclei in this structure. The LNTB and VNTB shared similar expression intensities of both subunits. In the MNTB, in addition to double-labelled neurons, there were also neurons predominantly labelled by the fluorophore tagged to $GABA_BR1$ but only weakly to the $GABA_BR2$ subunit. This is seemingly contrary to the theory that the $GABA_BR2$ subunit is required for the $GABA_BR1$ subunit to reach the plasma membrane as a heterodimer. One possibility could be the presence of an alternate binding partner that can mask the retention signal of $GABA_BR1$ upon binding and release it from the ER. Naturally, this binding partner would not be labelled due to the selectivity

of the antibody. This possibility has been raised in other studies where this type of labelling has been documented (Enna, 2001; Panzanelli et al., 2004). This partner may exist in neurons in the MNTB. For instance, $GABA_BR1$ subunits have been linked to other functions, including binding transcription factors for regulation of protein expression (Nakamura et al., 2011). Further experiments are needed to find whether the high level of $GABA_BR1$ receptor subunits is associated with this function in neurons in the MNTB.

In the LSO, MSO, and SPN, there were neurons that were labelled strongly by the $GABA_BR2$ subunit fluorophore and most likely did not represent a functional $GABA_B$ receptor. As discussed in section 1.4.5, previous knockout experiments have provided strong evidence for the necessity of the $GABA_BR1$ subunit in the formation of a functional receptor (Billinton et al., 2001). This could be indicative of a pool of available $GABA_BR2$ subunits for future heterodimerization and receptor transport (Jamal et al., 2011). Alternatively, like the $GABA_BR1$ subunit, the possibility of binding other partners not recognised by the $GABA_BR1$ antibody cannot be ruled out.

4.1.4 Cellular expression of the receptor and auditory function

There were differences in cell body and neuropil labelling across different subdivisions. These differences in could possibly be associated with pre- and/or post-synaptic $GABA_B$ receptor sites that play major roles in auditory function (Jamal et al., 2011).

As discussed previously, pre-synaptic $GABA_B$ receptors regulate the release of neurotransmitters. In the MNTB and AVCN, labelling suggestive of the Calyx of Held was found to be labelled by both subunits. In addition, these subdivisions had strong cell body immunoreactivity but relatively weak neuropil labelling. In the AVCN, pre-synaptic $GABA_B$

receptors were found that regulated the release of glycine in bushy cells (Lim et al, 2000). In the MSO, labelling also had strong cell body but weak neuropil labelling. This distribution is in agreement with a previous immunofluorescence study (Hassfurth et al., 2010). Furthermore, the same authors found pre-synaptic $GABA_B$ receptors in this subdivision that regulate the release of glycine. Pre-synaptic $GABA_B$ receptors have been found in the ICc as well (Ma et al., 2002; Sun et al., 2006). This coincides with the weak neuropil labelling observed in this subdivision by both subdivisions. Nevertheless, overall results from brainstem and midbrain structures that demonstrated high immunoreactivity to the subunits in cell bodies but weak in neuropil could suggest the presence of pre-synaptic $GABA_B$ receptors (Jamal et al., 2011). However, this cannot be concluded without further investigation.

Post-synaptic $GABA_B$ receptors have been found on neurons in the MGd and MGv in previous studies (Bartlett and Smith, 1999; Peruzzi et al., 1997). In the current study, both these regions were observed to have high immunoreactivity to both $GABA_BR1$ and $GABA_BR2$ subunits in cell bodies and neuropil. Layers II and III of the AC have been found to contain post-synaptic $GABA_B$ receptors as well (Bandrowski et al., 2001; Metherate and Ashe, 1994). Additionally, electron microscopy in the neocortex has found co-localisation of the $GABA_BR1$ and $GABA_BR2$ subunits neurons associated with pre- and post-synaptic sites in interneurons and pyramidal cells (López-Bendito et al., 2002). In the LSO, the $GABA_B$ receptor is found both pre- and post-synaptically (Magnusson et al., 2008; Chang et al., 2003). This coincides with the moderately strong cell body and neuropil labelling found in this subdivision. Previous research has found the ICd to also contain both pre- and post-synaptic $GABA_B$ receptors as well (Sun and Wu, 2009). This is interesting as the ICd was found to contrast in neuropil labelling to the ICc although both contained strong cell body labelling. Based on the examples cited here, labelling

of both cell body and neuropil could represent post-synaptic $GABA_B$ receptors (Jamal et al., 2011). Furthermore, the contrast seen in the IC could be an example of the different roles $GABA_B$ receptors can play within the same structure in addition to different structures of the auditory system. These associations raise interesting questions about the function of $GABA_B$ receptors in different auditory structures that can be addressed by future studies.

CONCLUSION AND FUTURE DIRECTIONS

This study represents a comprehensive analysis of the localisation and distribution of the $GABA_B$ receptor subunits in auditory structures in the albino rat. The $GABA_BR1$ and $GABA_BR2$ subunits were found in all subdivisions of auditory structures. In general, the two subunits were found to be parallel in distribution, with high levels of expression in higher structures and low levels of expression in brainstem structures. Differences in distributions across and within structures can be associated with differences in inputs and functions of these structures in the central auditory system.

$GABA_BR1$ and $GABA_BR2$ subunits were co-localised in the majority of auditory neurons. Co-localisation strongly suggests functional $GABA_B$ receptors that could be contributing to the mediation of auditory processes. Individual differences seen between the two subunits in co-localisation in some structures could be due to alternate functions of each subunit, in addition to involvement of the formation of $GABA_B$ receptors.

Studies in the future can further investigate $GABA_B$ receptors and their subunits in order to better understand their role in the auditory system. Additional co-localisation experiments of the $GABA_BR1$ and $GABA_BR2$ subunits in higher auditory structures can supplement and

confirm findings obtained in the present study. Subcellular distributions of both subunits in all auditory structures can be analysed with electron microscopy techniques and provide more insight into the localisation of each $GABA_B$ subunit pre- and post-synaptically. As well, the role of $GABA_B$ receptors in mediating auditory neurotransmission can be expanded. By using pharmacological manipulations that isolate responses from activation of $GABA_B$ receptors, physiological data can be compared to the data obtained here to better understand the function of these receptors in specific auditory pathways.

REFERENCES

Adams JC, Mugnaini E (1987) Patterns of glutamate decarboxylase immunostaining in the feline cochlear nuclear complex studied with silver enhancement and electron microscopy. J Comp Neurol 262:375–401.

Adams JC, Mugnaini E (1990) Immunocytochemical evidence for inhibitory and disinhibitory circuits in the superior olive. Hear Res 49:281–298.

Adams JC, Wenthold RJ (1987) Immunostaining of GABAergic and glycinergic inputs to the anteroventral cochlear nucleus. Soc Neurosci Abstr 13:1259.

Bajo VM, Nodal FR, Bizley JK, Moore DR, King AJ (2007) The ferret auditory cortex: descending projections to the inferior colliculus. Cereb Cortex 17:475–491.

Bandrowski AE, Aramakis VB, Moore SL, Ashe JH (2001) Metabotropic glutamate receptors modify ionotropic glutamate responses in neocortical pyramidal cells and interneurons. Exp Brain Res 136:25–40.

Barnes-Davies M, Forsythe ID (1995) Pre- and postsynaptic glutamate receptors at a giant excitatory synapse in rat auditory brainstem slices. J Physiol 488 (Pt 2):387–406.

Bartlett EL, Smith PH (1999) Anatomic, intrinsic, and synaptic properties of dorsal and ventral division neurons in rat medial geniculate body. J Neurophysiol 81:1999–2016.

Bartlett EL, Stark JM, Guillery RW, Smith PH (2000) Comparison of the fine structure of cortical and collicular terminals in the rat medial geniculate body. Neuroscience 100:811–828.

Benke D, Michel C, Mohler H (2002) Structure of $GABA_B$ receptor in rat retina. J Recept Signal Transduct Res 22:253–266.

Billinton A, IGE AO, Bolam JP, White JH, Marshall FH, Emson PC (2001) Advances in the molecular understanding of GABA(B) receptors. Trends Neurosci 24: 277-282.

Bordi and LeDoux, 1994 Response properties of single units in areas of rat auditory thalamus that project to the amygdala. I. Acoustic discharge patterns and frequency receptive fields. Exp Brain Res 98: 261-74.

Bowery NG, Hudson AL, Price GW (1987) $GABA_A$ and $GABA_B$ receptor site distribution in the rat central nervous system. Neuroscience 20:365–383.

Buonomano DV, Merzenich MM (1998) Net interaction between different forms of short-term synaptic plasticity and slow-IPSPs in the hippocampus and auditory cortex. J Neurophysiol 80:1765–1774.

Cant NB, Hyson RL (1992) Projections from the lateral nucleus of the trapezoid body to the medial superior olivary nucleus in the gerbil. Hear Res 58:26–34.

Caspary DM, Lawhorn RA, Armour BA, Pippin J, Arnerić SP (1990) Immunocytochemical and neurochemical evidence for age-related loss of GABA in the inferior colliculus: Implications for neural presbycusis. J Neurosci 10: 2363-2372.

Chalifoux JR, Carter AG (2011) $GABA_B$ receptor modulation of synaptic function. Curr Opin Neurobiol 21: 339-344.

Chang EH, Kotak VC, Sanes DH (2003) Long-term depression of synaptic inhibition is expressed postsynaptically in the developing auditory system. J Neurophysiol 90:1479-1488.

Charles KJ, Evans ML, Robbins MJ, Calver AR, Leslie RA, Pangalos MN (2001) Comparative immunohistochemical localisation of GABAB1a, GABAB1b and GABAB2 subunits in rat brain, spinal cord, and dorsal root ganglion. Neuroscience 106:447–467.

Chu DC, Albin RL, Young AB, Penney JB (1990) Distribution and kinetics of GABAB binding sites in rat central nervous system: a quantitative autoradiographic study. Neuroscience 34:341–357.

Chung SH, Kim CT, Hawkes R (2008) Compartmentation of GABAB receptor2 expression in the mouse cerebellar cortex. Cerebellum 7:295–303.

Collía FP, Pérez EC, Méndez JAG, Carrascal E (1990) Corticocortical connections of the auditory cerebral cortex in the albino rat, a PHA-L study. Eur J Neurosci Suppl 3:155.

Enna SJ (2001) A $GABA_B$ mystery: The search for pharmacologically distinct $GABA_B$ receptors. Mol Interv 1:208-218.

Faingold CL, Gehlbach G, Caspary DM (1989) On the role of GABA as an inhibitory neurotransmitter in inferior colliculus neurons: iontophoretic studies. Brain Res 500:302–312.

Faye-Lund H, Osen KK (1985) Anatomy of the inferior colliculus in rat. Anat Embryol 175: 35-52.

Faye-Lund H (1986) Projection from the inferior colliculus to the superior olivary in the albino rat. Anat Embryol 175:35-52.

Feliciano M, Potashner SJ (1995) Evidence for a glutamatergic pathway from the guinea pig auditory cortex to the inferior colliculus. J Neurochem 65:1348–1357.

Friauf E, Ostwald J (1988) Divergent projections of physiologically characterized rat ventral cochlear nucleus neurons as shown by intra-axonal injection of horseradish peroxidase. Exp Brain Res 73:263-284.

Fubara BM, Casseday JH, Covey E, Schwartz-Bloom RD (1996) Distribution of GABAA, GABAB, and glycine receptors in the central auditory system of the big brown bat, *Eptesicus fuscus*. J Comp Neurol 369:83–92.

Gaese BN, Ostwald J (1995) Temporal coding of amplitude and frequency modulations in the rat auditory cortex. Eur J Neurosci 7:438-450.

Games KD, Winer J (1988) Layer V in rat auditory cortex: Projections to the inferior colliculus and contralateral cortex. Hear Res 34:1-26.

Gehlert DR, Yamamura HI, Wamsley JK (1985) Gamma-aminobutyric acid B receptors in the rat brain: quantitative autoradiographic localisation using [3H](-)-baclofen. Neurosci Lett 56:183–188.

González-Hernádez TH, Galindo-Mireles D, Castaneyra-Perdomo A, and Ferres-Torres R (1991) Divergent Projections of projecting neurons of the inferior colliculus to the medial geniculate body and the contralateral inferior colliculus in the rat. Hear Res 52:17-21.

Grothe B, Koch U (2011) Dynamics of binaural processing in the mammalian sound localization pathway - The role of $GABA_B$ receptors. Hear Res doi:10.1016/j.heares.2011.03.013.

Gulick WL, Gescheider GA, Frisna RD (1989): Hearing: Physiological acoustics, neural coding, and psychoacoustics. Oxford, UK: Oxford University Press.

Hassfurth B, Grothe B, Koch U (2010) The Mammalian Interaural Time Difference Detection Circuit Is Differentially Controlled by $GABA_B$ Receptors during Development. J Neurosci 30:9715–9727.

Helfert RH, Bonneau JM, Wenthold RJ, Altschuler RA (1989) GABA and glycine immunoreactivity in the guinea pig superior olivary complex. Brain Res 501:269–286.

Huang Z (2006) $GABA_B$ receptor isoforms caught in action at the scene. Neuron 50:521-524.

Huffman RF, Henson OW Jr (1990) The descending auditory pathway and acousticomotor systems, connections with the inferior colliculus. Brain Res Rev 15:295-323.

Hutson KA, Morest DK (1996) Fine structure of the cell clusters in the cochlear nerve root: stellate, granule, and mitt cells offer insights into the synaptic organization of local circuit neurons. J Comp Neurol 371:397–414.

Ige AO, Bolam JP, Billinton A, White JH, Marshall FH, Emson PC (2000) Cellular and sub-cellular localisation of GABAB1 and GABAB2 receptor proteins in the rat cerebellum. Mol Brain Res 83:72–80.

Irie T, Ohmori H (2008) Presynaptic $GABA_B$ receptors modulate synaptic facilitation and depression at distinct synapses in fusiform cells of mouse dorsal cochlear nucleus. Biochem Biophys Res Commun 367:503–508.

Isaacson JS (1998) GABAB receptor-mediated modulation of presynaptic currents and excitatory transmission at a fast central synapse. J Neurophysiol 80:1571–1576

Jamal L, Zhang H, Finlayson PG, Porter LA, Zhang H (2011) The level and distribution of the $GABA_BR2$ receptor subunit in the rat. Neuroscience 181:243-256.

Jones KA, Borowsky B, Tamm JA, Craig DA, Durkin MM, Dai M, Yao W-J, Johnson M, Gunwaldsen C, Huang L-Y, Tang C, Shen Q, Salon JA, Morse K, Laz T, Smith KE, Nagarathnam D, Noble SA, Branchek TA, Gerald C (1998) $GABA_B$ receptors function as a heteromeric assembly of the subunits $GABA_BR1$ and $GABA_BR2$. Nature 396:674-679.

Juiz JM, Albin RL, Helfert RH, Altschuler RA (1994) Distribution of $GABA_A$ and $GABA_B$ binding sites in the cochlear nucleus of the guinea pig. Brain Res 639:193–201.

Kelly JB, van Adel BA, Ito M (2009) Anatomical projections of the nuclei of the lateral lemniscus in the albino rat (*Rattus norvegicus*). J Comp Neurol 512:573–593.

Kolston J, Osen KK, Hackney CM, Ottersen OP, Storm-Mathisen J (1992) An atlas of glycine- and GABA-like immunoreactivity and colocalization in the cochlear nuclear complex of the guinea pig. Anat Embryol (Berl) 186:443–465.

Kornau HC (2006) GABA (B) receptors and synaptic modulation. Cell Tissue Res 326: 517-533.

Kotak VC, Korada S, Schwartz IR, Sanes DH (1998) A developmental shift from GABAergic to glycineric transmission in the central auditory system. J Neurosci 18:4646-4655.

Kulesza RJ Jr, Berrebi AS (2000) The superior paraolivary nucleus of the rat is a GABAergic nucleus. J Assoc Res Otolaryngol 1: 255–269.

Kulik Á, Vida I, Luján R, Haas CA, López-Bendito G, Shigemoto R, Frotscher M (2003) Subcellular localization of metabotropic GABA(B) receptor subunits GABA(B1a/b) and GABA(B2) in the rat hippocampus. J. Neurosci 23:11026-11035.

Kumoi K, Saito N, Tanaka C (1993) Immunohistochemical localization of gamma-aminobutyric acid- and aspartate-containing neurons in the guinea pig superior olivary complex. Hear Res 68:173–179.

Kuner R, Kohr G, Grunewald S, Eisenhardt G, Bach A, Kornau HC (1999) Role of heteromer formation in GABAB receptor function. Science 283:74–77.

LeDoux JE, Ruggiero DA, Forest R, Stornetta R, Reis DJ (1987) Topographic organization of convergent projections to the thalamus from the inferior colliculus and spinal cord in the rat. J Comp Neurol 264:123-146.

Lim R, Alvarez FJ, Walmsley B (2000) GABA mediates presynaptic inhibition at glycinergic synapses in a rat auditory brainstem nucleus. J Physiol 525 (Pt 2):447–459.

López-Bendito G, Shigemoto R, Kulik A, Paulsen O, Fairén A, Luján R (2002) Expression and distribution of metabotropic GABA receptor subtypes $GABA_BR1$ and $GABA_BR2$ during rat neocortical development Eur J Neurosci, 15: 1766-1778.

Luján R, Shigemoto R (2006) Localization of metabotropic GABA receptor subunits GABAB1 and GABAB2 relative to synaptic sites in the rat developing cerebellum. Eur J Neurosci 23:1479–1490.

Luján R, Shigemoto R, Kulik A, Juiz JM (2004) Localization of the GABAB receptor 1a/b subunit relative to glutamatergic synapses in the dorsal cochlear nucleus of the rat. J Comp Neurol 475:36–46.

Ma CL, Kelly JB, Wu SH (2002) Presynaptic modulation of GABAergic inhibition by $GABA_B$ receptors in the rat's inferior colliculus. Neuroscience 114:207–215.

Magnusson AK, Kapfer C, Grothe B, Koch U (2005) Maturation of glycinergic inhibition in the gerbil medial superior olive after hearing onset. J Physiol 568:497-512.

Magnusson AK, Park TJ, Pecka M, Grothe B, Koch U (2008) Retrograde GABA signalling adjusts sound localization by balancing excitation and inhibition in the brainstem. Neuron 59:125-137.

Malcangio M, Bowery NG (1996) GABA and its receptors in the spinal cord. Trends Pharmacol Sci 17:457-462.

Malmierca MS, Merchán MA, Oliver DL (1999a) Convergence of dorsal and ventral cochlear nuclei input onto frequency-band laminae of the inferior colliculus: A double tracer study in rat and cat. ARO Abstr 22:221.

Malmierca MS, Oliver DL, Merchán MA (1999b) Convergence laminar projections from dorsal (DCN) and ventral cochlear nucleus (VCN) to inferior colliculus (IC) of rat and cat. SFN Abstr 25:1418.

Malmierca MS, Merchán MA (2005) Auditory system. In: The rat nervous system, 3rd edition (Paxinos G, ed), pp 997–1082. San Diego: Academic Press.

Malmierca MS, Merchán MA, Henkel CK, Oliver DL (2002) Direct projections from cochlear nuclear complex to auditory thalamus in the rat. J Neurosci 22:10891-10897.

Margeta-Mitrovic M, Jan YN, Jan LY (2000) A trafficking checkpoint controls $GABA_B$ receptor heterodimerization. Neuron 27:97-106.

Merchán MA, Collía FP, López DE, Saldaña E (1988) Morphology of cochlear root neurons in the rat. J Neurocytol 17:711-725

Metherate R, Ashe JH (1994) Facilitation of an NMDA receptor-mediated EPSP by paired-pulse stimulation in rat neocortex via depression of GABAergic IPSPs. J Physiol 481 (Pt 2):331–348.

Milbrandt JC, Albin RL, Caspary DM (1994) Age-related decrease in GABAB receptor binding in the Fischer 344 rat inferior colliculus. Neurobiol Aging 15:699–703.

Montero VM (1983) Ultrastructural identification of axon terminals from the thalamic reticular nucleus in the medial geniculate body of the rat: an EM autoradiographic study. Exp Brain Res 51:338 –342.

Moore DR, Kotak VC, Sanes DH (1998) Commissural and lemniscal synaptic input to the gerbil inferior colliculus. J Neurophysiol 80: 2229–2236.

Morest DK (1973) Auditory neurons of the brain stem. Adv Otorhinolaryngol 20:337-356.

Mugnaini E, Osen KK, Dahl A-L, Friedrich Jr. VL, Korte G (1980a) Fine structure of granule cells and related interneurons (termed Golgi cells) in the cochlear nuclear complex of cat, rat, and mouse. J Neurocytol 9:537-570

Mungaini E, Warr WB, Osen KK (1980b) Distribution and light microscopic features of granule cells in the cochlear nuclei of cat, rat, and mouse. J Comp Neurol 191:581-606.

Nabekura J, Katsurabayashi S, Kakazu Y, Shibata S, Matsubara A, Jinno S, Mizoguchi Y, Sasaki A, Ishibashi H (2004) Developmental switch from GABA to glycine release in single central synaptic terminals. Nat. Neurosci 7:17-23.

Nakamura Y, Hinoi E, Takarada T, Takahata Y, Yamamoto T, et al. (2011) Positive Regulation by $GABA_B$R1 Subunit of Leptin Expression through Gene Transactivation in Adipocytes. PLoS ONE 6(5): e20167. doi:10.1371/journal.pone.0020167

Osen KK, Ottersen OP, Storm-Mathisen J (1990) Colocalization of glycine-like and GABA-like immonoreactivities. A semi-quantitative study of individual neurons in the dorsal cochlear nucleus of the cat. In: Glycine neurotransmission (Ottersen OP, Storm-Mathisen J, eds), pp 417–451. Chichester: Wiley.

Osen KK, López DE, Ottersen OP, Storm-Mathisen J (1991) GABA-like and glycine-like immunoreactivities of the cochlear root nucleus in rat. J Neurocytol 20:17-25

Panzanelli P, López-Bendito G, Luján R, Sassoé-Pognetto M (2004) Localization and developmental expression of $GABA_B$ receptors in the rat olfactory bulb. J Neurocytol 33:87-99.

Paxinos G, Watson C (2007) The rat brain in stereotaxic coordinates, 6th edition. Amsterdam: Academic Press.

Peruzzi D, Bartlett E, Smith PH, Oliver DL (1997) A monosynaptic GABAergic input from the inferior colliculus to the medial geniculate body in rat. J Neurosci 17:3766–3777.

Pin J-P, Kniazeff J, Binet V, Liu J, Maurel D, Galvez T, Duthey B, Havlickova M, Blahos J, Prezéau L, and Rondard P (2004) Activation mechanism of the heterodimeric $GABA_B$ receptor. Biochem Pharmacol 68:1565-1572.

Pooler AM, Gray AG, McIlhinney RA (2009) Identification of a novel region of the GABA(B2) C-terminus that regulates surface expression and neuronal targeting of the GABA(B) receptor. Eur J Neurosci 29:869-878.

Restituito S, Couve A, Bawagan H, Jourdain S, Pangalos MN, Calver AR, Freeman KB, Moss SJ (2005) Multiple motifs regulate the trafficking of GABA(B) receptors at distinct checkpoints within the secretory pathway. Mol Cell Neurosci, 28:747-756.

Romanski LM, LeDoux JE (1993) Information cascade from primary auditory cortex to the amygdala: corticocortical and corticoamygdaloid projections of temporal cortex in the rat. Cereb Cortex 3:515–532.

Sakaba T, Neher E (2003) Direct modulation of synaptic vesicle priming by $GABA_B$ receptor activation at a glutamatergic synapse. Nature 424:775–778.

Saldaña E, Berrebi AS (2000) Anisotropic organization of the rat superior paraolivary nucleus. Anat Embryol 202:265-279.

Saldaña E, Feliciano M, Muganaini E (1996) Distribution of descending projections form primary auditory neocortex to inferior colliculus mimics the topography of intracollicular projections. J Comp Neurol 371:15–40.

Saldaña E, Merchán MA (1992) Intrinsic and commissural connections of the rat inferior colliculus. J Comp Neurol 319:417–437.

Schofield BR (1991) Superior paraolivary nucleus in the pigmented guinea pig: separate classes of neurons project to the inferior colliculus and the cochlear nucleus. J Comp Neurol 312:68 –76.

Schofield BR (1995) Projections from the cochlear nucleus to the superior paraolivary nucleus in guinea pigs. J Comp Neurol 360:135-149.

Schofield BR (2009) Projections to the inferior colliculus from layer VI cells of auditory cortex. Neuroscience 159:246-258.

Schofield BR, Cant NB (1999) Descending auditory pathways: projections from the inferior colliculus contact superior olivary cells that project bilaterally to the cochlear nuclei. J Comp Neurol 409:210–223.

Schofield BR, Coomes DL (2005) Auditory cortical projections to the cochlear nucleus in guinea pigs. Hear Res 199:89-102.

Schneiderman A, Henkel CK (1987) Banding of lateral superior olivary nucleus afferents in the inferior colliculus: A possible substrate for sensory integration. J Comp Neurol 266:519-534.

Shore SE, Moore JK (1998) Sources of input to the cochlear granule cell region in the guinea pig. Hear Res 116:33–42.

Silverthorn DU (2007) Human Physiology: An integrated approach, 4th ed. Pearson Education. San Francisco, CA.

Smith AJ, Owens S, Forsythe ID (2000) Characterisation of inhibitory and excitatory postsynaptic currents of the rat medial superior olive. J Physiol Pt 3:681-698.

Sommer I, Lingenhohol K, Friauf E (1993) Principle cells of the rat medial nucleus of the trapezoidal body: an intracellular *in vivo* study of their physiology and morphology. Exp Brain Res 95: 223–239.

Spangler KM, Cant NB, Henkel CK, Farley GR, Warr WB (1987) Descending projections from the superior olivary complex to the cochlear nucleus of the cat. J Comp Neurol 259:452-465.

Sun H, Ma CL, Kelly JB, Wu SH (2006) $GABA_B$ receptor-mediated presynaptic inhibition of glutamatergic transmission in the inferior colliculus. Neurosci Lett 399:151–156.

Sun H, Wu SH (2009) The physiological role of pre- and postsynaptic GABAB receptors in membrane excitability and synaptic transmission of neurons in the rat's dorsal cortex of the inferior colliculus. Neuroscience 160:198–211.

Thompson AM, Schofield BR (2000) Afferent projections of the superior olivary complex. Microsc Res Tech 51:330–354.

Thompson GC, Cortez AM, Lam DM (1985) Localization of GABA immunoreactivity in the auditory brainstem of guinea pigs. Brain Res 339:119–122.

Ulrich D, Bettler B (2007) GABA (B) receptors: synaptic functions and mechanisms of diversity. Curr Opin Neurobiol 17:298-303.

Vaughn MD, Pozza MF, Lingenhöhl K (1996) Excitatory acoustic responses in the inferior colliculus of the rat are increased by $GABA_B$ receptor blockade. Neuropharmacology 35:1761–1767.

Warr WB (1982) Parallel ascending pathways from the cochlear nucleus: Neuroanatomical evidence for functional specializations. Contrib Sensory Physiol 7:1-38.

Warr WB, Beck JE (1996) Multiple projections form the ventral nucleus of the trapezoid body in the rat. Hear Res 93:83–101.

Winer JA (1992) The functional architecture of the medial geniculate body and the primary auditory cortex. In: The mammalian auditory pathway: Neuroanatomy (Webster DB, Popper AN, Fay RR, Eds), pp. 222-409. Springer-Verlag, New York.

Winer JA (2005) Three systems of descending projections to the inferior colliculus. In: The inferior colliculus. Springer-Verlag. New York, pp. 231-247.

Winer JA, Larue DT (1988) Anatomy of glutamic acid decarboxylase immunoreactive neurons and axons in the rat medial geniculate body. J Comp Neurol 278:47–68.

Winer JA, Larue DT (1996) Evolution of GABAergic circuitry in the mammalian medial geniculate body. Proc Natl Acad Sci USA 93:3083–3087.

Winer JA, Prieto JJ (2001) Layer V in cat primary auditory cortex (AI): Cellular architecture and identification of projection neurons. J Comp Neurol 434:379-412.

Winer JA, Schreiner CE (2005) The central auditory system: A functional analysis. In: The inferior colliculus. Springer-Verlag. New York, pp. 1-49.

Winter IM, Robertson D, Cole KS (1989) Descending projections from auditory brainstem nuclei to the cochlea and cochlear nucleus of the guinea pig. J Comp Neurol 280:143–157.

Yamauchi T, Hori T, Takahashi T (2000) Presynaptic inhibition by muscimol through $GABA_B$ receptors. Eur J Neurosci 12:3433–3436.

Yang Y, Surette AM, Bishop D, Oliver DL (2000) Properties of local circuits in the central nucleus of the inferior colliculus (CIC). Soc Neurosci Abstr 26:674

Zhang Y, Wu SH (2000) Long-term potentiation in the inferior colliculus studied in rat brain slice. Hear Res 147:92–103.

Zhao M, Wu SH (2001) Morphology and physiology of neurons in the ventral nucleus of the lateral lemniscus in rat brain slices. J Comp Neurol 433:255-271.

APPENDICES

Solutions used in Western blotting procedures

Homogenization Buffer

For 10 ml

50 μL Tris base (pH= 7.4)

1.095 g Sucrose

in dH_2O

Protease Inhibitors

3 μl/ml aprotinin

10 μl/ml PMSF (phenylmethanesulfonyl fluoride)

1 μl/ml leupeptin

3 μl/ml pepstatin

Bovine Serum Albumin (BSA) Buffer for the Bradford Assay

The original concentration of BSA is 10 mg/ml

Standard 1: 1000 μl Bradford Reagent

Standard 2: 995 μl Bradford Reagent and 5 μl 0.313 mg/ml BSA

Standard 3: 995 μl Bradford Reagent and 5 μl 0.625 mg/ml BSA

Standard 4: 995 μl Bradford Reagent and 5 μl 1.250 mg/ml BSA

Standard 5: 995 μl Bradford Reagent and 5 μl 2.500 mg/ml BSA

Standard 6: 995 μl Bradford Reagent and 5 μl 5.00 mg/ml BSA

Electrophoresis Sample Buffer (4X Loading Buffer)

For 100 ml

40 ml 87% Glycerol

10 ml 2-mercaptoethanol

40 ml 10% SDS (sodium dodecyl sulphate)

100 ml 0.5 M Tris HCl

4 ml 1% Bromophenol blue

6 ml dH_2O

Lower Gel Buffer (pH=6.8)

For 1 L

182 g Tris base

4 g SDS

in dH_2O

12% Lower Gel

For about 30 ml

15 ml dH_2O

7.5 ml lower gel buffer

7.5 ml acrylamide

200 µl 10% APS (ammonium persulfate)

50 µl TEMED (N, N, N, N' - tetramethylenediamine)

Upper Gel Buffer (pH=6.8)

For 200 ml

12.1 g Tris base

0.8 g SDS

in dH_2O

Stacking Gel

For about 10 ml

2.5 ml dH_2O

1.1 ml lower gel buffer

6.4 ml acrylamide

30 µl 10% APS

20 µl TEMED

4X Running Buffer (pH=8.2)

For 1 L

12.11 g Tris base

57.60 g Glycine

in dH_2O

Transfer Buffer (pH=9.2)

For 1 L

5.82 g 48 mM Tris

2.93 g 39 mM Glycine

3.73 ml 10% SDS

200 ml methanol

in dH_2O

Tris Buffered Saline (TBS) (pH=7.6)

For 1 L

6.1 g Tris base

9.0 g NaCl

1 L dH_2O

TBS-Tween (TBST) Buffer

For 1 L

5 ml 10% Tween

995 ml TBS Buffer

Bovine Serum Albumin (BSA)

For 100 ml

3 g BSA

100 ml TBST buffer

Solutions used in immunohistochemistry procedures

0.5 M Sodium Phosphate Dibasic

For 1 L

70.98 g sodium phosphate dibasic powder ($NaH_2PO_4 \cdot H_2O$)

1 L dH_2O

0.5 M Sodium Phosphate Monobasic

For 1 L

68.99 g anhydrous sodium phosphate monobasic (NaH_2PO_4)

1 L dH_2O

0.4 M Sodium Phosphate Buffer (PB) (pH=7.4)

For 1 L

600 ml 0.5 M sodium phosphate dibasic solution

200 ml 0.5 M sodium phosphate monobasic solution

200 ml dH_2O

0.1 M Sodium Phosphate Buffer (PB) (pH=7.4)

For 1 L

250 ml 0.4 M PB

750 ml dH_2O

0.1 M Sodium Phosphate Buffer Saline (PBS) (pH=7.4)

For 1 L

250 ml 0.4 M PB

100 ml 9% physiological saline

650 ml dH_2O

4% Paraformaldehyde (PFA) in 0.1 M PB (pH=7.4)

For 1 L

40 g PFA powder

1 L 0.1M PB

1. Dissolve PFA powder into 0.1M PB by heating on a stir plate set to a low heat setting
2. Adjust pH to 7.4 with either HCl or NaOH

Cryoprotectant Solution

For 100 ml

30 g sucrose

100 ml PB

0.05% Triton in 0.1 M PBS (TPBS)

For 1 L

0.05 ml Triton X-100

1 L 0.1M PBS

3,3' diaminobenzidine tetrahydrochloride (DAB)- nickel solution

For 20 ml

5 ml 0.4M PB (pH= 7.4)

200 ul 0.4% NH_4Cl in 0.1M PB solution

200 ul Glucose

13.6 ml dH_20

200 ul of 50 mg/ml DAB (D5637, Sigma-Aldrich, Oakville, ON, Canada) in 0.1M PB

0.8 ml 1% Nickel sulfate in dH_20 solution

20 ul of Glucose oxidase (G3660, Sigma-Aldrich)

VITA AUCTORIS

NAME:	Lena Jamal
PLACE OF BIRTH:	Tennessee, U.S.A
YEAR OF BIRTH:	1987
EDUCATION:	Vincent Massey S.S. Windsor, Ontario 2005 University of Windsor, Windsor, Ontario 2005-2009 B. Arts. Sc. Honours Biological Sciences and Psychology 2009-2011 MSc. Biological Sciences